STRATIGRAPHIC ARCHITECTURE AND DIAGENETIC EVOLUTION OF EARLY MIOCENE SYN-RIFT CARBONATE PLATFORMS, MIDYAN BASIN, RED SEA RIFT, NORTHWEST SAUDI ARABIA

BY

ARDIANSYAH IBNU KOESHIDAYATULLAH

A Thesis Presented to the

DEANSHIP OF GRADUATE STUDIES

KING FAHD UNIVERSITY OF PETROLEUM & MINERALS

DHAHRAN, SAUDI ARABIA

In Partial Fulfillment of the
Requirements for the Degree of

MASTER OF SCIENCE

In

GEOLOGY

APRIL 2015

KING FAHD UNIVERSITY OF PETROLEUM & MINERALS

DHAHRAN- 31261, SAUDI ARABIA

DEANSHIP OF GRADUATE STUDIES

This thesis, written by ARDIANSYAH IBNU KOESHIDAYATULLAH under the direction his thesis advisor and approved by his thesis committee, has been presented and accepted by the Dean of Graduate Studies, in partial fulfillment of the requirements for the degree of **MASTER OF SCIENCE IN GEOLOGY**.

Dr. Khalid Al-Ramadan
(Advisor)

Dr. Abdulaziz Al-Shaibani
Department Chairman

Dr. Waleed Abdulghani
(Member)

Dr. Salam A. Zummo
Dean of Graduate Studies

Dr. Richard Collier
(Member)

١١/٥/١٤٣٥

Date

عمادة الدراسات العليا
DEANSHIP OF GRADUATE STUDIES

Dedication

To my beloved parents, wife and daughter

ACKNOWLEDGMENTS

In the name of Allah, the most gracious, most compassionate, most merciful and all the praises and thanks be to Allah that have given me the opportunity and capability to finish my study in KFUPM.

I am deeply indebted and most sincere appreciation goes to my advisor, Dr. Khalid Al-Ramadan, for knowledge, patience, encouragements, and guidance he has shown me over the past few years that I have been with this department, be it scientifically, personally, or academically.

I would like to thank my thesis committee members for their support and sharing their knowledge over the years: Dr. Waleed Abdulghani and Dr. Richard Collier. My appreciation also extended for Dr Wyn Hughes and Dr. Dave Cantrell from Saudi Aramco for the fruitful discussions throughout the research processes.

Further appreciation goes to Prof. Peter Swart from Stable Isotope Laboratory, University of Miami and other colleagues there for their guidance and help during my visit to perform laboratory analyses.

The help from Earth Sciences Department professors, staffs, and friends (Dr. Abdulaziz Shaibani, Dr. Mike Kaminski, Aziz, Abu Jihad, Abdulkarim Al-Hussaini and many more) during my study here are highly appreciated. Thanks also to KFUPM Indonesian community (Mas Syarif, Fandi, Ghazi, Septri, Dibi and many more). Thanks also goes to Cody Trigg for his comments and help in checking the English of the earlier version of this thesis draft.

Thank you to my wonderful family: my parents, Papah and Mamah, for their endless pray, love and support; my brothers, Kak Ditya and Kak Barkah, for keeping my spirit and encouragement during my master journey; and lastly — to my wife Vina Aliya and my daughter Aleena...your endless love, support and encouragement has been most influential and inspiring.

This research was fully supported by the Saudi Arabian government through NSTIP project "Sequence architectures of syn-rift carbonates: Midyan region, Saudi Arabia" for Dr. Khalid Al-Ramadan.

TABLE OF CONTENTS

LIST OF TABLES

LIST OF FIGURES

ABSTRACT

Full Name : [Ardiansyah Ibnu Koeshidayatullah]

Thesis Title : [Stratigraphic Architecture and Diagenetic Evolution of Early Miocene Syn-Rift Carbonate Platforms, Midyan Basin, Red Sea Rift, Northwest Saudi Arabia]

Major Field : [Geology]

Date of Degree : [April, 2015]

The Early Miocene of the Midyan Peninsula, NW Saudi Arabia represents an example of carbonate platform development in a region of active continental rifting. However, a complete characterization of the carbonate platforms in this study area has not previsously been realized. We present new architectural models that illustrate the formation of different carbonate platforms in the region and which allow the forcing mechanisms that likely drove their formation to be inferred. This study identified: a) a fault-block hangingwall dipslope carbonate ramp, which formed during active rifting, b) an isolated normal fault-controlled carbonate platform with associated slope deposits, and c) an attached fault-bounded, rimmed shelf platform developed on a fault footwall tip within a basin margin structural relay zone. Variations in cyclicity have been observed within the internal architecture of each platform and also between platforms. High-resolution sequence stratigraphic analysis has been carried out, with parasequences (probably 5th order cycles) observed as the smallest depositional packages within the platforms. The hangingwall dipslope carbonate ramp and the attached platform demonstrate aggradational-progradational parasequence stacking patterns. These locations appear to have been sensitive to sea-level cyclicities, despite the active tectonic setting. The isolated, fault-controlled carbonate platform reveals

less well organized stratal geometries in both platform-top and slope facies, suggesting a more complex interplay of tectonic rates of uplift and subsidence, variation in carbonate productivity, and resedimentation of carbonates, such that any sea-level cyclicity is obscure. The study explores the interplay between different forcing mechanisms in the evolution of carbonate platforms in active tectonic regions. Characterization of detailed parasequence-scale internal architecture allows the spatial variation in syn-depositional relative base-level changes to be inferred and is critical for understanding the development of rift basin carbonate platforms. Such concepts may be useful in the prediction of subsurface facies relationships beyond interwell areas in hydrocarbon exploration and reservoir modeling activities. This study also recognized two contrast post-depositional processes on two Early Miocene carbonate platform of Wadi Waqb Member (Wadi Waqb and Ad-Dubaybah localities). Integration of petrography, elemental (Mn, Fe, Sr, Na) and stable isotope analyses of carbon ($\delta^{13}C$) and oxygen ($\delta^{18}O$), were employed to decipher the diagenetic history and variatios of paleofluids on these carbonate successions. We found that: (i) early diagenesis is characterized by major microbial micritization, minor isopachous bladed cementation, and early dolomitization; (ii) the burial stage is represented by the presence of chemical compaction, aggrading neomorphism, and late stage dolomitization that formed after hydrocarbon migration. The carbonate sequence in the Wadi Waqb locality to the southwest shows relatively enriched on $\delta^{18}O$ values and trace elements (Fe, Mn, Sr, and Na) concentrations that may indicate extensive evaporation of pore water fluids with correspond to the dolomitization process. In contrast, Ad-Dubaybah locality to the northeast show both $\delta^{18}O$ values and trace element concentrations were significantly lower in comparison with the Wadi Waqb one. The indication of various

paleodiagenetic fluids likely controlled by local tectonic arrangements where Wadi Waqb locality being an isolated carbonate platform with respect to the Red Sea rift margin, whereas the Ad-Dubaybah platform was structurally attached and therefore potentially in communication with meteoric waters supported by a gravitational head from the rift margin footwall into its platform carbonates. Such relationships between platform geometry and rift flank proximity may have relevance to late syn-rift carbonate platforms elsewhere.

ملخص الرسالة

الاسم الكامل : أردينسيه إبنو كوشيديا طلحه

عنوان الرسالة **:** البنيويه التتابعيه وتطور النشأة المتأخره للأرصفه الجيريه ضمن فتره الصدع من بدايات عصر المايوسين، حوض مدين، شمال غرب المملكة العربية السعودية

التخصص **:** الجيولوجيا

تاريخ الدرجة العلمية : ليربأ- 2015

دائما ما يجذب نمو الرصيف الجيري وتطور النشأة المتأخرة في المناطق النشطة تكتونيا الاهتمام المتزايد نظرا لتعقيداته الداخلية الفريده من نوعها وغالبا ما يرتبط مع منظومة النفط والغاز. تتمثل هذه الحاله وبشكل مثالي في شبه جزيره مدين شمال غرب المملكة العربية السعودية حيث تكونت الأرصفة الجيرية ضمن النظام البحري لصدع البحر الأحمر. ومع ذلك، لم يتم فهم التوصيف الكامل للأرصفة الجيرية في منطقة الدراسه هذه. تقدم هذه الدراسة نماذج بنيويه حديثه والتي تستطيع وبشكل متكامل وصف تكون رصيفين جيريين في المنطقة: متكون المصير (20.5 مليون سنة)، بالإضافة إلى عضو وادي وقب (17.2 مليون سنة)، كما وتلخص الأليات الدافعه والتي من المحتمل أدت الى تكونها. حددت هذه الدراسة: المنحدر الجيري بزاويه ميل الحائط المعلق لكتله الصدع، والتي تكونت خلال فتره التحركات التكتونيه، ب) الرصيف الجيري المعزول نتيجه فالق عادي والذي صاحب فترات لحركات تكتونيه نشطه نسبيا، جـ) تكون الأرصفه المتعلقه بالجروف الحافيه على قمه الكتله المنخفضه للفالق ضمن منطقه تحول الحوض والحافه. أظهر كلا الرصيفين الجيريين تتابع متكرر يضمحل تصاعديا ذو نمط تراكمي- تقدمي. كما تصف هذه الدراسه عمليات ما بعد الترسيب للرصيف الجيري لبدايات عصر المايوسين في شمال غرب المملكة العربية السعودية. أستخدمت تقنيات دراسه الخصائص الصخريه المجهريه، تحليل العناصر والنظائر المستقرة للكربون ($\delta^{13}C$) والأكسجين ($\delta^{18}O$)، لمعرفه تاريخ النشأة المتأخرة لهذا التتابع الجيري. وجدت أنه: (1) تتميز بدايه النشأه المتأخره بتكون رئيسي للطين الجيري الميكروبي، سمنتة ثانويه مسننه متساويه السماكه، التحول المبكر إلى الدولومايت والتراص الميكانيكي، (2) تتمثل مرحلة الدفن بوجود التراص الكيميائي، تحول البنيه البلوريه تراكميا، والمرحله المتأخره من التحول إلى الدولومايت. أظهر التتابع الجيري في موقع وادي وقب إلى الجنوب الغربي علاقة عكسيه بين عنصرين من عناصر القليله التركيز (الحديد والمنغنيز) وبين نسب النظائر المستقره (الكربون $\delta^{13}C$ والأكسجين $\delta^{18}O$) والتى تعزى تقليديا للنشأة المتأخره المرتبطه بالأحوال الجويه. ومع ذلك، وفي هذه الرواسب، تدل القيم العاليه نسبيا للأكسجين ($\delta^{18}O$) للمياه الموجوده في المسامات على عمليه تبخير واسعه النطاق، أو وفره في كلا من الأكسجين ($\delta^{18}O$) والعناصر القليله في الدلوميات منها في الكالسيات. في موقع الضبيبة بإتجاه الشمال الشرقي، كانت قيم تركيز النظائر المستقرة للأكسجين ($\delta^{18}O$) والعناصر القليله التركيز إلى حد كبير أقل. وأختتم بأن النشأة المتأخره المرتبطه بالأحوال الجويه (بدلا من النشأة المتأخره المرتبطه بعمليات الدفن) قد تكون مسئوله عن الأنماط الملاحظة في هذا الموقع في الضبيبة.

CHAPTER 1

INTRODUCTION

In the last decades, carbonate rocks have been the subject of many researches working both in the field and laboratory. The presence of carbonate rocks as one of the main reservoir facies in the world has driven geologist to develop new techniques to understand the complexity and heterogeneity of carbonates. Understanding these variations is crucial in the prediction of subsurface reservoir architecture in terms of the distribution of reservoir properties and connectivity.

Many giant carbonate reservoir fields in the world's are located within an active tectonic region however relatively little work has been carried out to characterize the stratigraphic architecture response of carbonate systems in syn-rift settings. A framework within which syn-rift, siliciclastic sequence stratigraphic architectures may be analysed has been outlined by Gawthorpe et al (1994) and applied by, for example, Jackson et al (2005). Developing a sequence stratigraphic framework within which to study sedimentary process, petrological and diagenetic variation and hence reservoir character in syn-rift carbonates will improve our fundamental understanding of the controls upon carbonate deposition. It follows that this will improve our predictive capabilities with respect to the key features of hydrocarbon reservoirs, namely their subsurface geometries, petrophysical variation and reservoir quality. Such a framework will allow the recognition of patterns of petrophysical variation arising from both 1) initial depositional facies and 2) from diagenetic alteration related to relative changes in sea level.

1.1 Motivation

The Midyan region offers an opportunity to assess carbonate sedimentology and depositional geometries in a mappable structural context (after Hughes and Johnson 2005), allowing syn-depositional faults and displacement fields to be identified. Structural mapping and the identification of faults active at the time of carbonate deposition will allow the relative sea level and accommodation space changes associated with carbonate platform or basinal facies development to be inferred. This will allow construction of generic models of sequence architecture to improve prediction and correlation within syn-rift carbonate sequences. These would contrast, for example, the spatial distribution of high porosity and permeability facies within transgressive versus regressive sequence sets controlled by tectonic subsidence or uplift. Reservoir geometry and quality predictions are of profound need in the exploration of new fields in the Midyan Basin. Understanding the sedimentological and diagenetic evolution of syn-rift carbonate sequences in both surface and subsurface systems will enhance reservoir architecture and quality predictions along the Saudi Red Sea subsurface.

1.2 Problem Statements and Objectives

In the last decade, Cenozoic carbonate deposits have been identified as potential future oil and gas targets, particularly in this study area, which belongs to Red Sea rift basin area. The Cenozoic rift basin petroleum system not only occurs in Saudi Arabia but also in several other countries around the world, such as Egypt, Brazil, and Indonesia where the petroleum systems are already proven (Rudolf and Lehmann, 1989; Vahrenkamp et al.,

2004). The petroleum potential of the Middle Cenozoic strata in Red Sea, Saudi Arabia is noteworthy in view of the correlations with proven petroleum systems in neighboring Egypt. For this reason, an understanding of the basin, facies, palaeoenvironment, paleogeography and carbonate platform architecture together with the cyclicity and its stacking patterns and diagenesis, are vital to identify the potential petroleum system in the Early to Middle Miocene Carbonate strata. In addition, this succession has only little information available and is not well understood compared to other carbonate successions in Saudi Arabia (e.g. Mesozoic carbonate). This is largely due to the poor seismic resolution in subsalt intervals.

Therefore, the main objectives of this thesis are summarized as follow:

1). Detailed analysis of the sedimentology, biofacies, and petrographic properties of selected carbonates and their geometries, stacking patterns, and lateral extent.

2). To characterize the carbonate platform architecture and relate it to the syn-depositional structural context. It is important in order to better understand the spatial and temporal distribution of carbonate facies that are difficult to resolve in the seismic section.

3). To assess controlling mechanisms on the evolution and development of carbonate platforms in Midyan Peninsula. Hence, its cyclicity variations within the internal platform architecture and between different platform location.

4). To understand the diagenetic evolution of the carbonate successions and its influence in the porosity development throughout the platform.

5). To decipher the variations of paleodiagenetic fluids that affected the post depositional alteration of the carbonate sequences.

1.3 Methodology

1.3.1 Fieldwork

This study was approached through sedimentology, stratigraphy and structural field mapping and sampling of targets which includes:

1. Shallow platform carbonates of the Early Miocene (20. 5 Ma) Musayr Formation from selected representative outcrops.
2. Shallow platform carbonates of the Early Miocene (17.2 Ma) Wadi Waqb Member of the Jabal Kibrit Formation from both hangingwall and footwall crest locations, of particular relevance as a local hydrocarbon reservoir (Fig. 1.1).
3. Key outrcrops for studying the impact of lateral facies distribution and diagenetic alteration on porosity evolution.

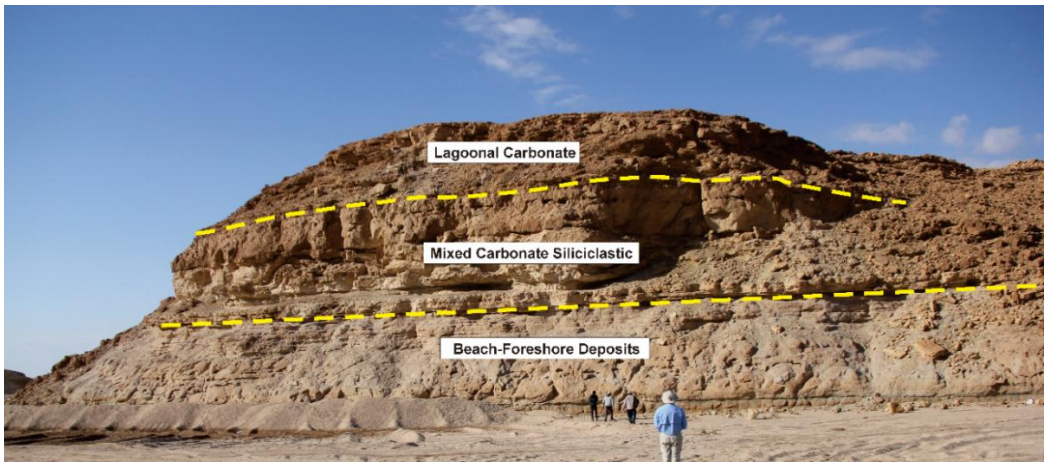

Figure 1.1. Outcrop of Wadi Waqb member of Jabal Kibrit Formation located in the Ad-Dubaybah location. The outcrop shows the vertical variations of carbonate facies.

1.3.2 Laboratory Work

Collected samples were subjected to different types of preparation and analysis as follow:

1. Preparation of polished thin sections, subsequent to vacuum impregnation of the collected samples with colored (blue) epoxy, which enhances the study of porosity in the host rocks and staining by alizarin Red-S to distinguish between calcite and dolomite.
2. Modal analyses based on counting 300 points of the various rock components (minerals, cement, and matrix) and porosity types in each thin section. Thin section analysis to determine the grain component, cement geometry and distribution.
3. Scanning Electron Microscopy (SEM) and Cathodoluminescence (CL) microscopy were performed in order to unravel the variations in crystal morphology and small-scale zonation and sequence of diagenetic events to be linked to changes in pore-water chemistry.
4. Semi-quantitative powder X-ray Diffraction (XRD) for minerals identification and later to select suitable samples for stable isotope analysis (Fig 1.2). This analysis will be focused on identifying major carbonate minerals (aragonite, calcite and dolomite).

Figure 1.2 X-ray Diffraction equipment in the mineralogy laboratory of University of Miami used for analyzing whole rock carbonate samples. This analysis will provide a bulk mineralogy information of the samples.

5. Stable isotope (^{13}C and ^{18}O) analysis were performed on the selected samples to determine geochemical signature of diagenetic fluids. The carbon and oxygen analyses were conducted at Stable Isotope Laboratory, University of Miami using the following procedure:
    - 100 -200 µg of powdered carbonate samples were placed into twenty five small sample holders and then placed it into Thermo Finnigan MAT 251 equipment.
    - Manually inject 200µl of phosphoric acid and left it for 1 hour so the samples will have time to react before the Thermo Finnigan MAT 251 equipment run.

- Samples were calibrated using pure calcite standards (NBS-18 and NBS-19) and reported as ‰ on the VPDB scale. Precision of this technique may reach 0.1‰ for both $\delta^{13}C$ and $\delta^{18}O$ (Swart, 2002).

This technique may also help to determine the origin of diagenetic fluids such as meteoric, marine and high temperature fluids. The equipments set up are shown in the figures 1.3A and B.

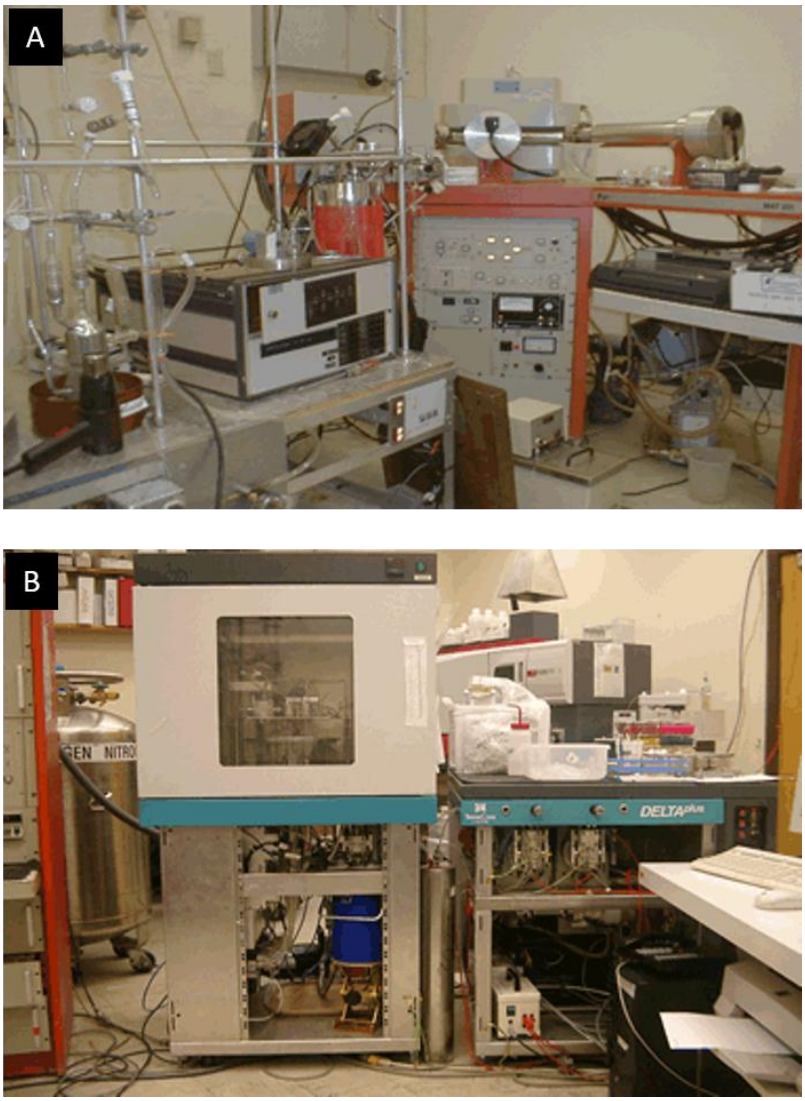

Figure 1.3 (A). Different components of stable isotope Finnigan MAT 251 equipment at Stable Isotope Laboratory, University of Miami for analyzing carbon and oxygen isotopes.

(B). Delta-PLUS with Kiel. The difference between this equipment and the Finnigan MAT 251 is that this equipment almost fully automated and requires less amount of sample.

6. Trace elemental analysis (Ca, Si, Na, Fe, Al, Mg, K, Ba, Sr, Mn, Zn, P, Ti and S) of carbonate samples using ICP-OES (Inductively Coupled Plasma Optical Emission Spectrometer) was carried out to unravel the origin of carbonate materials and different diagenetic environment (Fig. 1.4). 20 mg powders were weighed and placed in vials of 20 ml together with 20 ml (5%) HNO3. The solution was left reacting for at least 2 hours. This instrument has a detection limit of 50 ppm wt% with measurement uncertainty around 0.5 to 3% relative to the reported value.

Figure 1.4 Varian ICP-OES in the University of Miami used for analyzing trace elements concentration in the carbonate rock samples.

1.4 Thesis Structure

This master thesis contains five chapters: An introductive chapter (1), about the motivation, problem statement and objectives of this master thesis. In this chapter, field and laboratory methodologies performed in this study are also discussed. Literature review chapter (2), an overview about the study area including its geological setting and tectonic evolution. This chapter briefly discusses the different controlling mechanisms that affected carbonate platform evolution and diagenesis from literature sources that have direct and indirect relation with this study. In addition, it discusses the occurrence of carbonate rocks as important major reservoirs around the world. Chapter (3) deals with the results obtained in this study. Lithofacies description, associations and diagenetic features results are presented in this chapter. A discussion chapter (4) is devoted to discuss the main objectives in this master works including carbonate platform architecture and controlling mechanisms in the Early Miocene carbonate of Midyan rift basin and diagenetic evolution within the carbonate successions. A final conclusive (Chap. 5) presents the main findings, answers to the questions introduced in this chapter and perspectives, followed by stating future recommendations that will help to develop this study in the future.

CHAPTER 2

LITERATURE REVIEW

2.1 Geological Background

Cenozoic carbonate platforms represent one of the most extensive carbonate deposits within active tectonic regions (Bosence, 2005), and a large body of literature now exists for such sites around the world, (i.e. Coniglio et al., 1996; Wilson, 2000; Pomar et al., 2005 Brandano et al., 2009; Benisek et al., 2012; Hughes, 2014 and reference therein). Red Sea, in particular the Egyptian side has been one of the most well studied Miocene carbonate platform because it represents carbonate platform development in an active tectonic region. The Red Sea rift developed in response to the Oligo-Miocene separation of the Arabian and African plates (Lyberis, 1988; Bosworth et al., 2005), and Early to Middle Miocene syn-rift formations are exposed across the Midyan Peninsula, offering the opportunity for detailed sedimentology and structural mapping (Fig. 2.1).

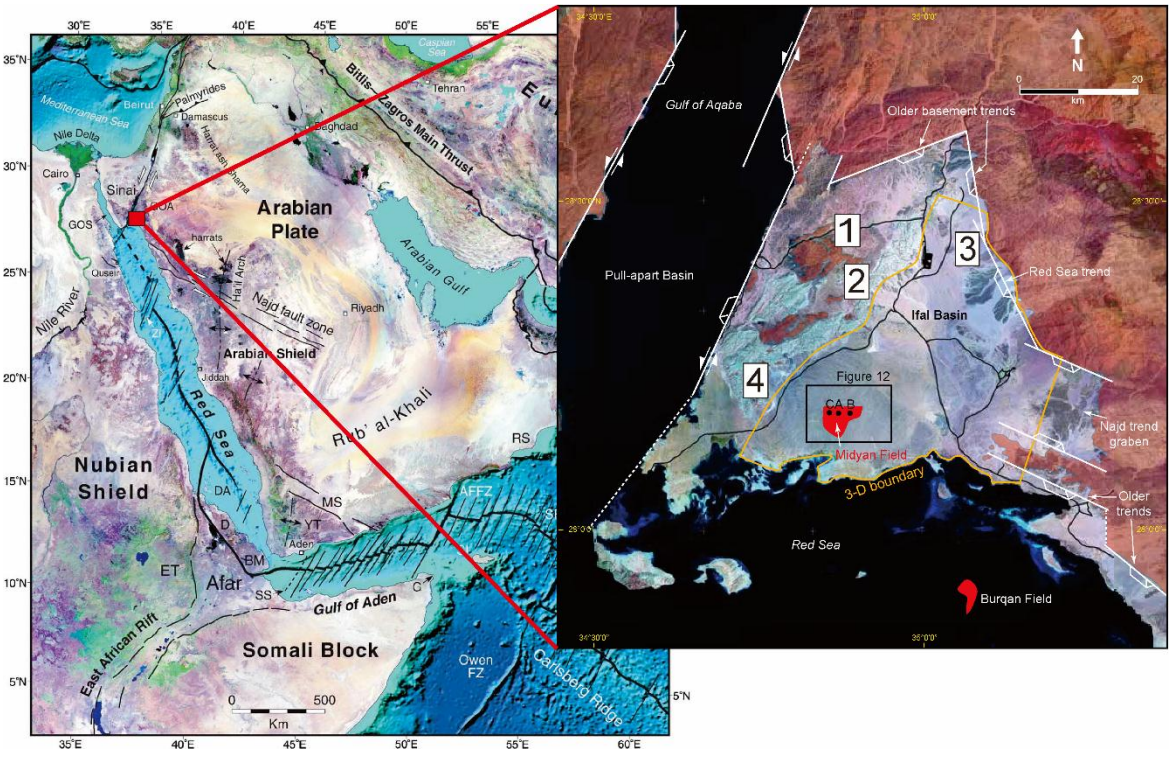

Figure 2.1 Landsat image of Red Sea and Gulf of Aden Area (after Bosworth et al., 2005). Study area is marked by red rectangle. Satellite image of the Midyan basin, NW Saudi Arabia (modified after Tubbs et al., 2014). Numbers represent study locations used for this study: 1. Maqna area, 2. Wadi Al-Hamd, 3. Ad-Dubaybah, and 4. Wadi Waqb.

The two Early Miocene carbonate sequences studied here are exposed on the western part (locations 1-2 in Fig. 2.1), eastern (location 3 in Fig. 2.1) and southern (location 4 in Fig. 2.1) part of the Midyan Peninsula, on the NW margins of the present day Red Sea. The outcrops mostly coincide with structural highs in the area (Kamal and Hughes, 1993; Hughes and Johnson, 2005; Fig. 2.2), a result of rifting during the Late Oligocene to Recent (Bosworth and McClay, 2001).

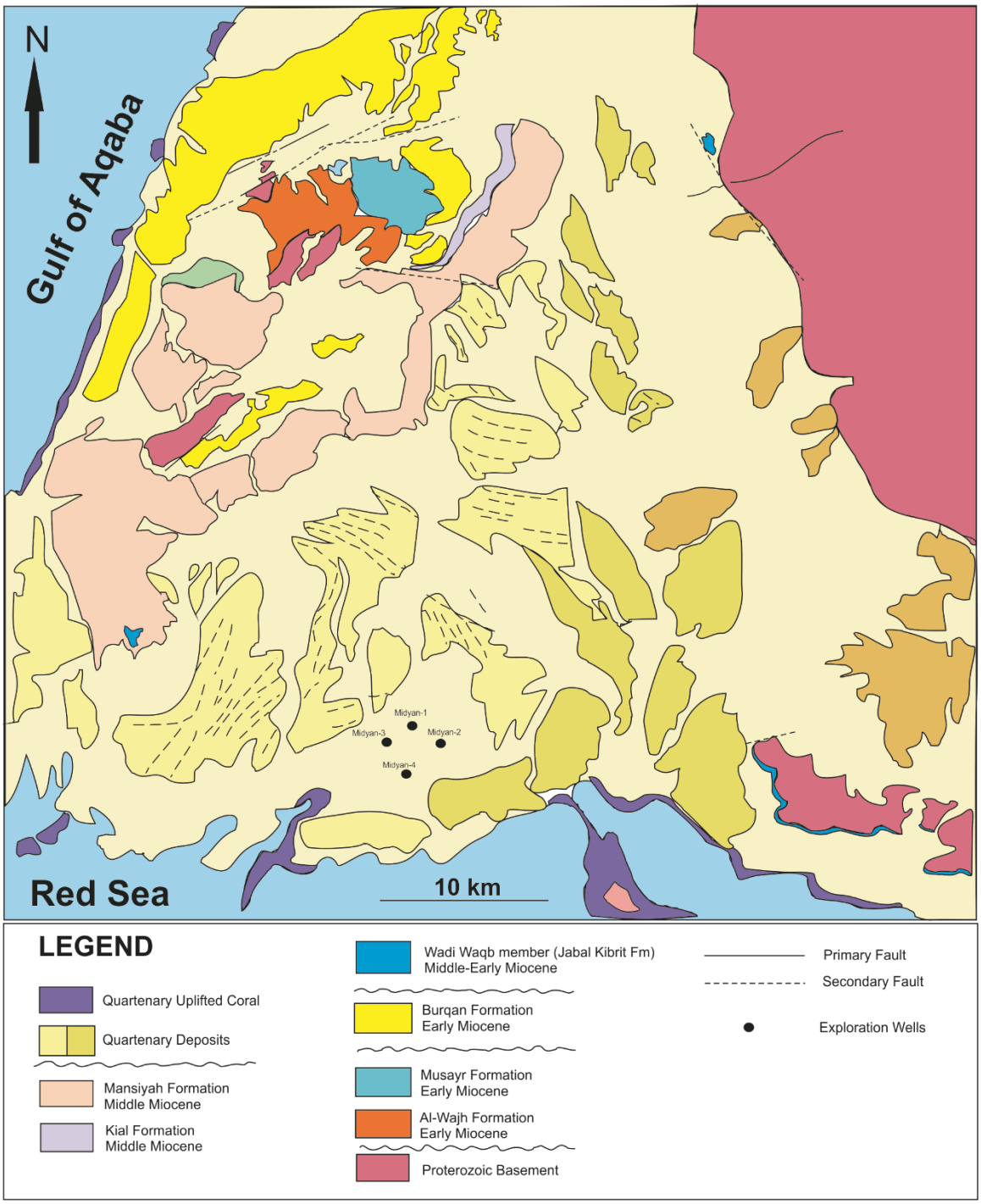

Figure 2.2 Geological map of Midyan Peninsula (modified after Clark, 1986) showing different sedimentary sequences from Early Miocene to Quartenary. The presence of Proterozoic basement also found in the eastern side and scaterred in the study area.

2.2 Tectonic Evolution of Midyan Peninsula

There are at least three major structural episodes that have influenced the evolution of Midyan Peninsula through time (Bosworth et al., 2005) (Fig. 2.3). Rifting began in the Late Oligocene due to mantle upwelling and also the increasing rates of Arabian Plate movement towards the NE direction that associated with subduction in the Zagros Mountain. After that, the development of the Dead Sea Transform (DST) occurred and resulted in rotation of different fault blocks. Lastly, the transition from continental rift to the drift regime that correspond to the oceanic seafloor spreading happened during Plio-Pleistocene (Polis et al., 2005). Hughes and Johnson (2005) indicated that the Midyan Peninsula shares similar tectonic and geologic history with the Gulf of Suez and entire Red Sea basins.

Different fault trends can also be observed from the satellite images (Fig. 2.1), corresponding to the several structural regimes of the Phanerozoic eon. NW-SE trend mostly corresponds to the Late Oligocene Red Sea rifting whereas the NE-SW trend follows the Dead Sea transform. In addition, older structural trends such as Najd graben trend (Proterozoic age) is recognized in the Midyan Peninsula with NE-SW trend (Fig. 2.1).

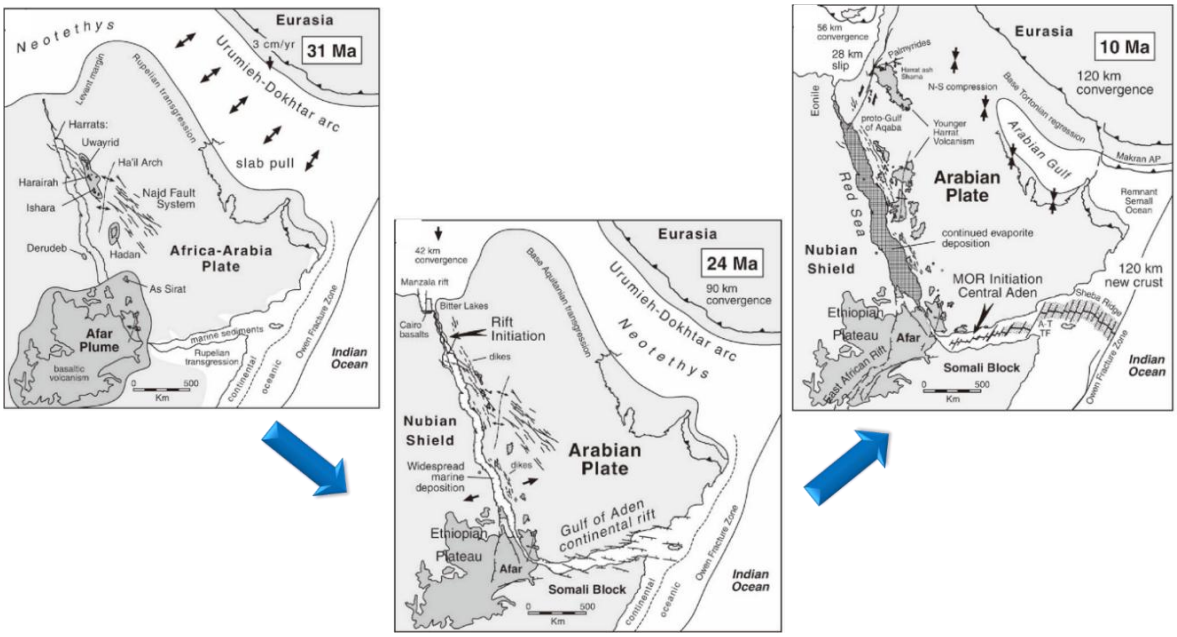

Figure 2.3 Reconstruction and evolution of Red Sea rifting throughout time (30 my – Recent). It started by the initiation of Afar Plume and slab-pull movement of Arabian Plate followed by several episodes of continental rifting and transition from rift to drift from the last 10 m.y (after Bosworth et al., 2005).

2.3 Red Sea Rift Stratigraphy

2.3.1 Proterozoic Basement

The Proteozoric basement has been encountered in several exploration wells around the Red Sea area, consisting primarily of metasedimentary rocks and granitic plutons with basalt dyke intrusions (Figs. 2.2 and 2.4). Based on Gardner et al., (1996) the basement rocks were formed about 600–700 million years ago. Fractured and leached basement succession has been recognized in both surface and subsurface. Bosworth and others 1993 suggest the domination of granitic plutons in this Proterozoic basement suggests a

continental origin for the proto-Red Sea rather than generation of oceanic crust and spreading that formed along an accreting Proterozoic volcanic arc. The distribution of this sequence is scatterred throughout the study area, but prominent in the eastern and northern sides of Midyan Peninsula. This Proterozoic granitoid sequence may provide an information about the crustal evolution of the Midyan Peninsula and possibly northern part of Nubian Shield. Clark (1985) suggest island-arc accretion and compressional tectonics (625 Ma) and rifting have involved in the crustal evolution in this area.

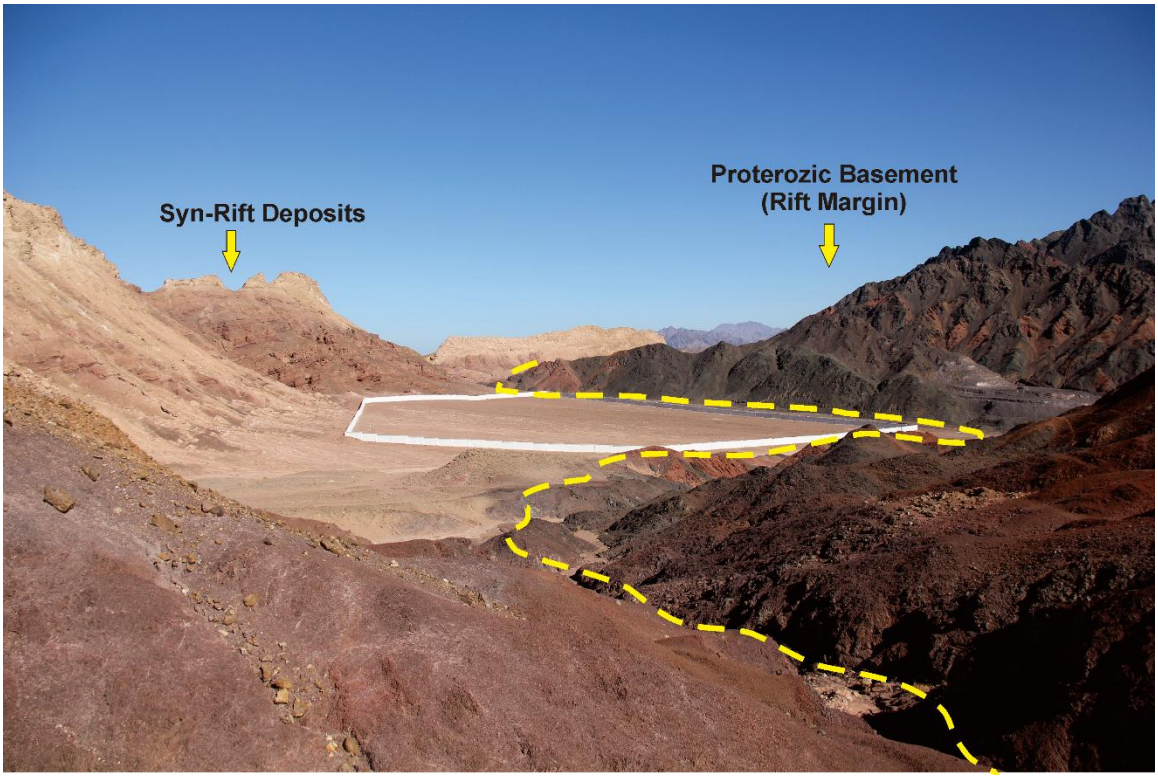

Figure 2.4 Proterozoic basement located in the Maqna area. This basement mostly composed of granitoid rocks that may suggest continent origin and basalt dyke intrusions. The basement also form as a rift margin for this basin.

2.3.2 Pre-Rift

Th pre-rift succession in the Midyan Peninsula and surroundings consist of siliciclastic of Upper Cretaceous sequences (Adaffa and Usfan formations) that unconformbaly overlain the Proterozoic basement. These sequences have been recognized from both surface and subsurface, and it is outcropping in the Midyan Peninsula (Fig. 2.5). The depositional setting of these successions are interpreted as fluvial environment based on the lines of evidence found in the outcrop such as cross-bedding, fining upward and the presence of phosphatic nodules in the mud-dominated facies (Hughes and Johnson, 2005). Bosworth and others (1998) reported almost similarities sequences in the southern Gulf of Suez, which consist of mixed siliciclastic and carbonate successions.

Figure 2.5 Cretaceous sandstones of Adaffa Formation showing high-angle cross-bedding. This sandstone is part of the Pre-Rift sequence in the Midyan basin.

2.3.3 Syn-Rift

Two syn-rift episodes have been recognized in this study area that are marked by different sedimentary successions (Hughes et al., 1999). Ravnas and Steel (1998) highlighted the architecture of syn-rift sequences in the maritime rift basin with its internal complexity. This complexity can be observed in the Midyan Peninsula area where the syn-rift successions are composed of mixed between siliciclastic, carbonate and evaporites. The Proterozoic basement is overlain by the first sedimentary unit, the Al-Wajh Formation. This formed immediately after rifting initiated and consists of immature continental fluvio-lacustrine sediments deposited in an alluvial fan (Fig. 2.6). The thickness of the coarse-grained siliciclastic Al-Wajh Formation is variable throughout the basin because of the irregularity of fault segments and underlying basin topography (Tubbs et al., 2014). Later, the Yanbu and Musayr formations were deposited after the first major marine incursion towards the Midyan basin (Fig. 2.5). The Musayr Formation therefore represents the first major carbonate unit in the Midyan Basin (Hughes, 2014; Tubbs et al., 2014). The synchronous development of the evaporitic Yanbu Formation was due to basin restriction from open marine circulation. A sudden increase in subsidence rates led to the deposition of the deep marine Burqan Formation, dominated by sediment gravity flow deposits (Fig. 2.6). Following the Burqan Formation, a non-deposition event that is represented by a quiescent tectonic period is recognized in the Midyan basin. As a series of local blocks was subsequently uplifted due to tectonic re-adjustment, facilitating the development of the second major carbonate succession, the Wadi Waqb member of the Jabal Kibrit Formation (Hughes & Johnson, 2005; Tubbs et al., 2014). The Jabal Kibrit Formation, deposited in the paleo-highs and adjacent basin during the mid to early Miocene (17-17.5 Ma), consists

of a mixed carbonate-siliciclastic succession (Fig. 2.5). This succession is capped by Kial evaporites, formed in response to the gradual closure of the northern Gulf of Suez due to the differential widening of the Red Sea (Bosworth & McClay, 2001). Collectively, this entire sequence comprises the first syn-rift stratigraphy in this basin and can be recognized from the seismic section (Fig. 2.7).

The development of thick succession of Mansiyah evaporites is used to define the base of the second syn-rift sequence. Gradual development of hypersaline environment during the Middle-Late Miocene time (Maqna Group) may responsible for the formation of of thick evaporites sequence (Hughes et al., 1999). The deposition of Ghawwas Formation that composed of mixed evaporites and siliciclastic overlain the thick Mansiyah evaporites. This sedimentary evolution of marginal and shallow marine environment may be related to either decrease in the rate of vertical subsidence or global eustatic sea-level fall (Hughes et al., 1999).

2.3.4 Post-Rift/Drift

This episode is represented by the deposition of Lisan group sequence that consist of mixed siliciclastic and carbonates coinciding with the Rift Stage II (Bayer et al., 1988) and post-rift stage (Purser et al., 1990). This post-rift stage also recognized in the seismic section by the similarity in thickness throughout the section (Fig. 2.7). This feature may indicate limited and calm tectonic activity.

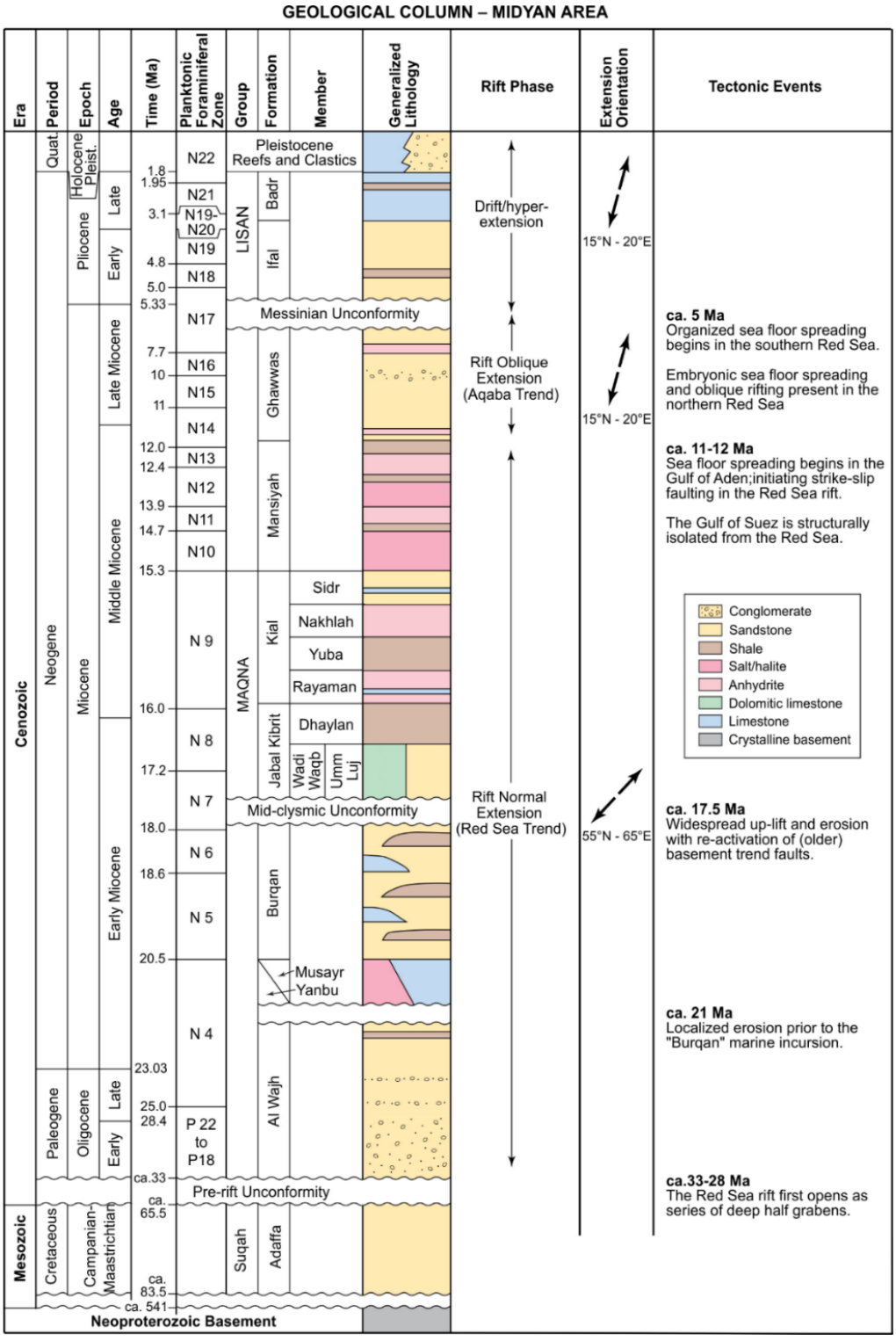

Figure 2.6 Generalized lithostratigraphy of Midyan area. It shows that the Musayr Formation is unconformably underlain by Al-Wajh Formation and conformably overlain

by the Burqan Formation.The Wadi Waqb member was deposited unconformably over the Burqan Formation (after Tubbs et al., 2014).

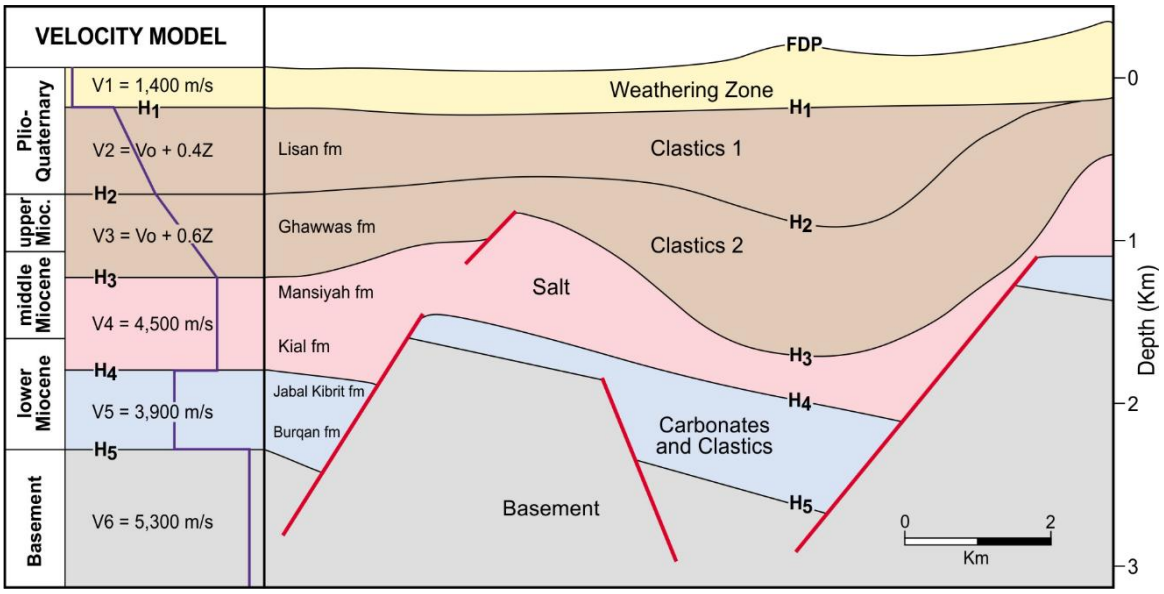

Figure 2.7 Geological sketch section showing the location of the reference horizons. The faulted basement is buried under a thick Neogene sedimentary pile, which includes formations of contrasting lithologies and propagation velocities (Mougenot and Al-Shakhis, 1999).

2.4 Challenges in Subsalt Exploration around the World

Subsalt exploration has been encountered in different major hydrocarbon basins around the world, such as Gulf of Suez, Noth Sea, Red Sea and Gulf of Mexico (Mougenot and Al-Shakhis, 1999). The main challenge in doing subsalt exploration is the presence of strong internal multiples due to the presence of salt deposit overlain the reservoir target. This creates difficulty in imaging and build a proper velocity model of the pre- and syn-rift

structures beneath the salt (Western and Ball, 1992). Based on Polis et al 2005 the exploration history of the Gulf of Suez and Red Sea area is not similar even though they are adjacent to each other and possessed almost similar tectonic history and sedimentary sequences. Instead, the Red Sea area may have more similarity to the North Sea subsalt system where the salt deposit evolution and movement was related to the extensional fault in the region (Fig. 2.8).

In the Midyan Peninsula the exploration targets are also belong to subsalt structures with high structural complexity that increases with depth due to the presence faultls, fold related faults and salt diapirs. In this study area, seismic sections are mostly distorted which hinder the geometry of the reservoir targets and make the imaging effort of any structural features difficult. Mougenot and Al-Shakhis (1999) indicated the importance of pre-stack depth migration in generating seismic sections that have also been performed in other subsalt prospects around the world in order to remove theses distortions and precisely identify the structural features. Additionaly, an outcrop study in this area will also help in revealing the geometry and architectural features of the sedimentary sequences along with its tectonic context.

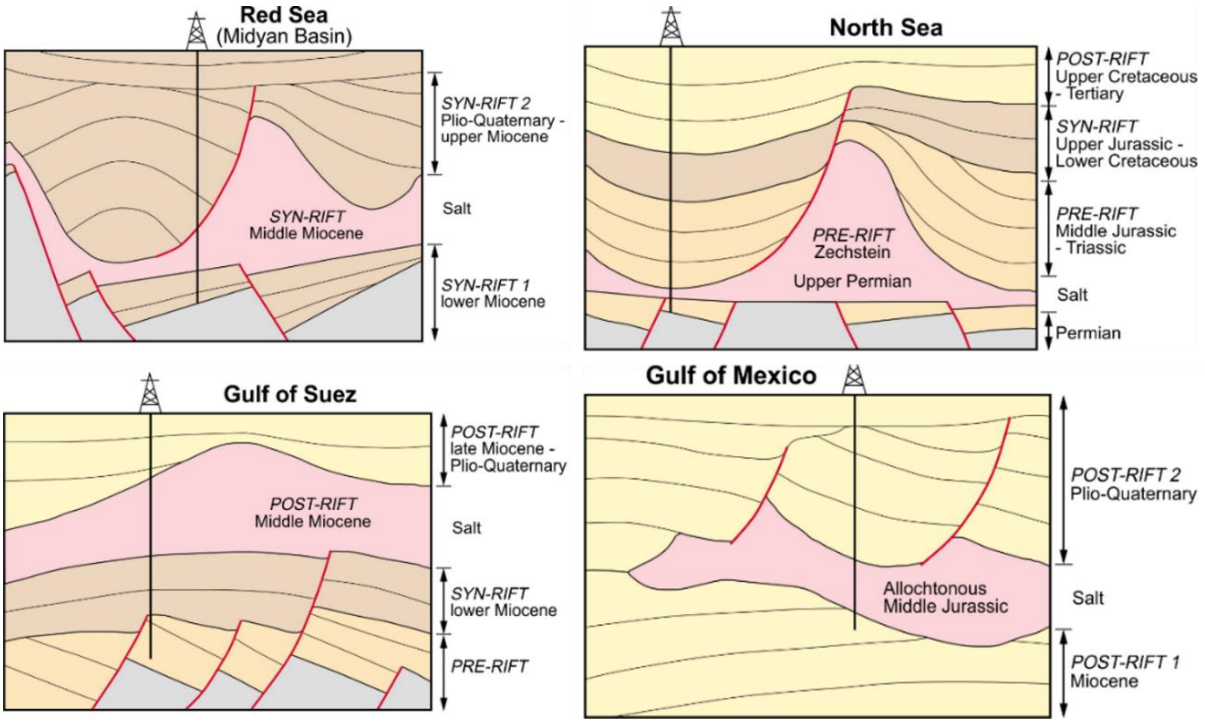

Figure 2.8 Sub-salt plays corresponding to four mature basins are represented with respect to the chronology of the depositions in an extensional basin (pre-, syn and post-rift formations (Mougenot and Al-Shakhis, 1999).

2.5 Controlling Mechanisms on Carbonate Platform

The sedimentology and stratigraphy of carbonate platforms act as useful proxies that can help sedimentologist understand the evolution of marine basins (i.e. Tucker, 1985), and the prevailing paleoenvironmental conditions at the time, including seawater chemistry and biological affinities (James, 1983; Schlager 1992; Schlager, 2005). Even so, the interplay between different forcing mechanisms that account for the growth and evolution of carbonate platforms remains a matter of debate, especially in active tectonic settings. Three

major controls have been proposed to account for the development and evolution of carbonate platforms:

2.5.1 Tectonic

Subsidence and footwall uplift caused by tectonic activity create accommodation space for the accumulation of carbonate sediments, provide topographic areas for carbonate producers to nucleate, terminate carbonate productivity by drowning, and control the evolution of the carbonate platform geometry (Leeder and Gawthorpe, 1987; Gawthorpe and Leeder, 2000; Bosence, 2005; Mack et al., 2009) (Fig. 2.9). In tectonically active rift regions, constantly evolving fault geometries result in significant spatial variability in accommodation space (Gawthorpe and Leeder, 2000). A number of published studies on shallow marine clastic strata within active rifts demonstrate that the stratigraphic evolution and heterogeneity of syn-rift sequences are significantly influenced by the evolution of normal fault segments over large distances (kilometers; e.g., Carr et al., 2003; Jackson et al., 2005). The concept of tectonic control on stratigraphic evolution of shallow marine clastic strata in syn-rift sequence is starting to be applied to carbonate depositional environments, allowing for the development of models of initial depositional facies architecture and interpretation of successions within syn-rift tectonic settings (Dorobek, 2008; Cross and Bosence, 2008). For example, sedimentary records within syn-rift strata may provide important insights necessary to model the structural evolution and sedimentological response at divergent margins, where economically significant hydrocarbon reservoirs are often found (Steel, 1993; Dorobek, 2008).

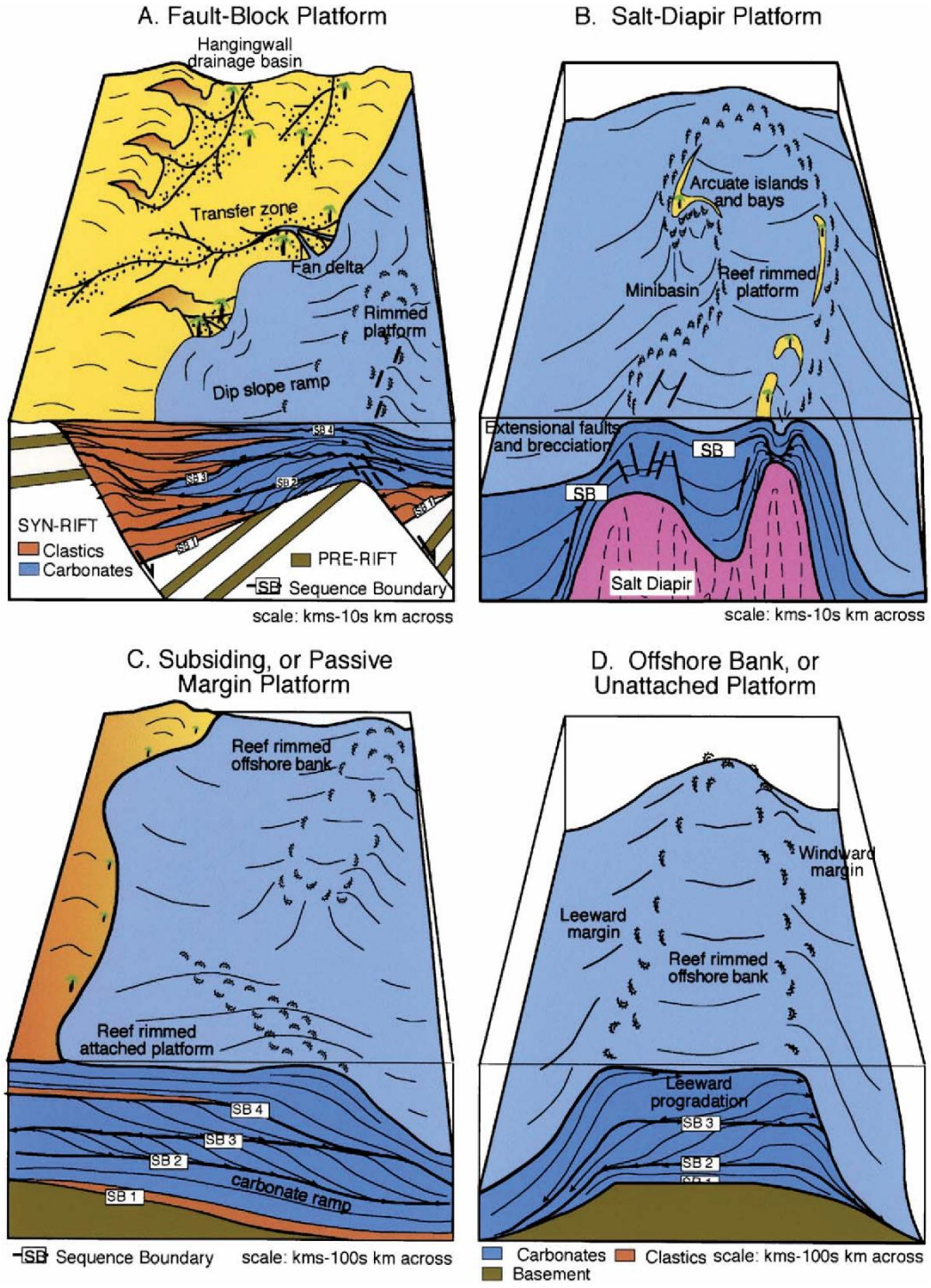

Figure 2.9 Different models of carbonate platform based on their tectonic settings. **(A)** Fault-Block carbonate platforms, **(B)** Salt Diapir platforms, **(C)** Subsiding Margin platforms and **(D)** Offshore Bank (Bosence, 2005).

2.5.2 Sea-Level Variations

Different mechanisms controlling the sea level variations with their amplitude and duration have been discussed in Miller et al., 2005 (Fig. 2.10). Sea level fluctuations play a major role in determining the extent of accommodation space created, and the capacity for carbonate generation by light-dependent producers, such as corals, algae, and other photosymbionts (Kendall and Schlager, 1981; Strasser et al., 1999; Pomar and Kendall, 2007; Bover-Arnal et al., 2009). Trends in relative sea level fluctuations can be identified by the presence and nature of foraminiferal biofacies. Over long time periods, eustatic sea level variation results in crudely predictable relative sea level curves (Fig. 2.11). These can then be used to produce predictive models of reservoir architectures in marine settings (Gawthorpe et al., 1994), although this may be outweighed on a localized scale by the effect from local tectonic displacement fields and lateral variations in sediment flux (Collier & Gawthorpe, 1995; Jackson et al, 2005).

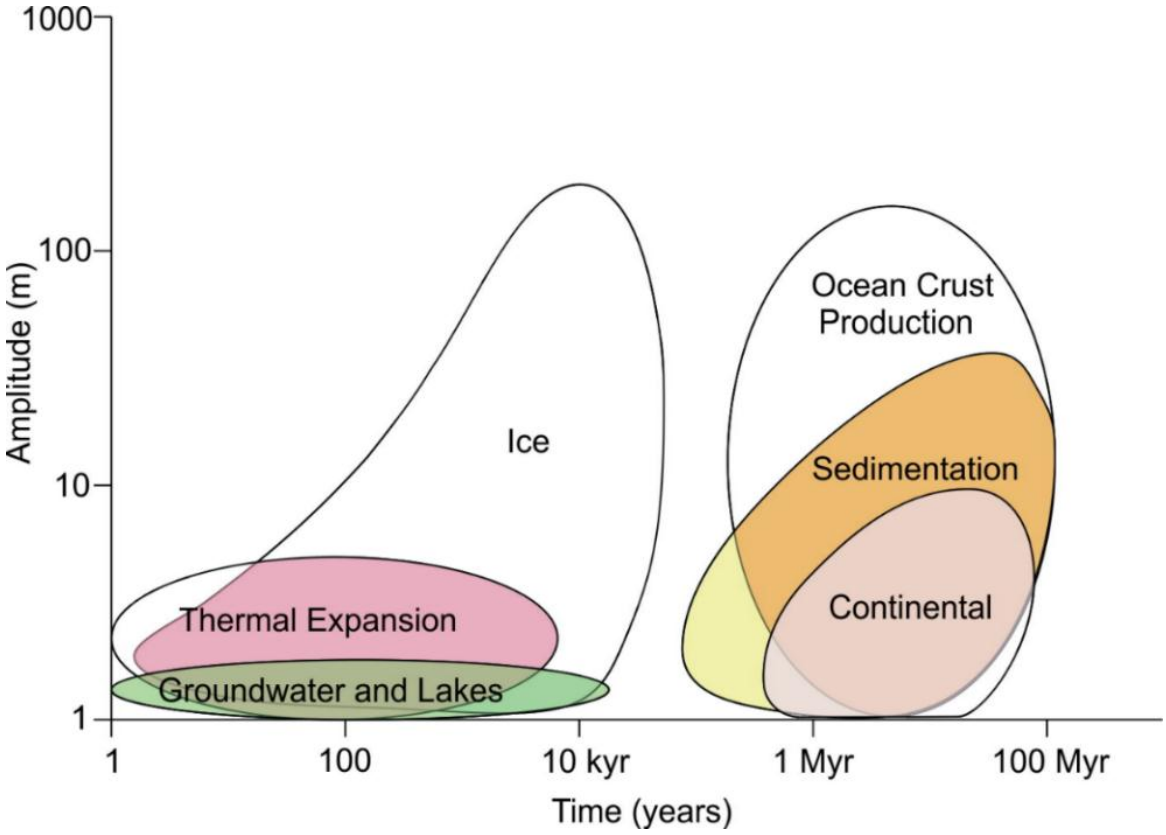

Figure 2.10 Several major and minor mechanisms responsible for the sea level changes (Modified after Miller et al., 2005).

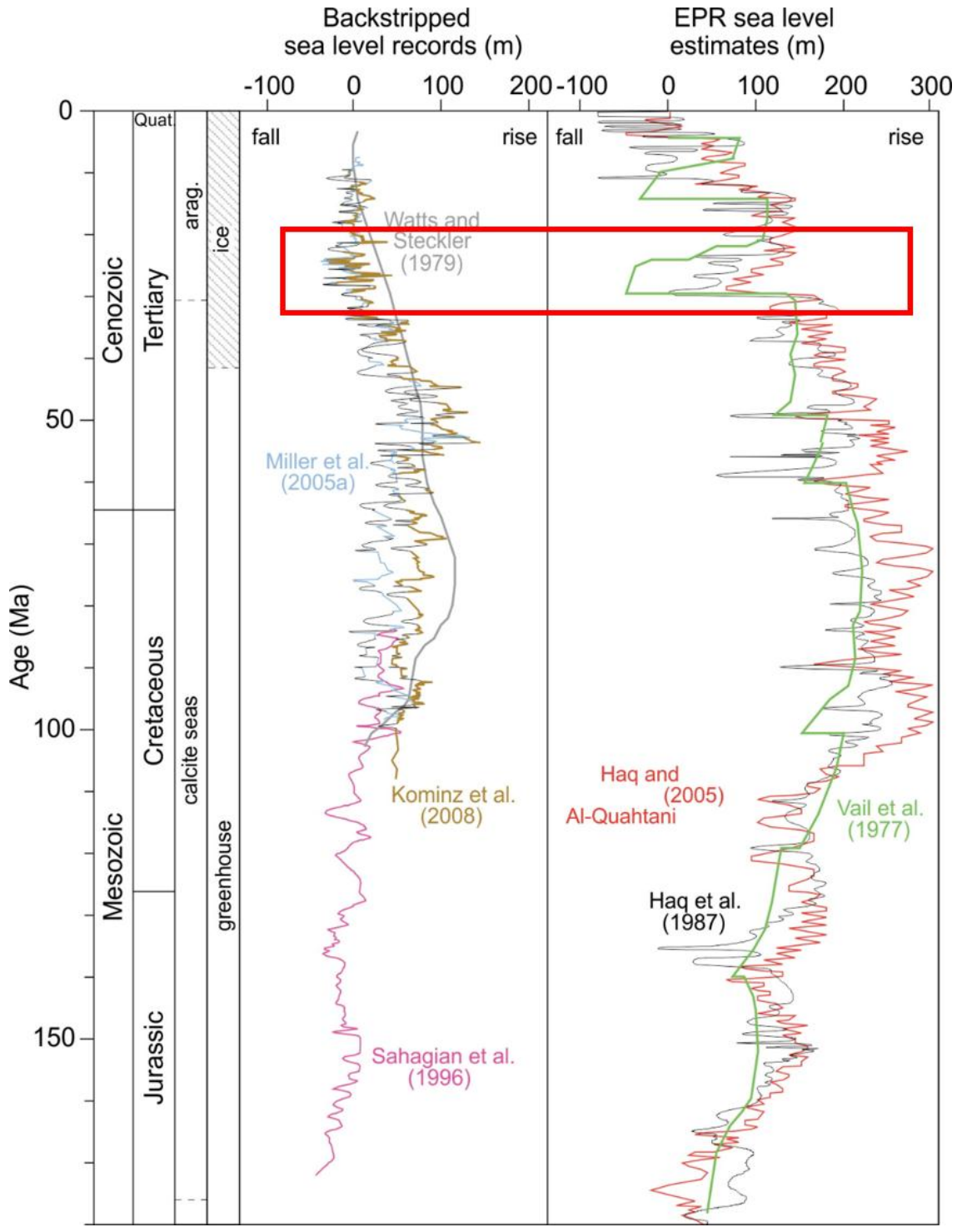

Figure 2.11 Comparison of different global sea level records (blue, Miller et al., 2005a; brown, Kominz et al., 2008) (modified after Miller et al., 2005). It can be noted that the Miocene sea level (red rectangle) has almost similar position with Recent position.

2.5.3 Ecological Accommodations

The presence of carbonate-producing biota associated with particular hydrodynamic levels and other ecological factors – makes carbonate systems distinct from siliciclastic systems (Sarg, 1988; Pomar 2001a; 2001b). The type of carbonate producing biota, cementation factor and transportability may also govern the evolution and development of different types of carbonate platform (Wright, 2011; Fig. 2.12).

Besides these three main factors, other subordinate controls on the temporal and spatial evolution of carbonate platforms include clastic input, temperature, salinity, nutrients, and other physico-chemical variables (Hallock and Schlager, 1986; Weissert et al., 1998; Pomar, 2001a; Mutti and Hallock, 2003; Pomar and Kendall, 2007).

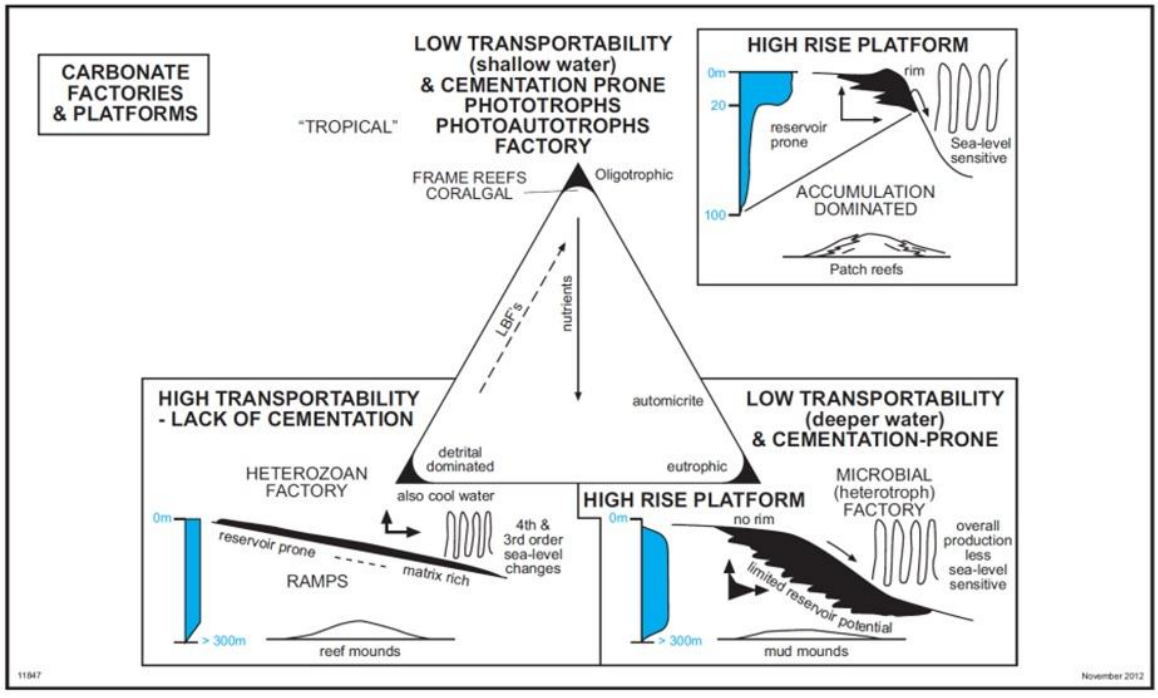

Figure 2.12 Different geometry of carbonate platforms controlled by the variations of carbonate factories. The degree of cementation and transportability may also play a significant role in determining the platform development (Wright, 2011).

2.6 Carbonate Reservoir

Carbonate rocks (both limestones and dolomites) account for approximately 50% of oil and gas production around the world (Roehl and Choquette, 1985; Mazzullo, 2004), and provide for a significant proportion of the world's truly giant fields. Reef and reef-related carbonate deposits comprise a significant proportion of these reservoirs, and occur most prominently in carbonate systems of Siluro-Devonian, Cretaceous, and Neogene age (Sarg, 2011).

Coral reef and related reservoir-prone deposits most commonly occur as thick to massively bedded boundstones in platform margin and in platform interior patch reef settings, and as skeletal rudstones, floatstones, grainstones, and packstones interbedded with the boundstones in fore-slope debris (Sarg, 1998). Reef deposits typically occur over relatively small areas (square km to 10's of square km), and range in thickness from meters to 100's of meters (up to a 1000 m or more). The most common depositional pore types in reefs and reef associated beds include interparticle, intraparticle, and growth-framework shelter porosity (Table 2.1), although these depositional pore systems may be extensively modified by post-depositional alteration (most notably dissolution, cementation and dolomitization). Although porosity in these reef related reservoirs is typically very heterogeneous, they constitute some of the most prolific reservoirs in the world (Trice, 2005).

Table 2.1 A partial list of significant Miocene aged carbonates as main oil and gas reservoirs in production fields. Different types of faunas and porosity types are also recognized (Trice, 2005).

Field Name	Country	Depositional Component	Porosity Types	Est. Porosity Range (%)	Estimated Ultimate Recovery (MMBOE)
Arun	Indonesia	Coral/Algal/ Foram/Molluscs	Chalky, Vug, Mo, WP, Fr	5-25	3900
Kampung Baru	Indonesia	Coral/Algal/ Foram/Molluscs	Mo, Vug, Chalky, Fr	25-30	90
Krisna	Indonesia	Coral/Algal/ Foram/Molluscs	Vug, Mo, Chalky, Fr	10-35	55
Lho Sukon A	Indonesia	Coral/Algal/ Foram/Molluscs	Vug, Mo, Chalky	5-20	85
Liuhua	China	Coral/Algal/ Foram	Vug, Mo, BP, WP, Chalky	15-35	115
Nido	Indonesia	Coral/Algal/ Foram	Vug, Mo, Fr	1-10	20
NSO A	Indonesia	Coral/Algal/ Foram/Molluscs	Vug, Mo, Chalky, Cav, Fr	15-30	245
Natuna L	Indonesia	Coral/Algal/ Foram/Molluscs	Vug, Mo, BP, WP, Cav	10-30	26250
Luconia F6	Malaysia	Coral/Algal/ Foram/Molluscs	Vug, Mo, BP,	5-35	740
Salawati A	Indonesia	Coral/Algal/ Foram/Bryozoan/ Molluscs	Vug, Mo, Fr, BC	~15	20
Kasim	Indonesia	Coral/Algal/ Foram/Bryozoans/ Molluscs	Vug, Mo, BC, Fr	5-40	60
Walio	Indonesia	Coral/Algal/ Foram/Bryozoans/ Molluscs	Vug, Mo, BC, Fr	5-30	200
Rama	Indonesia	Coral/Foram	Chalky, Vug, Mo, BP, WP	15-40	125
Bima	Indonesia	Foram/ Molluscs/ Coral/Algal	Vug, Mo, Chalky, WP	20-40	90
Ramba	Indonesia	Foram/Coral	Vug, Mo, Chalky, Ch, Fr	5-30	90
Bombay High	India	Coral/Algal/ Foram	Vug, Mo, Chalky, Fr	15-25	5015
Ras Fanar	Egypt		Vug, Mo, Chalky, BC, Fr	10-30	140

As can be seen in Table 2.1, reservoir quality in reef reservoirs can be impressive, with porosity ranging from 5 to 40%, and reservoir thickness of approximately 1000 feet (Jintan field-Vahrenkamp et. al., 2004) to 3000 feet. Reservoir quality usually occurs in coral-algal boundstones, rudstones, floatstones, grainstones, and packstones that were deposited as isolated reef platforms of Middle to Late Miocene. In addition, periodic and significant subaerial exposure occurred, which lead to secondary porosity enhancement and cementation.

While Saudi Arabia produces prolifically from a variety of carbonate reservoirs at present, very few of these reservoir are true reefs – and this is the point of this thesis. Future exploration opportunities in the Red Sea will focus on Neogene carbonates, many of which are reef and detrital reef related deposits, and this study will allow us to examine outcrops that are equivalent in age and character to potential exploration targets in the subsurface. Previous works in the northern Red Sea/Midyan area have been limited in scope, and have focussed on a biostratigraphic analysis of the mid-Miocene interval (Hughes and Johnson, 2005). This study seeks to conduct an in-depth analysis of the depositional architecture and diagenetic history – with special emphasis on reservoir quality controls – on a variety of syn-rift reef and reef related deposits in the Midyan area. As such, information gained from this study will be invaluable to the future success of the Kingdom's exploration and development efforts there.

2.7 Variation in reservoir properties in syn-rift carbonates

Predictive models of 3-dimensional variation in reservoir properties are fundamental to the hydrocarbon exploration process and to the modelling of internal reservoir quality and heterogeneity for hydrocarbon production. Reservoir properties will relate to a) initial depositional facies variation and b) to post-depositional diagenetic alteration, which may modify porosity and permeability distributions through porosity destruction or enhancement. Reservoir properties have also been shown to reflect sequence stratigraphic context, which determines environments and rates of deposition, and sediment provenance/composition (e.g. Posamentier et al., 1992; Allen & Posamentier, 1993; Catuneanu 2006).

The conceptual relationship between carbonate depositional facies architectures and sequence stratigraphic setting is well established (e.g. Sarg, 1988; Kerans & Tinker, 1997; Pomar, 2001). This has provided a framework within which post-depositional alteration of carbonates may be characterized (Moore, 2001). But to date there are few published examples of the relationship between carbonate reservoir quality and sequence stratigraphy around the Red Sea margins. The early to middle Miocene Wadi Waqb member of the Jabal Kibrit Formation (Hughes & Johnson, 2005; Hussain & Al-Ramadan, 2009), exposed on the Midyan peninsula, is an important target as this forms an significant hydrocarbon reservoir in the region (Kamal & Hughes, 1995). Crucially, this and other younger carbonate depositional analogues on the Gulf of Aqaba coast have accumulated in syn-rift tectonic settings (Hughes & Johnson, 2005). This requires an integrated approach encompassing sedimentary, micropaleontological and petrological characterization within a structural and sequence stratigraphic context.

In tectonically active rift environments, evolving fault geometries and fault linkages determine the vertical displacement fields around faults. Accommodation generation therefore varies spatially, controlled by the deformation fields of individual faults or interacting faults. Areas of most rapid accommodation generation (subsidence) will tend to be in the centre of the hangingwall of fault segments, with subsidence rates decaying away from the active fault (Gawthorpe et al., 1994; Fig. 2.13). Uplift rates will be at a corresponding maximum at approximately the centre of the footwall crest. Transgressive to aggradational depositional architectures therefore tend to develop in hangingwall areas, whereas forced regressive depositional trends may be developed in footwall locations where sediment supply and preservation allow. Such trends in relative sea level will be reflected by the foraminiferal biofacies. When combined with any eustatic sea level variation through time, relative sea level curves will vary in a crudely predictable manner throughout the deforming fault block or blocks (Gawthorpe et al., 1994). As a result, the stacking patterns of higher order (4^{th} or 5^{th} order) sequences provide a predictive model for reservoir architectures in nearshore and coastal settings, although in some areas the eustatic signal may be either enhanced or suppressed by the relative impacts of local displacement fields and lateral variations in sediment flux (Collier & Gawthorpe, 1995; Jackson et al, 2005).

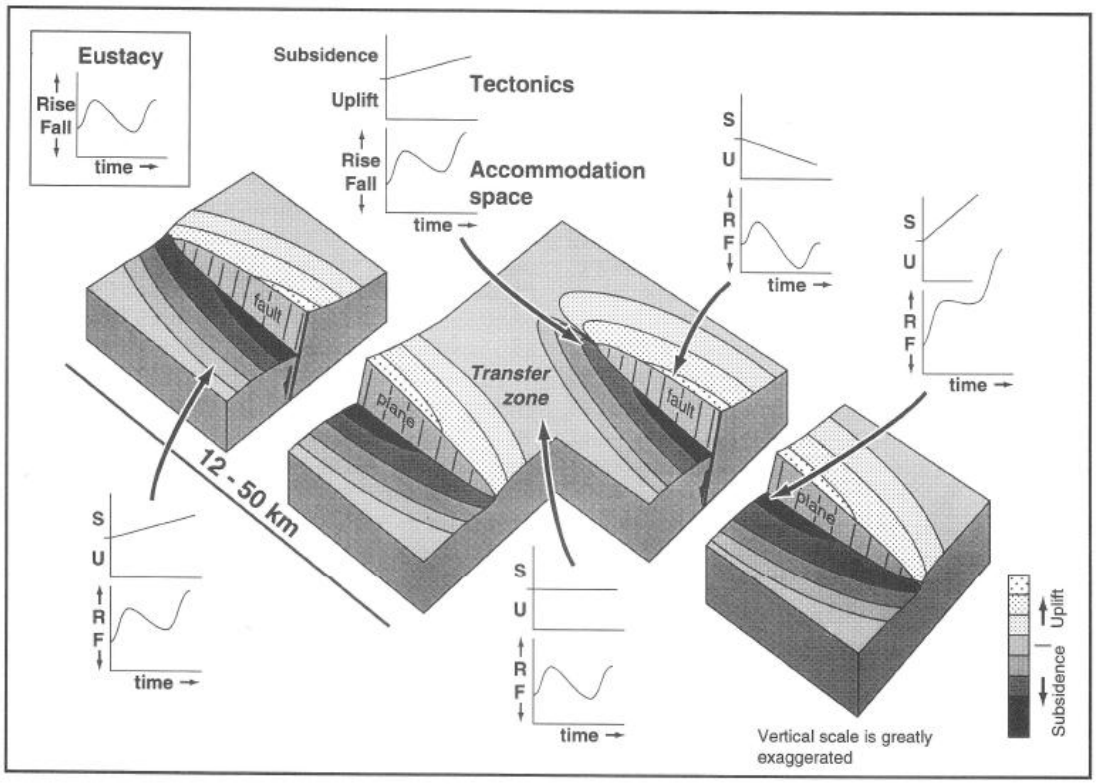

Figure 2.13 Cartoon showing the interaction of eustatic sea-level change and tectonic subsidence or uplift in controlling accommodation space around two rift margin fault segments (after Gawthorpe et al., 1994). The lower graph at each location represents relative sea-level through time.

2.8 Carbonate Diagenesis

Carbonate diagenesis may occur in three different settings, which are meteoric, marine and deep burial environments (Fig. 2.14). Over the last two decades, there have been many extensive reviews on carbonate diagenesis (Longman, 1980; Roehl and Choquette, 1985; Schroeder and Purser, 1986; Choquette and James, 1988; Melim et al., 2002; Miller et al., 2012). However, due to their spatial and temporal complexity, and heterogeneity, the dominant controlling mechanisms of diagenetic alteration in carbonate rocks are still not

entirely understood. Carbonate platforms are a useful proxy to understand this post-depositional history because of their sensitivity to paleoenvironmental changes over time. In particular, their development is largely controlled by sea level fluctuations and tectonic activity (Tucker and Wright, 1990; Flugel, 2004; Bosence, 2005); however, physicochemical parameters may play an especially important role in the subsequent diagenetic evolution of carbonate rocks (Hallock and Schlager, 1986; Weissert et al., 1998; Pomar, 2001; Mutti and Hallock, 2003; Pomar and Kendall, 2007). These physiochemical factors have shown a significant control on determining the variability of facies across the platform and consequently diagenetic alterations.

Studies of carbonate platform development and diagenesis of shallow marine early Miocene carbonates in the northern Red Sea are of particular interest because they are often associated with economically important hydrocarbon resources. Many platform deposits are therefore fairly well documented – for example in the Gulf of Suez, where a hydrocarbon reservoir is located in the subsurface (Aissaoui et al, 1986; Coniglio et al., 1988). However, the variation in diagenetic processes from the platform interior to the platform slope in this area are not fully understood. To date, the majority of published studies of these sequences have focused solely on sedimentology and micropaleontology (Hughes and Johnson, 2005; Hughes, 2014), which tell us very little about the diagenetic alteration conditions. Elsewhere, geochemical parameters such as trace elements (Mn, Na, Ca, Mg, and Fe) and stable isotopes of carbon ($\delta^{13}C$) and oxygen ($\delta^{18}O$) can have been successfully employed to elucidate the nature and evolution of pore water fluids and diagenetic environments (Tucker and Wright, 1990; Flugel, 2004).

Typically Mn, Fe, Na, Sr, Mg, and Ca values are used to determine diagenetic changes in carbonate rocks (Brand and Veizer, 1980; Rao, 1996; Bolhar & Van Kranendonk, 2007), and to differentiate between calcite and aragonite (Milliman, 1974; Brand & Morrison, 1987). For example, Sr and Na concentrations are significantly decreased during burial diagenesis in paleo-carbonates (Winefield et al., 1996). More generally, the predominant mineralogy in modern tropical carbonates is characterized as aragonite and high-Mg calcite (Morse & Mackenzie, 1990; Flugel, 2004), whereas in modern, low-temperate marine waters it is often a mixture of high-Mg calcite to low-Mg calcite with minor contributions of aragonite (Lees & Butler, 1972; Rao & Adabi, 1996; Morse & Mackenzie, 1990).

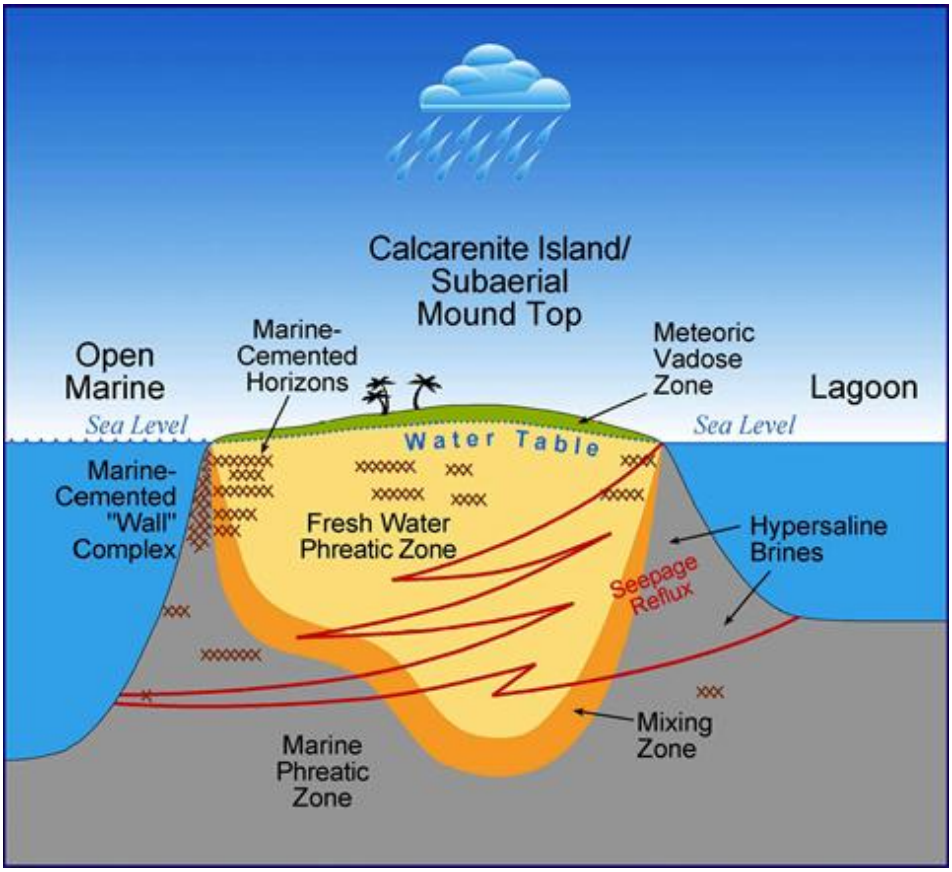

Figure 2.14 Cartoon showing different carbonate diagenetic environments (modified after Tucker and Wright, 1990).

CHAPTER 3

RESULTS

3.1 Carbonate Lithofacies and Facies Association

This section describes the carbonate lithofacies and facies associations and from these information the depositional models will be derived. The lithofacies descriptions are largely based on field observation, which when combined with thin section work, define rock textures, skeletal and non-skeletal components, and geometric relationships. This study uses the widely known nomenclature of Dunham (1962), later modified by Embry & Klovan (1971), to describe the rock textures and compositions.

3.1.1 Musayr Formation

Musayr Formation studied locations are restricted to the north-western part of the Midyan peninsula (location 1 and Fig. 2.1). The Maqna half graben lies to the west of the Jabal Tayran fault block high, which displays an east-dipping hangingwall dipslope to the broader half graben controlled by the Ifal Fault system on the eastern side of the basin. Jabal Tayran provides excellent continuous outcrop of the Musayr Formation for sedimentological study (Fig. 3.1). Eleven lithofacies were recognized in the Musayr Formation, these lithofacies in turn being grouped into three facies associations. All facies are summarized in Table 3.1.

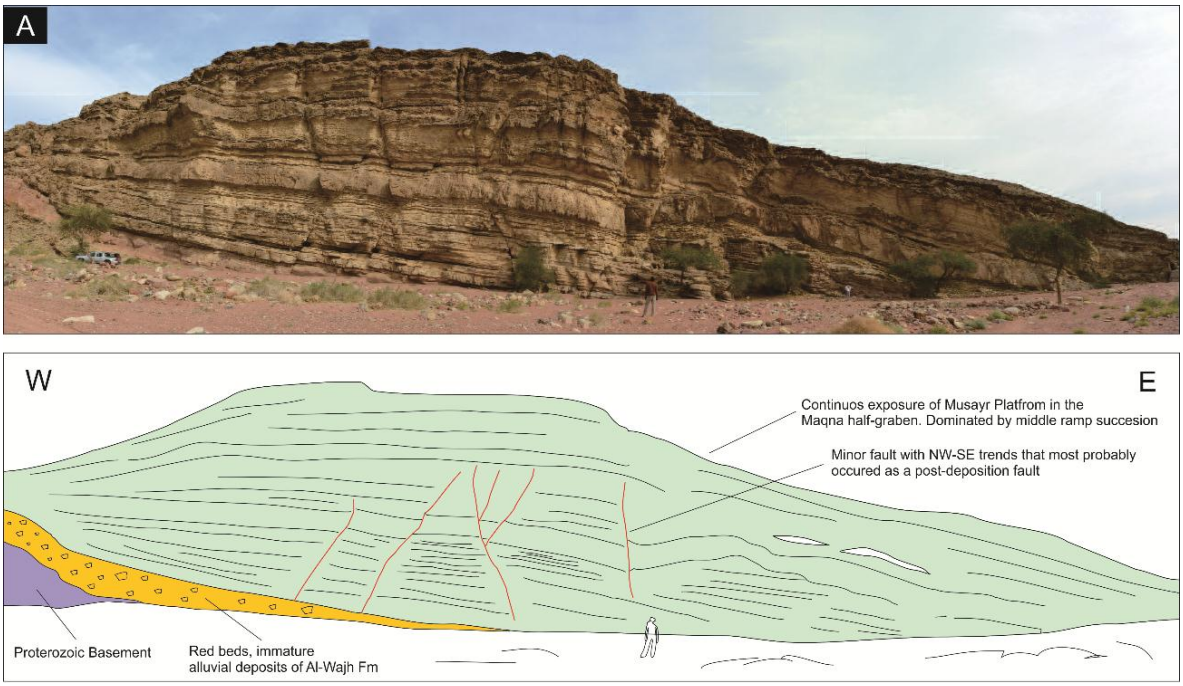

Figure 3.1 Well-exposed Musayr Formation in the Maqna area (location 1-Fig 2.1) directly overly the siliciclastic Al-Wajh Formation. The succession is dipping towards the east (32^{o}).

Facies Association 1 (FA1): Inner Ramp

This facies association comprises facies F1 to F4 (Table 3.1). It is mainly dominated by interbedded bioclastic packstone and calcareous sandstone, stromatolitic boundstones with dolomitized fractures in the basal part (Fig. 3.2A to C), and contains miliolids foraminifera (Fig. 3.2D). The calcareous sandstone facies has high angle cross bedding and is intensively burrowed. Two different morphologies of stromatolite boundstone, planar and domal shapes are also observed in the field (Fig. 3.2A). Pebble lenses occur within the calcareous sandstone facies in the lower part of the successions.

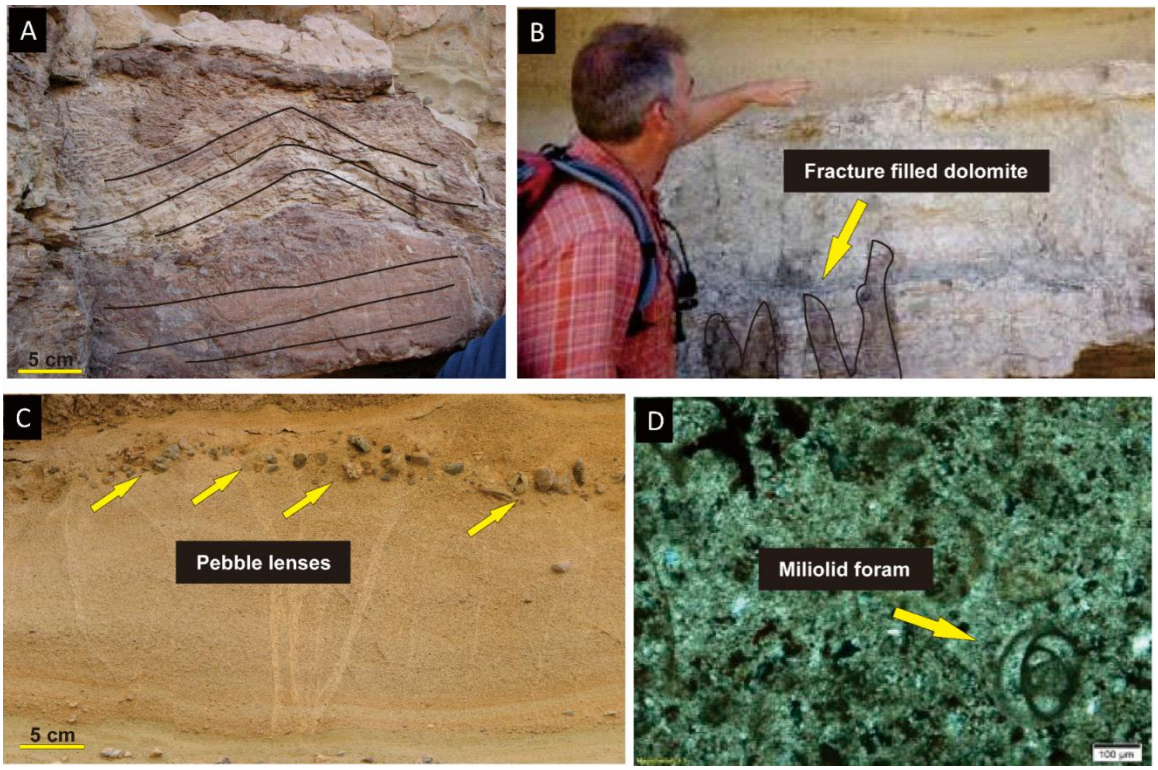

Figure 3.2 Macro- and microscopic features of Musayr Formation facies. **(A).** Dark brown stromatolite boundstone facies, it occurs in two different morphologies: planar and domal shapes. **(B).** Light grey stromatolite facies intruded by dark brown fractures filled dolomite. **(C).** Calcareous sandstone facies with pebble-cobble lenses (arrow), which observed alternating with wackestone-packstone facies. **(D).** Foraminiferal packstone facies characterized by the presence of miliolid forams (arrow) observed in the thin section (XPL).

Facies Association 2 (FA2): Shoal Complex

This facies association is made up of two main lithofacies, which are the oolitic and peloidal grainstone lithofacies (F5 to F6; Table 3.1). The main sedimentary structures observed in these facies are planar parallel-bedding and low-angle cross-bedding (Fig. 3.3A). Petrographically, the oolitic grainstone has tangential cortices and nuclei are mostly

composed of subrounded-rounded quartz grains (Fig. 3.3B). Peloidal grainstone facies (Fig. 3.3C) occurrs as a thin bed associated with the oolitic grainstone.

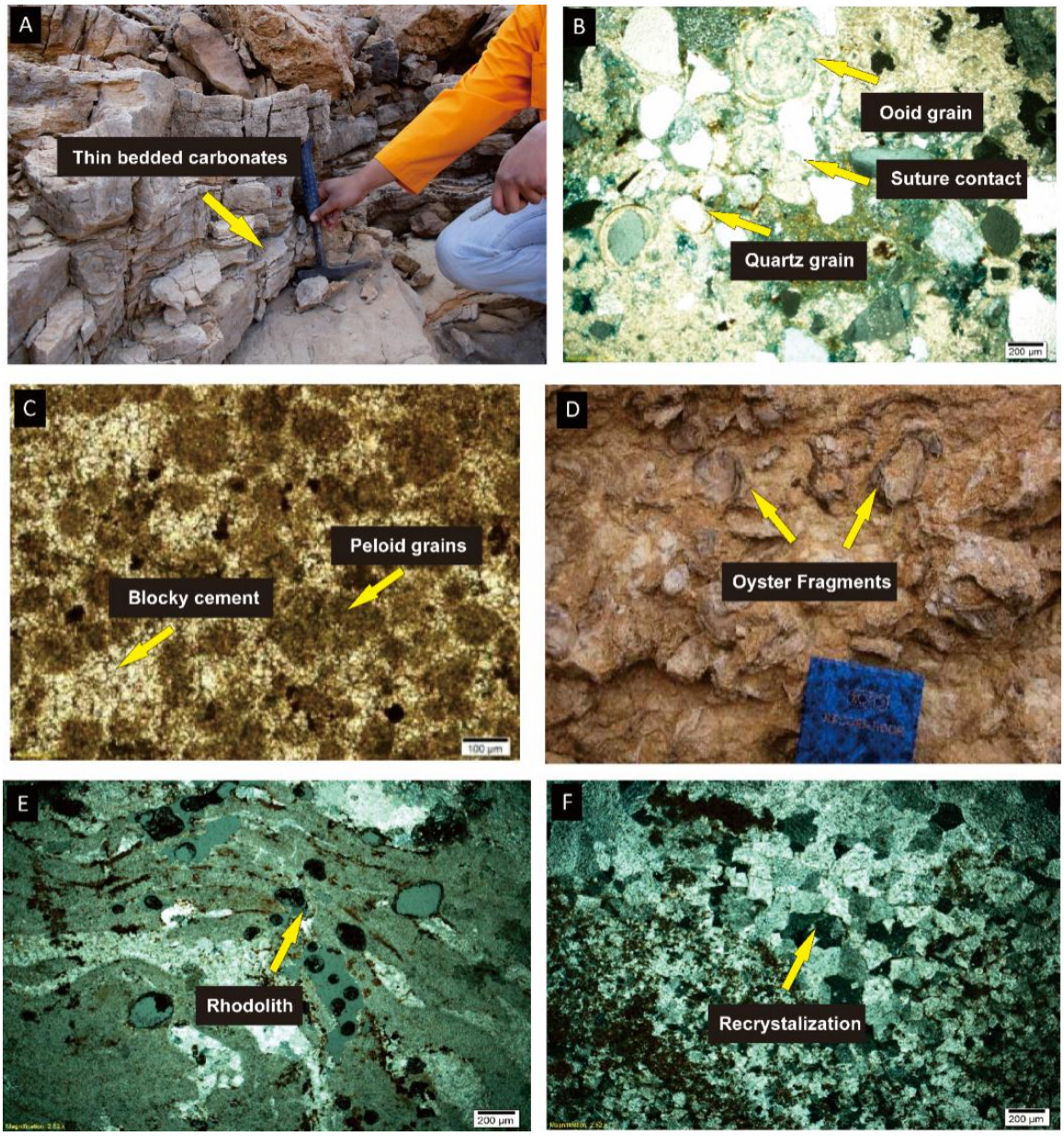

Figure 3.3 Macro- and microscopic features of Musayr Formation facies. **(A)**. Well bedded grainstone succession, comprise of oolitic grainstone and thin bed of peloidal grainstone **(B)**. Ooilitic grainstone (XPL). The nuclei consist of quartz grains with subrounded-rounded shapes. Suture contacts between quartz grains and ooids are commonly observed

in this facies (red arrow) and suggest deep burial and/or chemical compaction. **(C)**. Peloidal grainstone-packstone (XPL; arrow), found associated with ooid grainstone. **(D)**. Oyster rudstone, likely formed as a product of storm processes which indicated by the abundance of oyster fragments (allochtonous). **(E)**. Rhodoliths, commonly found as fragments and an encrusting agent on the skeletal and non-skeletal grains. **(F)**. Recrystallized matrix within oyster-rich rudstone.

Facies Association 3 (FA3): Middle Ramp

This facies association is composed of five lithofacies (F7 to F11; Table 3.1). Oyster rudstone and floatstone (Fig. 3.3D) facies were observed at both study locations. The oyster shells were found broken and fragmented, suggesting that the oysters were reworked and transported from their origin further upslope to this inferred middle ramp environment. The bioclastic-rhodolithic packstone is dominated by gastropods, bivalve fragments, large benthic foraminifera *(Miogypsina sp* and *Miogypsinoides sp)* and rhodolithic fragments (Fig. 3.3E), with some minor intraclasts. This facies was observed in the field as a well-bedded package and associated with the oyster-rich rudstone/floatstone facies. Two lithofacies, F10 and F11 are mostly dominated by mud-supported limestone, namely bioclastic and micritic wackestones (Fig. 3.3F).

Depositional Architecture

The eleven lithofacies described in Table 3.1 are collectively characterized by laterally extensive continuity of facies over hundreds of metres and by the absence of wave-resistant reef frameworks at the studied outcrops. Thus, this study infer that deposition of the Musayr Formation occurred on a storm-dominated, hangingwall dip-slope carbonate ramp,

which is observed to deepen toward the east (Fig. 3.4). The Musayr Formation does not exhibit an outer ramp environment towards the basin, instead passing directly into shallow to progressively deeper marine siliciclastics to the east, which can be ascribed lithostratigraphically to the Burqan Formation. Generally, the Musayr Formation represents the first major marine incursion into this segment of the Red Sea rift basin. The carbonate parasequences of the Musayr Formation are revealed by a repetitive pattern of shoaling and an abrupt flooding surface. Overall, parasequence stacking patterns at the studies outcrops show aggradational to slightly progradational parasequence sets within an inner to middle ramp environment.

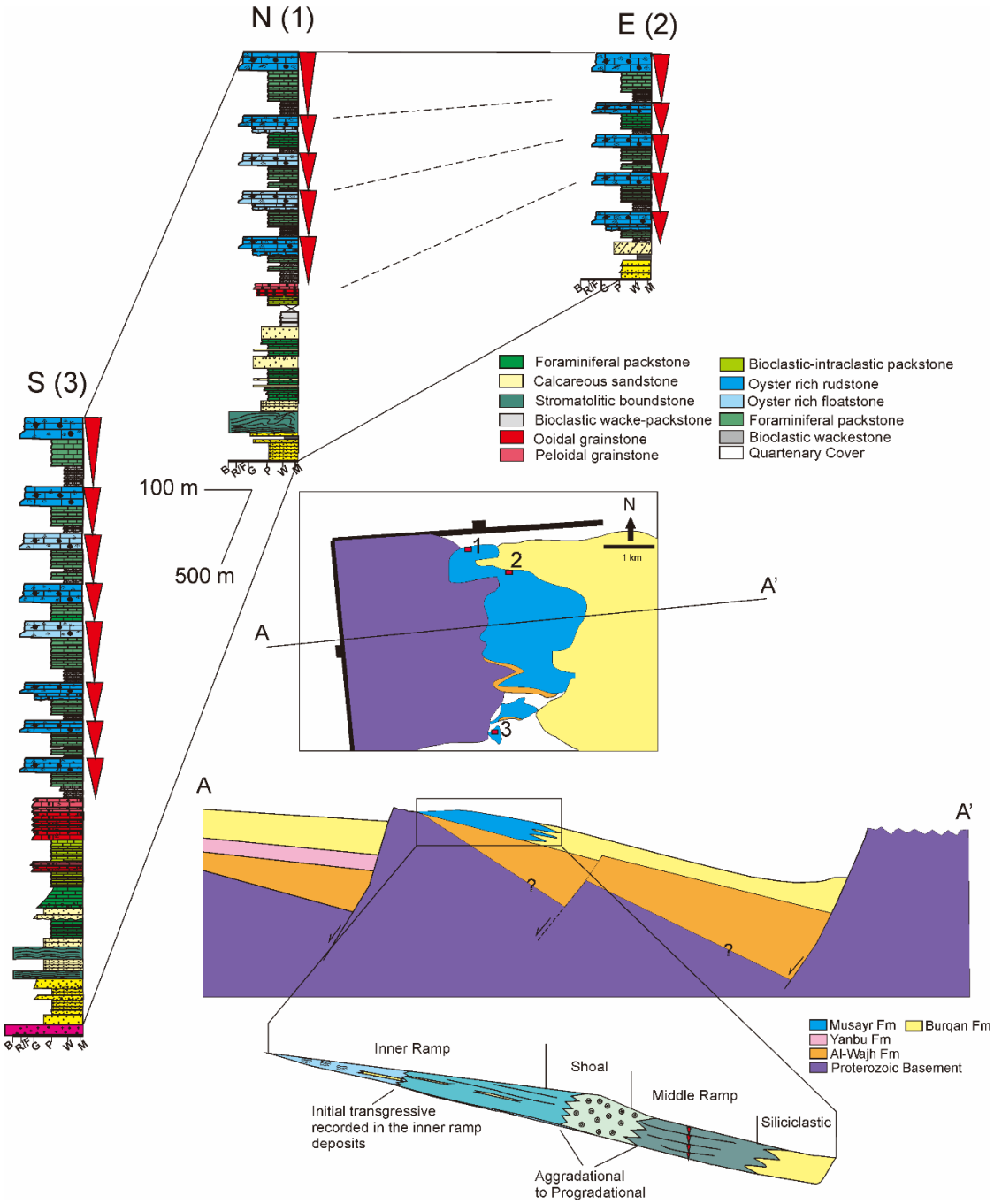

Figure 3.4 Depositional architecture of Musayr Formation showing hangingwall dipslope carbonate ramp that passed into siliciclastic towards the basin. Please note that the aggradational to progradational stacking patterns are observed in the shoal and middle ramp environment whereas the initial transgression is recognized only in the inner ramp environment.

Table 3.1 Musayr lithofacies descriptions and its interpreted depositional environments.

Lithofacies code	Lithofacies	Facies Association	Description	Porosity type	Hydrodynamic energy	Depositional environment
F1	Foraminiferal packstone	FA1	Typically found interbedded with calcareous sandstone. Composed mostly of miliolids foraminifera (*Quinqueloculina spp*) and other skeletal fragments, such as bivalves and gastropods.	Intergranular, Intragranular	Low	Lagoon to protected inner ramp. RMF[2] 16, RMF[2] 20
F2	Calcareous sandstone	FA1	Composed of mostly quartz and plagioclase grains. The grains are subangular to subrounded. Lenses of pebbles are commonly associated with this facies. Burrows are common. Cross-stratification found in some cases.	Intergranular, Fracture	Moderate to High	Intertidal
F3	Bioclastic wacke-packstone	FA1	Normally graded and well stratified. Composed of a mixture of skeletal fragments, such as rhodoliths, foraminifera, gastropods, and bivalves. Intensive micritization and poorly sorted.	Intergranular, Fracture	Low to Moderate	Open inner ramp, RMF 14
F4	Stromatolitic boundstone	FA1	Common fenestral fabric. Most of the grains are recrystallized.	Fenestral	Low to moderate	Peritidal to intertidal RMF 24
F5	Ooidal grainstone	FA2	Well stratified and extensive lateral continuity. Well sorted ooid grains with concentric cortex arrangements. The nuclei are mostly composed of quartz fragments. Suture grain contacts are a common feature in this facies	Intergranular, Intragranular	High	Shallow subtidal shoals above fair weather wave base SMF[1] 15-C, RMF 29
F6	Peloidal grainstone	FA2	Typically found associated with ooidal grainstone. Massive and with lime mud pellets, micritic intraclasts, variable amounts of silt-sized quartz, minor bioclasts (gastropods, brachiopods). Intensive recrystallization and isophachous blocky cements.	Intercrystalline porosity	Moderate	Shallow subtidal setting, behind the shoal, RMF 30

F7	Bioclastic-rhodolithic packstone	FA3	Normal grading, mostly composed of various bioclast fragments (benthic foraminifera, rhodoliths) and intraclasts. Intensive bioturbation.	Intergranular	Moderate to High	Agitated middle ramp, below fair weather wave base. RMF 8
F8	Oyster floatstone	FA3	Typically found associated with the rudstone and bioclast-intraclast packstone facies. Floating oyster fragments within packstone matrix.	Intergranular, vuggy	High	Storm-influenced middle ramp setting below the fair weather but above storm wave base. RMF 8, RMF 9
F9	Oyster rudstone	FA3	Typically found associated with the floatstone facies (F8). Oyster fragments more dominant, matrix <10%. Planar to low angle cross stratification.	Intergranular, vuggy	High	Storm-influenced middle ramp setting below the fair weather but above storm wave base. RMF 8, RMF 9
F10	Foraminiferal packstone	FA3	This facies mostly comprise ramp-derived fragments. Abundant benthic forams (*Miogypsina sp*) and minor bioclasts (bivalves, gastropods) characterize this facies.	Intergranular	Moderate to High	Deposited by strong currents or waves induced by storms. RMF 9
F11	Bioclastic wackestone	FA3	Diverse fossil content and abundant micrite. Associated with the oyster rudstone and found commonly at the base of cycles. Bioturbation is observed in this facies.	Intergranular	Low	Outer ramp, deposited below storm weather wave base. RMF 3, SMF 9

[1]SMF = standard microfacies type based on Wilson (1975) and Flügel (1972, 1982)

[2]RMF = ramp microfacies type of Flügel (2004).

3.1.2 Wadi Waqb Member at Wadi Waqb

The Wadi Waqb location is located in the southern part of the Midyan Peninsula (Figs. 2.1 and 2.2). It represents an uplifted and rotated footwall margin carbonate platform (Fig. 3.5). This area is surrounded by younger evaporite deposits of the Kial and Mansiyah formations. Twelve lithofacies were identified in the Wadi Waqb member (see Table 3.2).

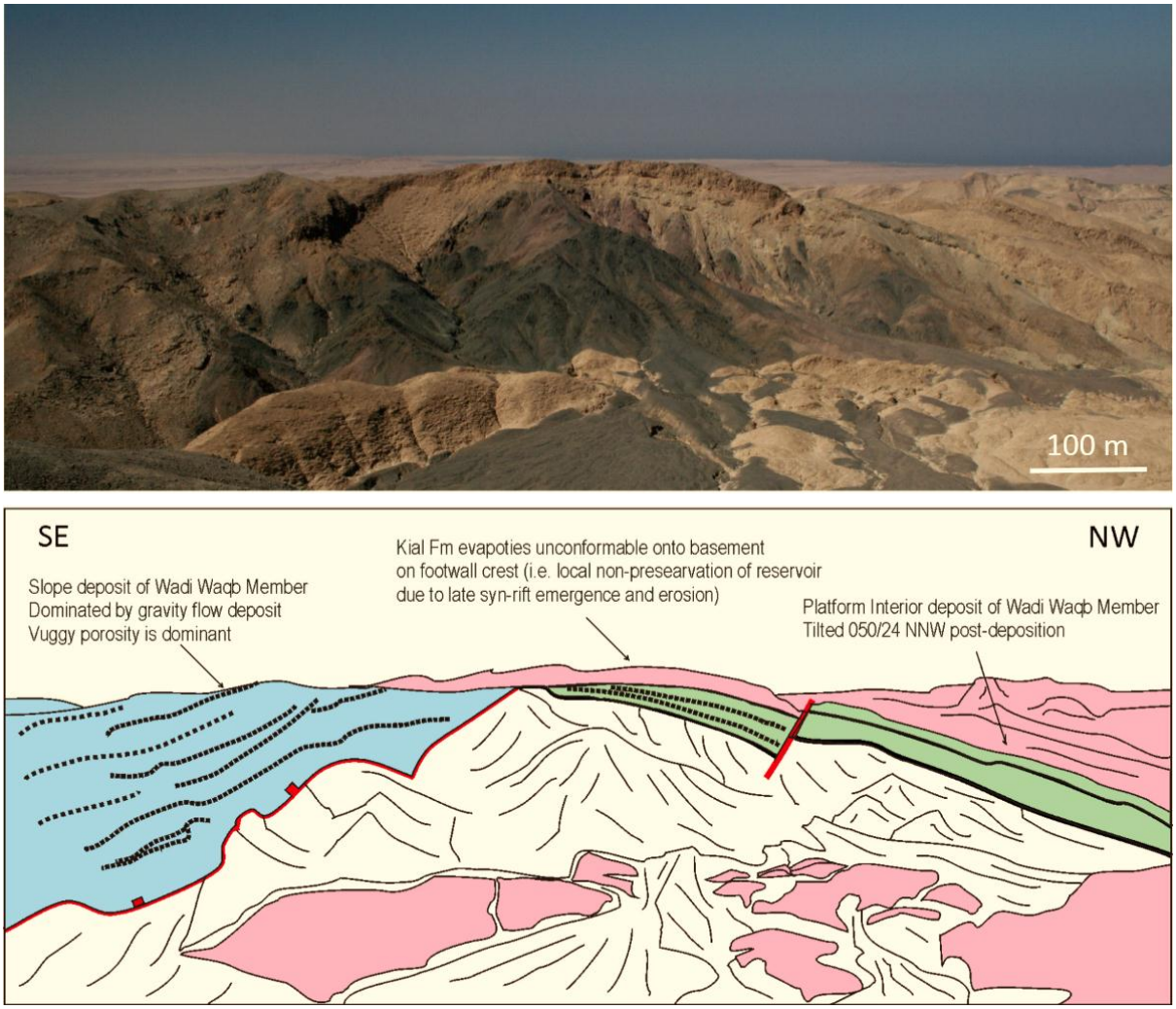

Figure 3.5 Field-view of approximately 700 m long, isolated late syn-rift carbonate platform of the Wadi Waqb member at the Wadi Waqb locality. This shows that Wadi Waqb member was deposited unconformably on top of the basement.

Facies Association 1 (FA1): Platform Interior

Five different lithofacies (C1 to C5) comprise the first facies association identified in this study of the Wadi Waqb member. They occur on the platform-top and consist of bioclastic wackestone, cross-bedded to wavy-bedded packstones, foraminiferal grainstone, bioclastic rudstone, and microbial boundstone (Fig. 3.6). This facies association is characterized by the presence of in-situ sand dollars in the basal sandstones and stromatolitic boundstones at the top of the succession (Figs. 3.7A and B). The presence of cross-bedded and wavy-bedded packstones (C2) are also observed in the middle part of the succession. The presence of well-cemented rudstone comprising colonies of coralline red algae (rhodoliths) and corals is one of the most characteristic features of this facies association.

Facies Association 2 (FA2): Upper Slope

Well-bedded rhodolithic grainstones, rudstones, and wackestones are dominant in the upper slope and correspond to facies E1 to E3 in Table 3.2 (Fig. 3.8). This facies association is dominated by repeated packages of rhodolith-rich grainstone (facies E3). The steep geometry of bedding, relatively small skeletal fragments, and the predomination of grain-flows suggest an upper slope environment (Wilson, 1975). The abundance of resedimented rhodolith spheres (> 5 cm), which are more abundant compared to the middle-lower slope environment, is one of the main characteristics of this facies association (Fig. 3.7C).

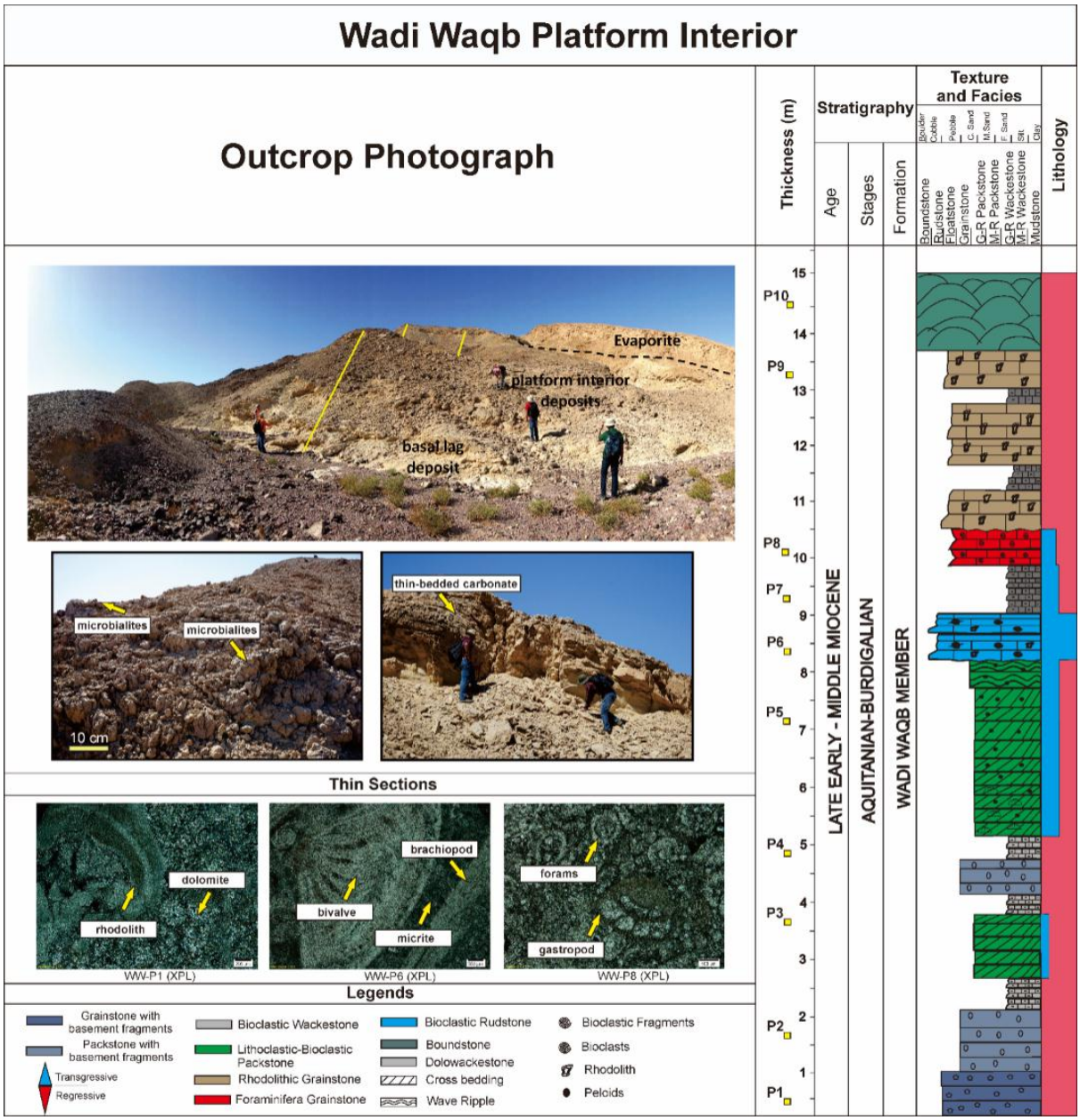

Figure 3.6 Sedimentary section measured in the platform interior of Wadi Waqb platform. The main features of this section are the presence of siliciclastic-rich carbonate in the lower part and microbial laminites in the upper part.

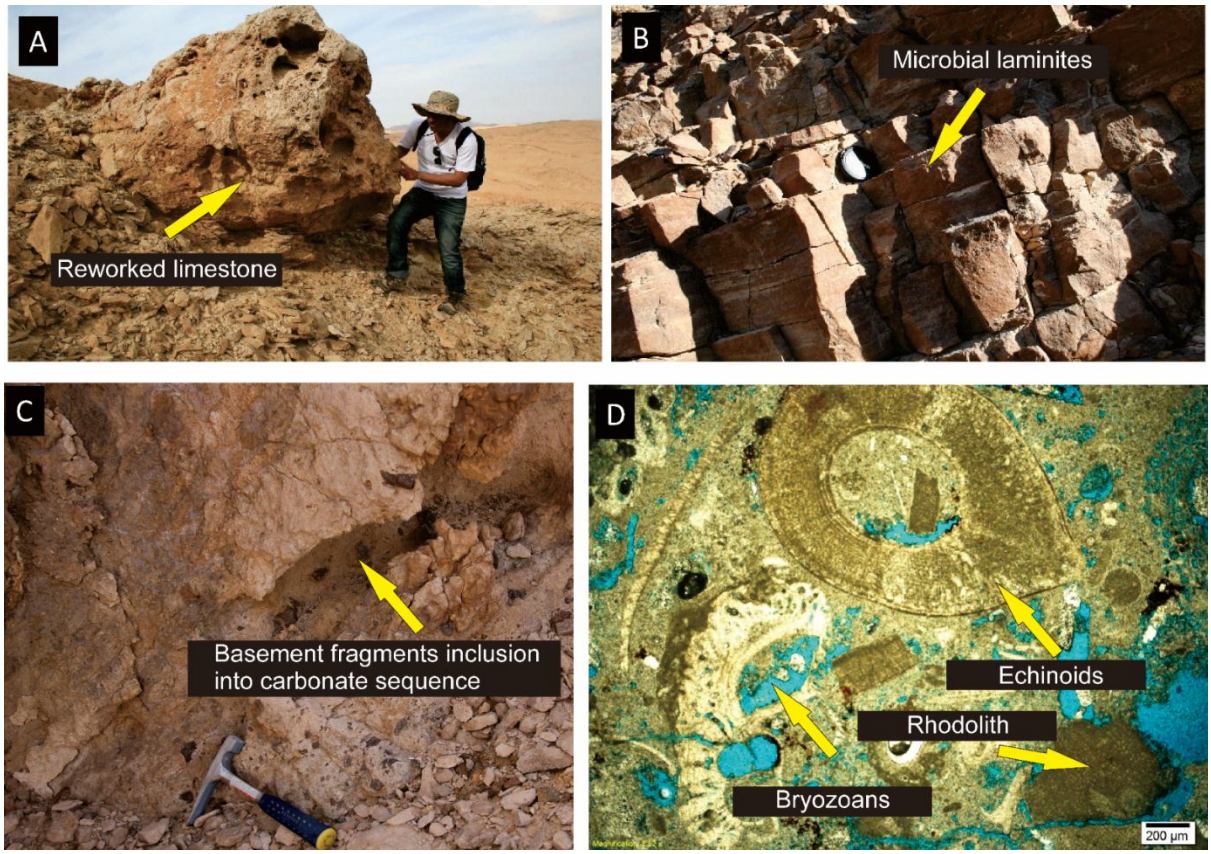

Figure 3.7 Macro- and microscopic features of Wadi Waqb member facies. **(A).** Reworked boulder of carbonate with vuggy porosity found in the platform interior. **(B).** Microbial laminites with planar shapes that found in the most upper part of the platform interior section. **(C).** Inclusion of basement fragment in the rhodolitic grainstone facies in the upper slope environment. **(D).** Bioclastic packstone with abundant intragranular and moldic porosities characterized the matrix of bioclastic rudstone recognized in the middle slope enviromment.

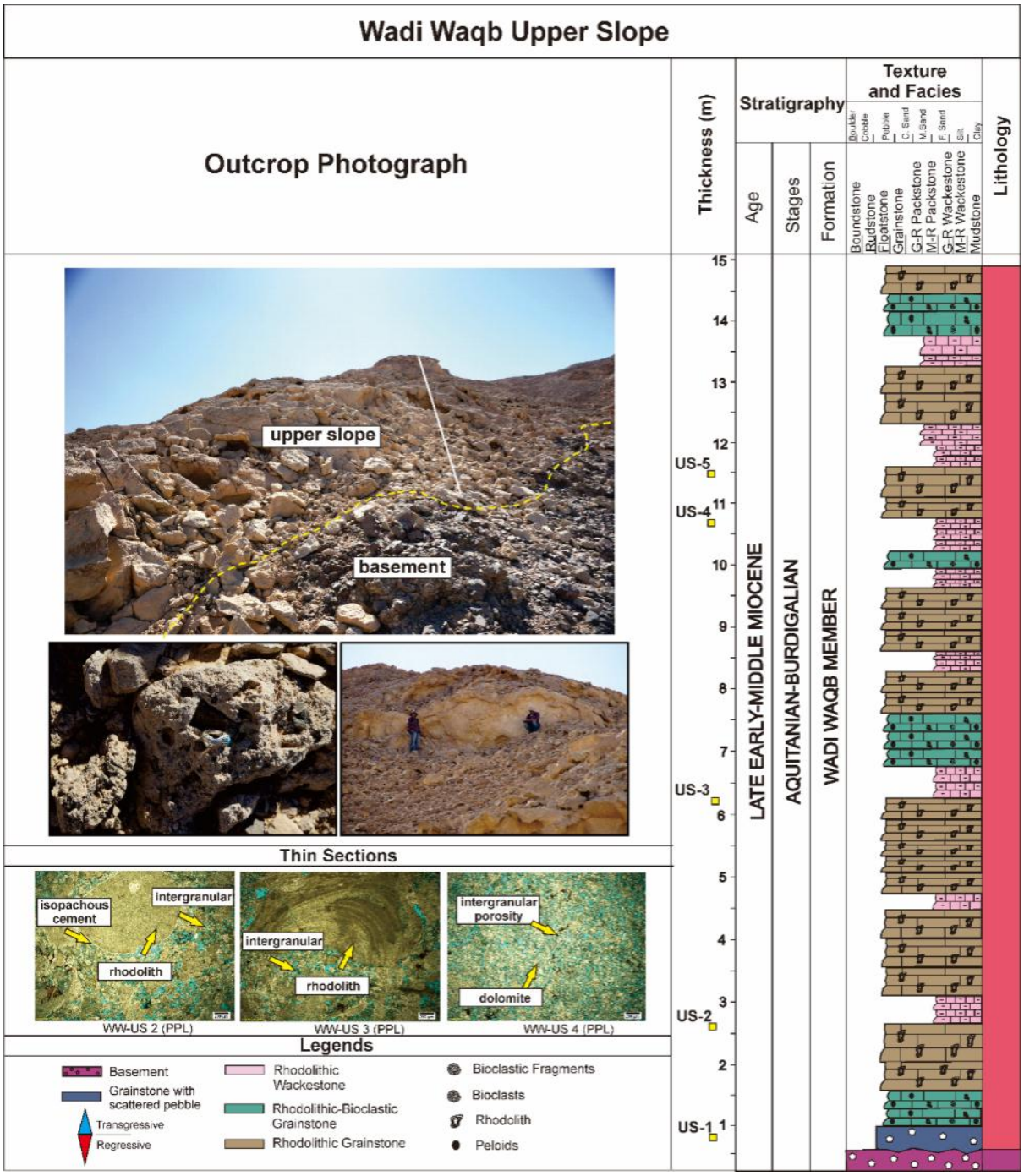

Figure 3.8 Sedimentary section measured in the upper slope of Wadi Waqb platform. The main features of this section are the presence of basal-lag transgressive sequence in the lower part and rhodolitic-rich carbonate throughout the section.

Facies Association 3 (FA3): Middle Slope

This facies association contains packstones, grainstones, and rudstones (F1 to F5, Table 2) that are composed of reworked materials from the platform margin (Fig. 3.9). The most common skeletal components are corals and rhodoliths, while other bioclasts, such as benthic foraminifera, bivalves, green algae, and gastropods are also common (Fig. 3.7D). The most characteristic feature of this facies association is the presence of outsized coral fragments and rhodolith spheres. The steeply bedded carbonate (>40°) is observed and characterized the middle slope section and is consistent with reworking of carbonate clasts off the structural platform by gravity flows (Fig. 3.9).

Depositional Architecture

The stratigraphy and depositional architecture of the Wadi Waqb member platform are presented in Figure 3.10. As described in the results section, these facies represent a series of platform interior and slope deposits. The Wadi Waqb carbonate platform is characterized as an isolated carbonate platform with steep, fault-bounded slopes. The major break in slope and the abundance of coral fragments in the slope deposits may suggest the presence of a wave-resistant reef margin that was dominated by tropical corals (e.g. *Scleractinians*). This characteristic geometry of tropical carbonate accumulation is directly related to the production and reworking of carbonate detritus. The slope deposits were likely developed as a result of earthquake-triggered slope collapse in combination with storm wave-generated gravity flows. The presence of post-depositional faults in the slope part are also prominent which characterized by the drop down of carbonate blocks and cut through the whole carbonate sequence.

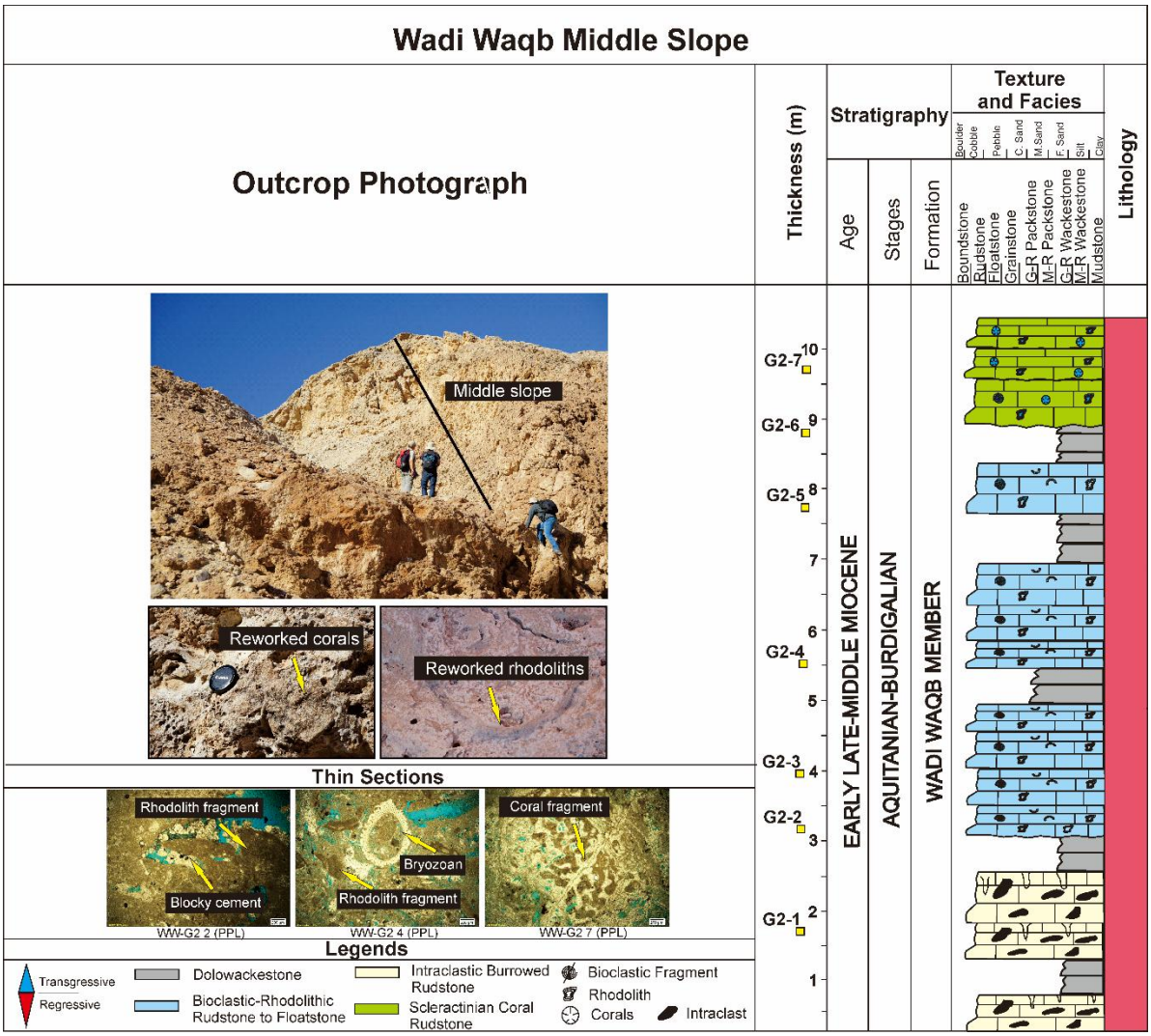

Figure 3.9 Sedimentary section measured in the middle to lower slope of Wadi Waqb platform. The main feature of this section is the presence of abundant of coral fragments with increasing abundancy towards the lower slope.

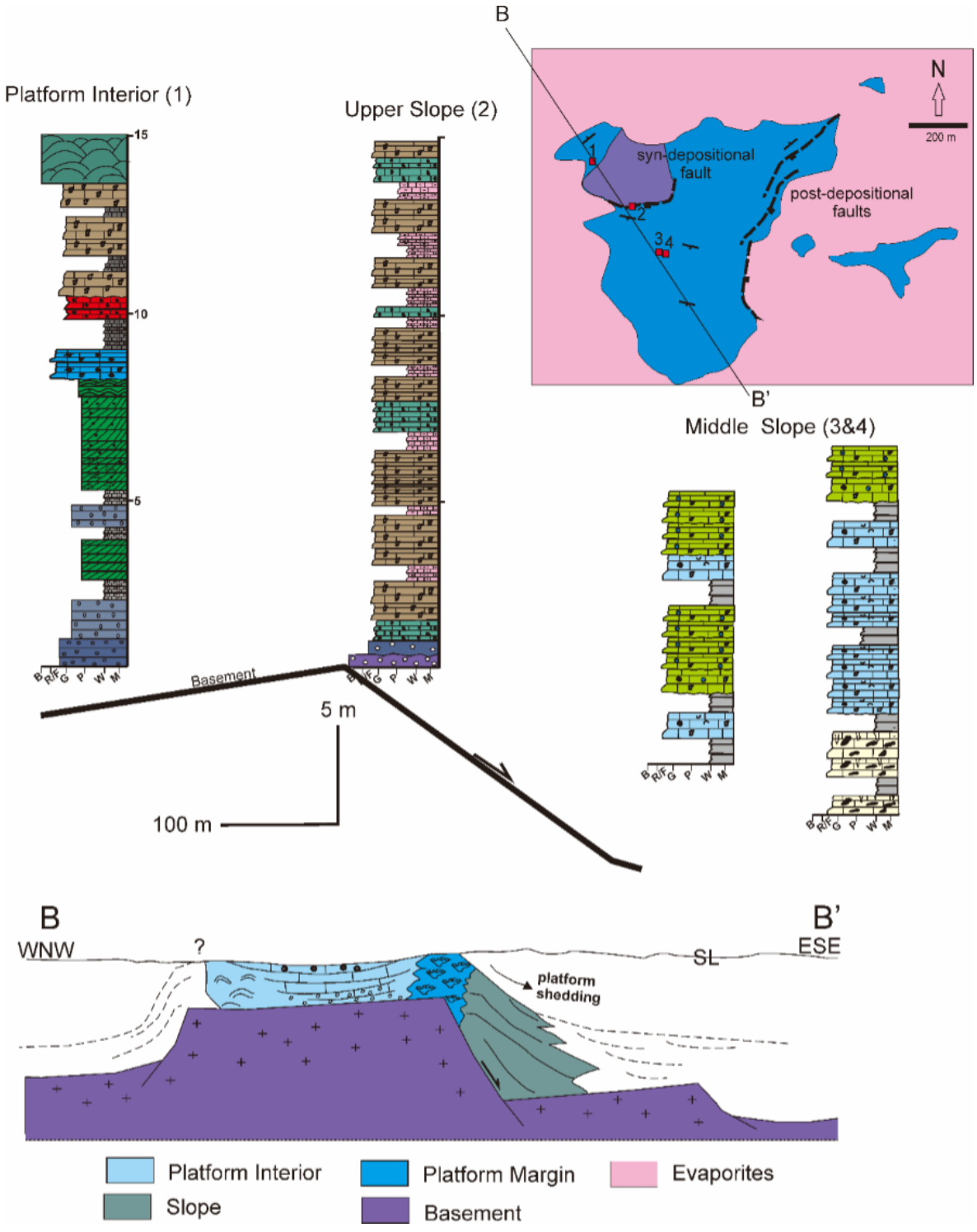

Figure 3.10 Isolated carbonate platform of Wadi Waqb member in Wadi Waqb locality. Thick slope deposits and absence of cycles may suggest active tectonic condition during the time of deposition. The syn-depositional fault is observed at the contact between the basement and carbonate sequence that shows thickening of strata towards the fault boundary.

3.1.3 Wadi Waqb Member at Ad-Dubaybah

Ad-Dubaybah is located in the eastern part of the Midyan Basin, against the rift shoulder (Figs. 2.1 and 3.11). It represents a carbonate platform developed on the upthrown side of the tip of one normal fault, in the zone of overlap with respect to the next rift-margin fault to the north. The normal fault-bounded platform was subsequently separated structurally from the rift footwall, when a hard-linked relay zone joined the two normal fault segments. Three facies associations are recognized based on the presence of twelve different lithofacies (Table 3.2).

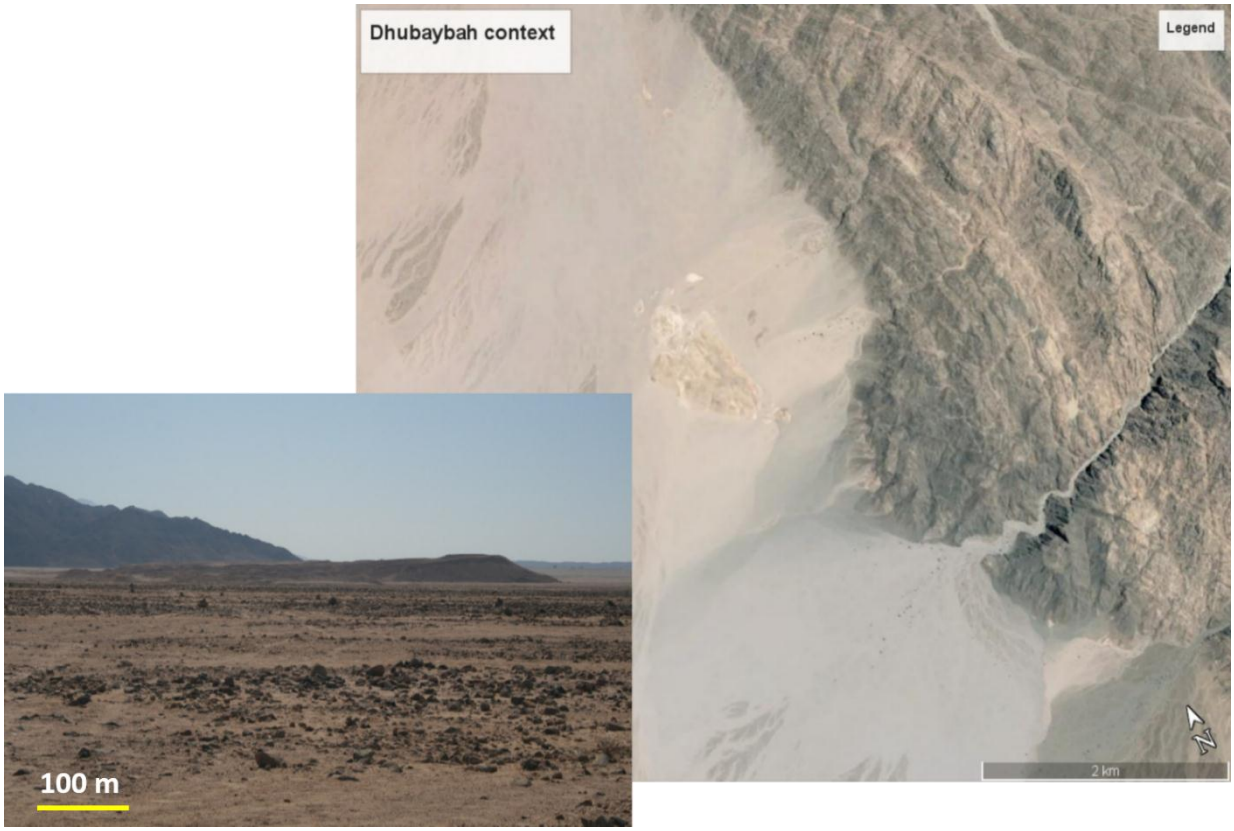

Figure 3.11 Field photograph and satellite image showing the geometry of Ad-Dubaybah locality where it is located adjacent to Proterozoic basement complex. The three dimensional outcrop of this carbonate sequence allow a detail stratigraphic architecture to be inferred.

Facies Association 1 (FA4): Beach to Intertidal Complex

The first facies association in the Wadi Waqb member here comprises facies A1 to A5, as detailed in Table 3.2. It is interpreted as a beach to intertidal complex, composed of conglomerate, conglomeratic sandstone, calcareous sandstone, seismites, and planar cross-bedded sandstone (Figs. 3.12 ands 3.13A and B) This association of facies is only present at the Ad-Dubaybah locality of the Wadi Waqb member. An extensive deformed and contorted calcareous sandstone also known as seismite is observed in the lower part of the section (Fig. 3.13C. Finally, extensive planar cross-bedded sandstones (A3) may represent subaqueous dunes in this upper shoreface zone. An oolitic grainstone facies (G1) (Fig. 3.13D) generally caps the facies association at the Ad-Dubaybah locality. Intertidal environment is mainly characterized by the occurrence of stromatolite and intensive burrowed sandstones (Fig. 3.14).

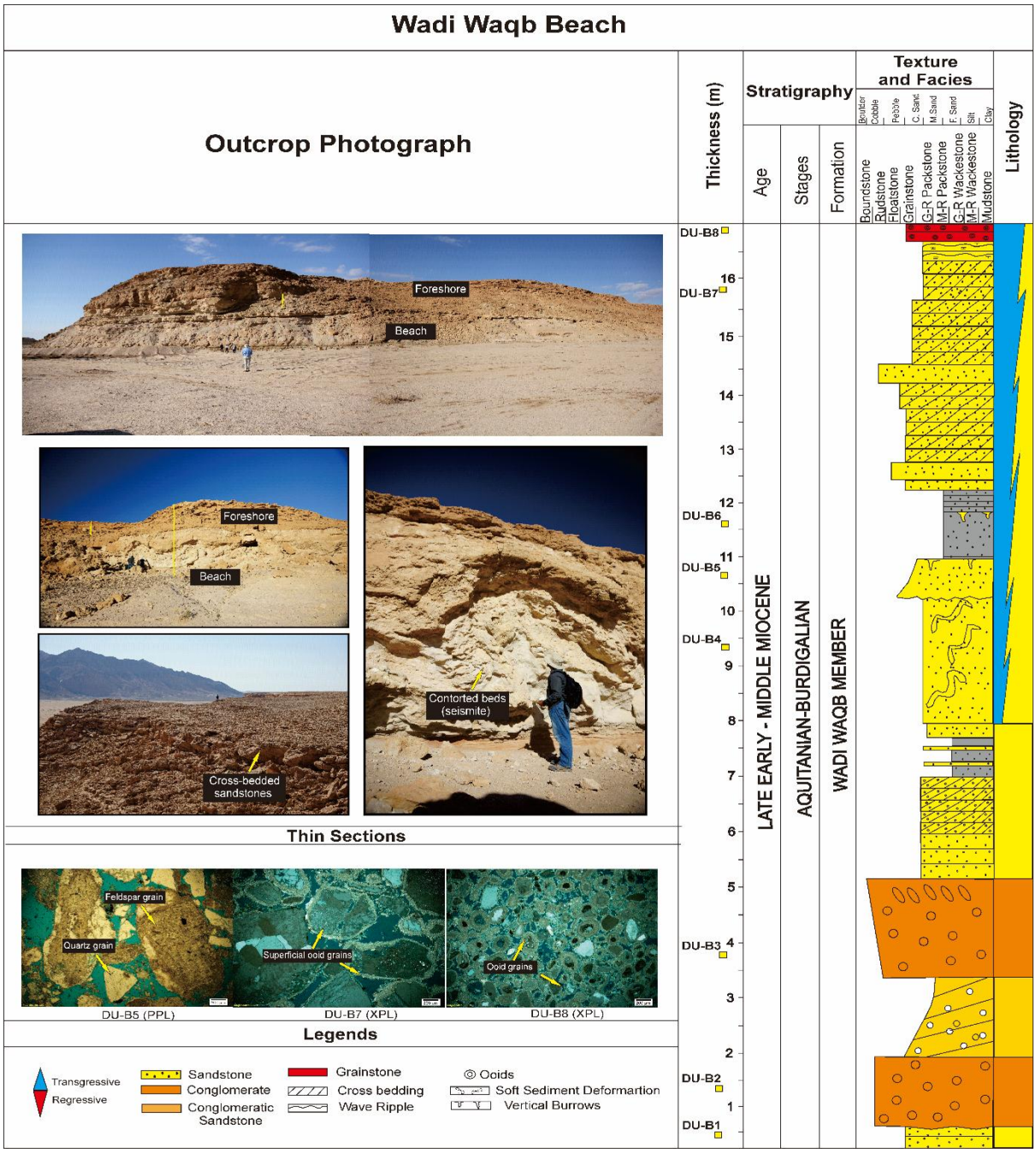

Figure 3.12 Stratigraphic section of the beach-foreshore subenvironment in the Ad-Dubaybah platform. The section is characterized by beach conglomerates in the lower part and cross-bedded sandstones in the middle part then capped by oolitic grainstones.

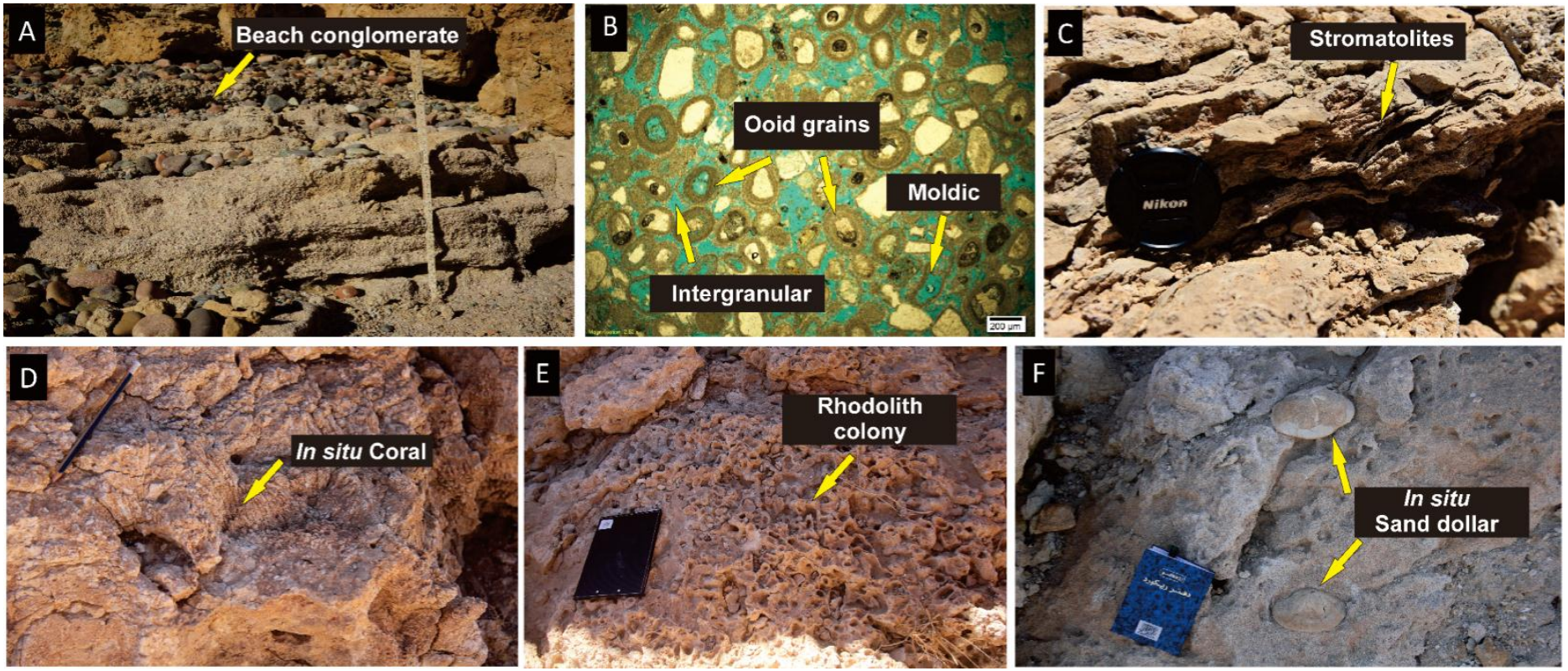

Figure 3.13 (A). Conglomeratic sandstone facies, found in the basal part of Wadi Waqb member succession in Ad-Dubaybah locality. **(B)**. Ooidal grainstone with concentric cortices and nuclei primarily composed of basement-derived fragments (PPL). **(C)**. Stromatolite boundstone facies showing clear laminations. **(D)**. In situ corals deposited in the original living position, surrounded by detrital limestone and siliciclastics. **(E)**. Well cemented rudstone comprises of rhodolith colony. **(F)**. *In situ* echinoids (sand dollars) mostly recognized in the lower part of platform interior.

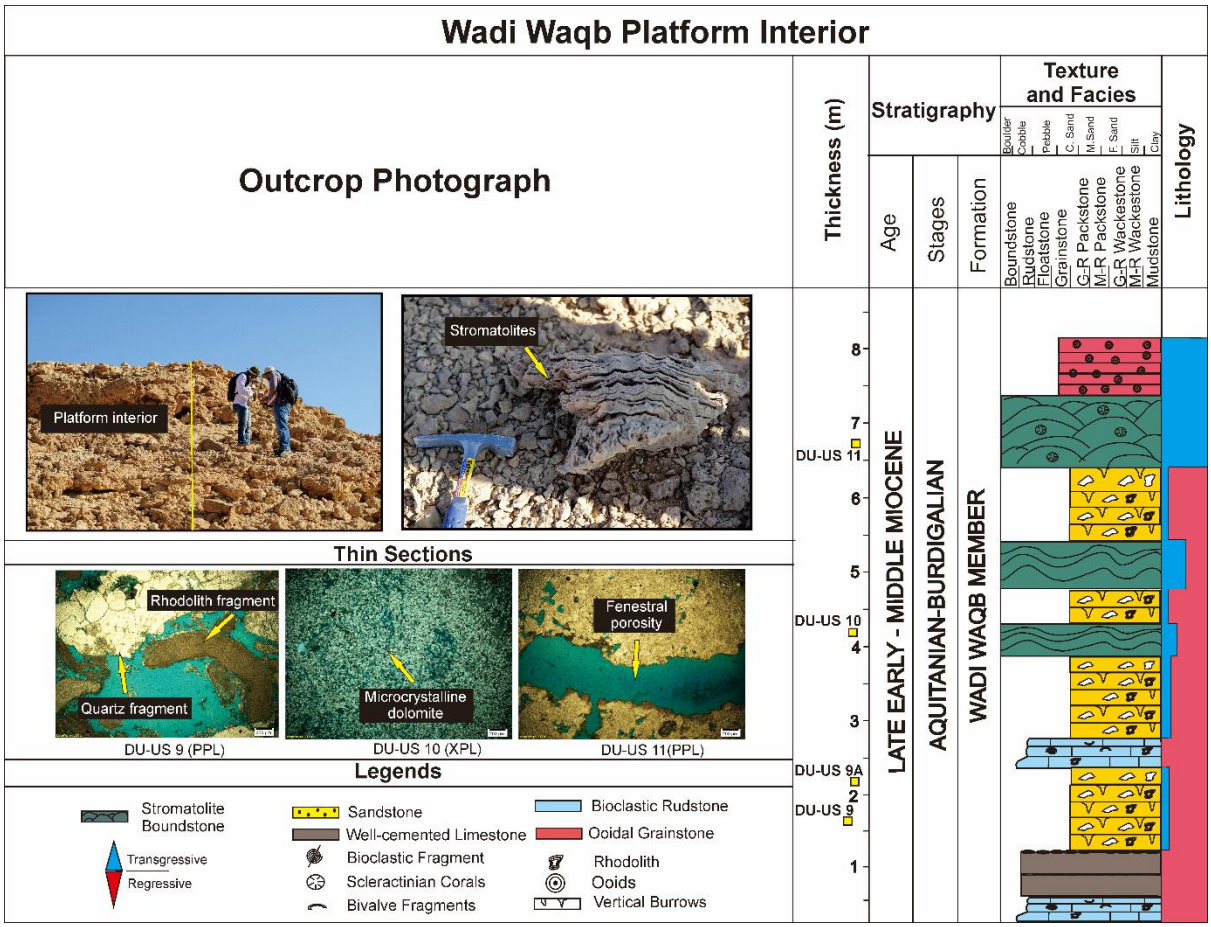

Figure 3.14 Sedimentary section measured in the intertidal environment of Ad-Dubaybah location. The main feature of this section is the presence of interbedded between siliclastic and stromatolites with grainstone cap.

Facies Association 2 (FA5): Constructed Reef Framework

Facies D1 and D2 collectively describe a constructed reef framework facies association dominated by coral boundstone and bioclastic packstone facies, alternating with calcareous sandstone (Fig. 3.15). Where they occur, corals (*Sclerectinians* and *Porites sp*) are observed in the living position, indicating that they remain in situ (Figs. 3.13E and F). The bioclastic packstone consists primarily of red algae and fragments of bivalves.

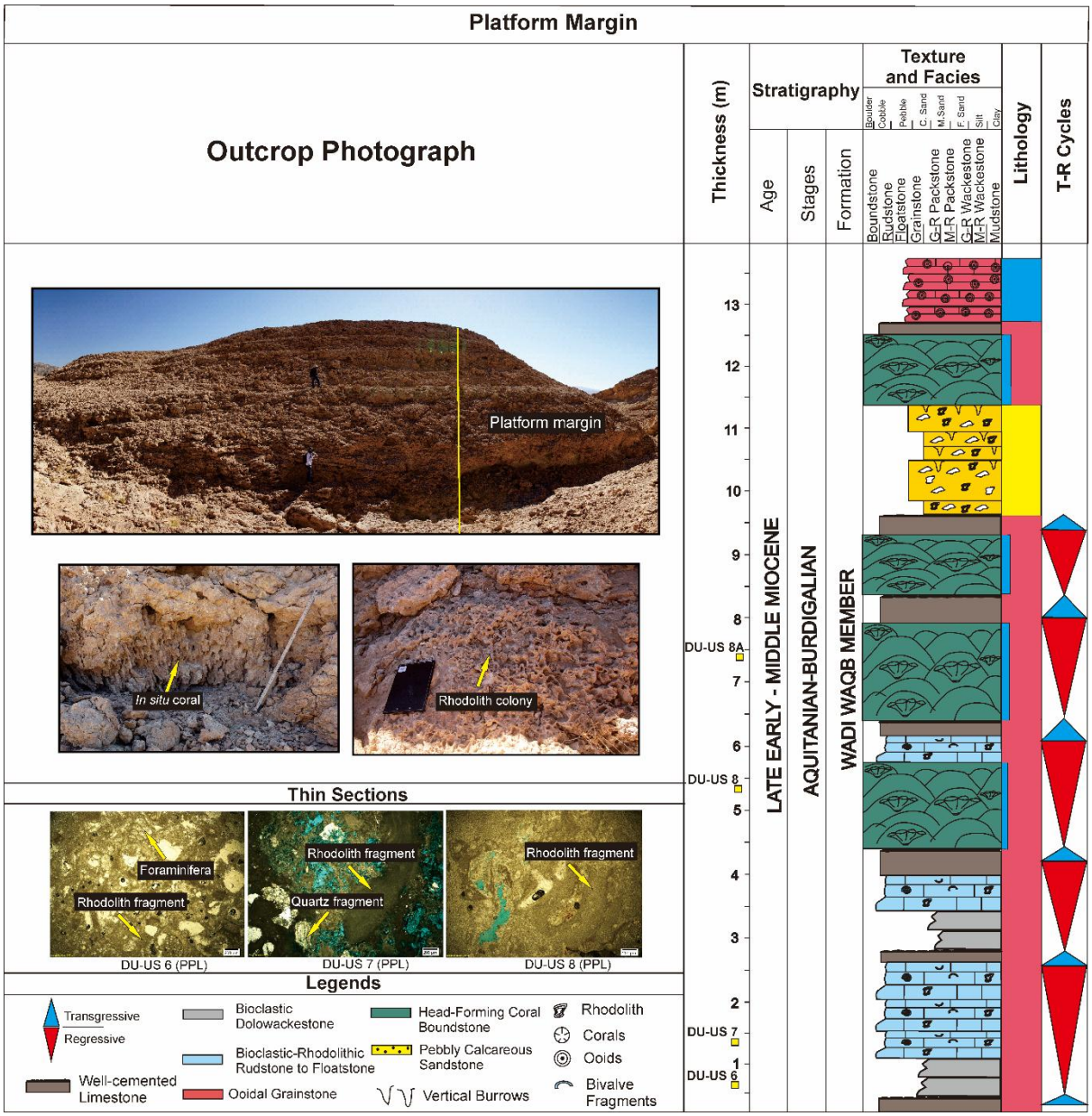

Figure 3.15 Sedimentary section measured in the platform margin environment of Ad-Dubaybah platform. The main feature of this section is the presence of in-situ corals.

Facies Association 3 (FA3): Upper Slope

This facies association is dominated by bioclastic- and rhodolithic-rich rudstones (Fig. 3.16). It comprises of three different lithofacies (F1 to F3; Table 3.2). Similar features of slope characteristics observed in the Wadi Waqb locality are also recognized here, such as steeply

bedded carbonates with outsized clasts. The bedding geometries reveal clinoform packages, divided by well-cemented dolostone surfaces. Based on the rock textures, this facies association was produced mostly by gravity flows.

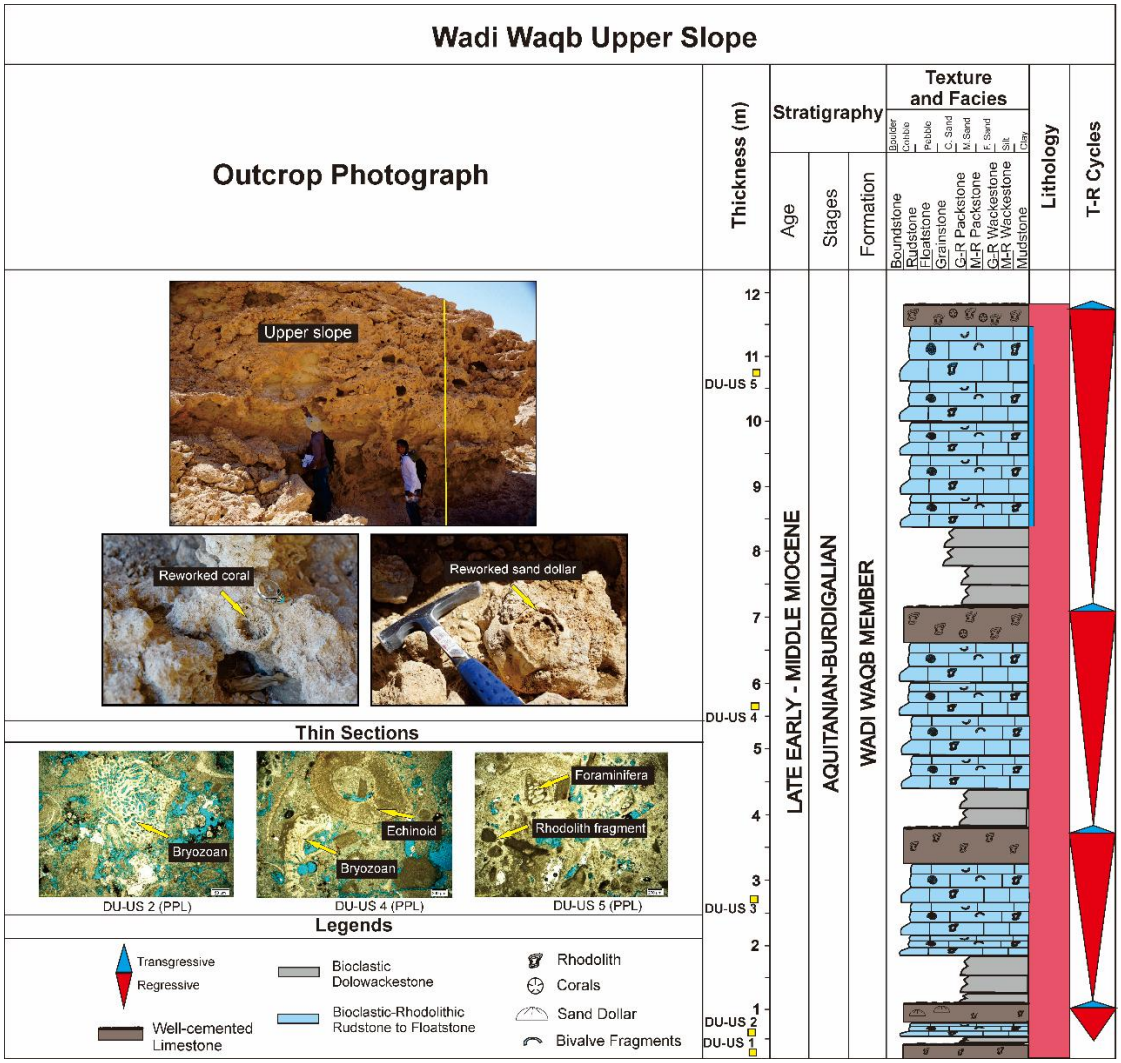

Figure 3.16 Sedimentary section measured in the intertidal environment of Ad-Dubaybah platform. The main feature of this section is the presence of bioclastic rich rudstone capped with well cemented rudstone. Shallowing upward sequences are readily recognized in this section.

Depositional Architecture

Based on the spatial lithofacies distribution, the Ad-Dubaybah carbonate platform represents an attached, fault-bounded, rimmed shelf located within the fault transfer zone. The occurrence of siliciclastic-dominated sequences in the platform interior suggests significant silicilastic input during the depositional period. However, siliciclastics rapidly disappear from east to west across the platform, implying that there was an eastwards depositional tilt across the platform. This allowed the siliciclastics to be trapped to the east of the platform and carbonate productivity and coral colonization to occur on the western crest of the platform. The repetitive, stacked, shallowing-upward parasequence pattern is recognized in the upper slope to platform margin environments, in an overall combined progradational-aggradational manner (Fig. 3.17). The parasequences are interpreted as the basic building blocks of the Wadi Waqb carbonate platform at this location. The presence of parasequence cycles varies laterally (east-west) across the platform (Fig. 3.17), probably due to differences in tectonic displacement rates and differing siliciclastic flux rates from platform crest to the sand fairway to its east. A key feature of this rift margin-attached platform is that the structural configuration allowed clastic sediments to be diverted around the platform high, such that carbonate productivity was maximized away from the clastic fairways (Fig. 3.17).

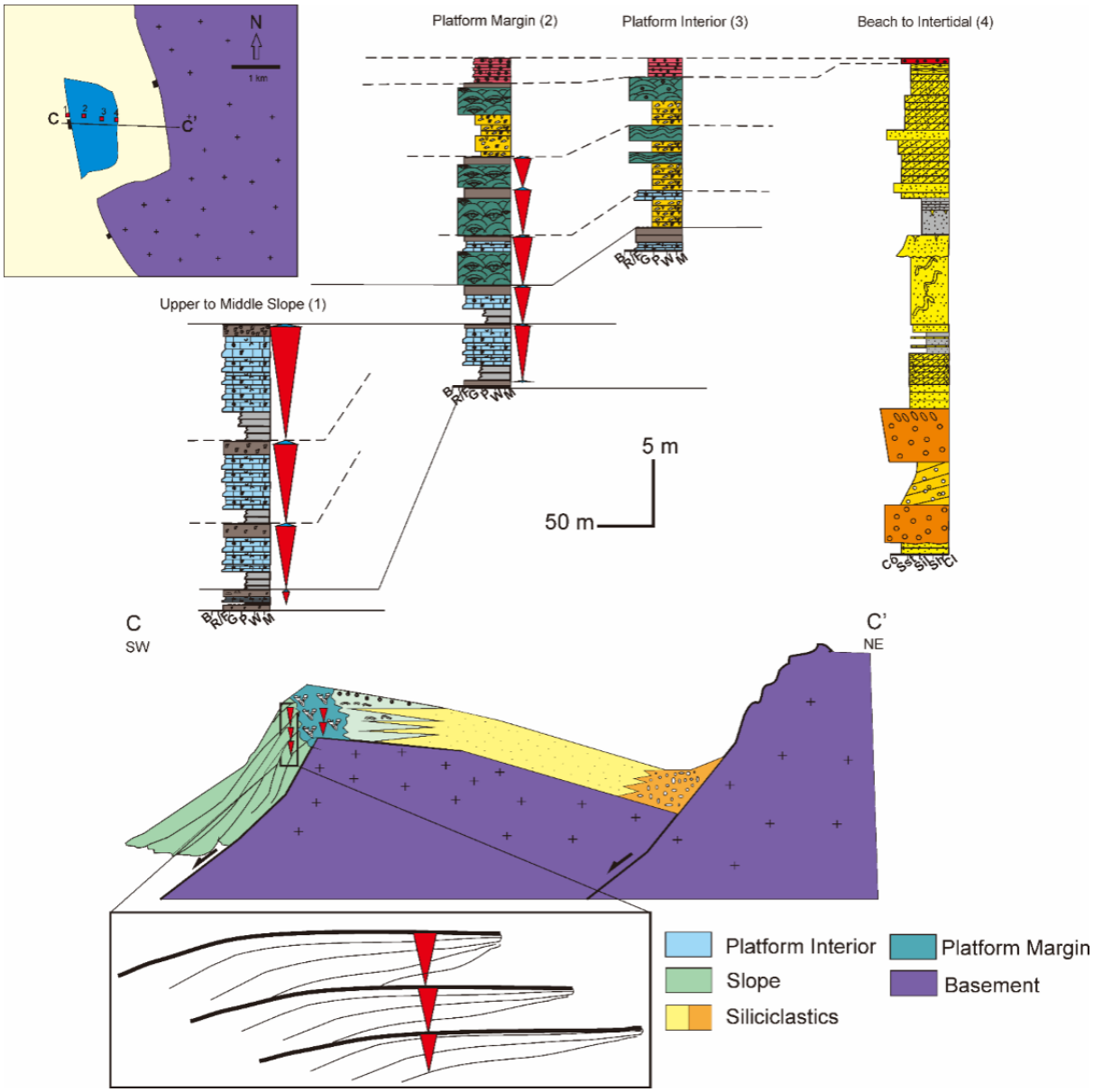

Figure 3.17 Attached rimmed shelves carbonate platform of Wadi Waqb member in Ad-Dubaybah locality. Please note that major part of the siliciclastic successions only observed in the proximal part of the platform with respect to the rift margin. The aggradation to progradation shallowing upward parasequences are recognized in the platform margin and platform interior part and create clinoformal features.

Table 3.2 Main features and interpretations of the Wadi Waqb carbonate facies from both localities.

Lithofacies code	Lithofacies	Facies Association	Description	Porosity type	Hydrodynamic energy	Depositional environment
C1	Bioclastic-peloidal packstone	FA1	Composed of bioclastic fragments (i.e., gastropods), rhodoliths, peloids and foraminifera, sutured grain contacts.	Intergranular	Moderate	Platform interior, open marine SMF 17, SMF 18, FZ 7
C2	Lithoclastic-bioclastic packstone	FA1	Composed of lithoclast fragments (glauconite?), a few rhodoliths and miliolid foraminifera, bryozoans, strongly dolomitized, (dolomitization post-date the grain)	Intergranular, intragranular	Low to Moderate	Platform Interior, open marine. SMF 17, FZ 7
C3	Bioclastic packstone-rudstone	FA1	Composed of bioclastic fragments (i.e., gastropods, brachiopods, bivalves, echinoids, barnacles), large benthic foraminifera (LBF), (nummulites?), rhodolith fragments, intraclast or burrows (?), planktonic foraminifera (?), intergranular and vuggy porosity, strongly dolomitized, calcareous green algae (*Dasyclads sp*)?, micritic envelope. Most of the grains were replaced by calcite/dolomite.	Intergranular, intragranular, vuggy	Moderate to High	Platform Interior, open marine. SMF 18, FZ 7
C4	Bioclastic wackestone	FA1	Mostly composed of bioclastics (i.e., echinoids, gastropods and benthic foraminifer's fragments), ghost fabric, intercrystal porosity, strongly dolomitized, and matrix selective dolomitization.	Intergranular, moldic	Low to Moderate	Platform Interior, restricted. SMF 9, FZ 8
C5	Foraminiferal packstone-grainstone	FA1	Abundance of planktonic and benthic foraminifera (rotaliid-ammonite), minor echinoids, gastropods, and rhodoliths, strongly dolomitized.	Intergranular, moldic, intragranular	High	Platform Interior, restricted. SMF 18, FZ 8
E1	Rhodolithic wackestone	FA2	Fine-grained carbonate, strongly dolomitized, intergranular porosity, iron-oxide filled pore space with patchy distribution, ghost grain fabric, dolomitization-enhanced porosity.	Intergranular	Low to Moderate	Upper slope, active wave agitation. SMF 5, FZ 4
E2	Bioclastic-rhodolithic rudstone	FA2	Primarily composed of rhodolith, bioclastic (brachiopods, barnacles, bivalves, echinoids, gastropods, bryozoans), LBF, miliolid foraminifera derived from lagoons, grain fracturing, iron oxide cement, matrix selective dolomitization	Intergranular, vuggy	High	Upper slope-Middle slope, below fair weather wave base. SMF 5, FZ 4

E3	Rhodolithic grainstone	FA2	Primarily composed of rhodolith fragments, strongly dolomitized, ghost fabric, fabric-destructive dolomite, stylolites, iron oxide cements, patchy distribution.	Intergranular	High	Upper Slope, Restricted platform interior. SMF 5, FZ 8
F1	Burrowed-intraclastic floatstone	FA3	Composed of intraclast and bioclast fragments, burrows filled with micrite, strongly dolomitized, ghost fabric, partial grain dissolution, iron oxide cement.	Intergranular, vuggy	Moderate to High	Middle slope, below fair weather wave base. SMF 4, FZ 4
F2	Bioclastic-rhodolithic floatstone	FA3	Primarily composed of rhodolith fragments, bioclasts (gastropods, echinoids, barnacles?, brachiopods, LBF, bivalves), miliolid foraminifera within lithoclasts, intergranular porosity, grain fracturing, peloidal cements, iron oxide cement, matrix selective dolomitization, dolomitization-enhanced porosity, patchy distribution of iron oxide filling pore space.	Intergranular, vuggy	High	Middle slope, below fair weather wave base. SMF 5, FZ 4
F3	Well cemented rudstone	FA3	Grain supported, well cemented of rhodolith colony and corals. Isopachous cement. Show a decreasing of rhodolith towards the platform interior	Intergranular, Moldic and Vuggy	Low	Platfrom interior to Slope
F4	Burrowed wackestone-packstone	FA3	Composed of intraclast and bioclast fragments, burrows filled with micrite, strongly dolomitized, ghost fabric, partial grain dissolution, iron oxide cement, scattered rhodolith spheres at the outcrop scale.	Intergranular	Low to Moderate	Middle to lower slope, below fair weather wave base. SMF 4, FZ 4
F5	Sclerectinian rudstone	FA3	Primarily composed of head-forming corals, partial dissolution lead to the creation of moldic porosity, bioturbation filled by micrite, minor bioclastic (echinoids) fragments.	Intragranular, vuggy, moldic	High	Middle to lower slope, below fair weather wave base. SMF 5, FZ 4
A1	Arkosic sandstone	FA4	Primarily composed of quartz, mica and feldspar grains, partial grain dissolution	Intergranular	Moderate	Intertidal channel. FZ 8
A2	Conglomeratic sandstone	FA4	Primarily composed of quartz, mica and feldspar grains, partial grain dissolution, cemented by calcite.	Intergranular	High	Intertidal, Beach. FZ 8
A3	Calcareous subarkosic sandstone	FA4	Primarily composed of quartz, mica and feldspar grains, partial grain dissolution, calcite cements.	Intergranular	Moderate	Intertidal. FZ 8
A4	Stromatolitic boundstone	FA4	Fine-grained carbonate, strongly dolomitized, siliciclastic grains.	Fenestral, intracrystalline	Low	Intertidal to low subtidal. SMF 20, SMF 21, FZ 8

A5	Boundstone	FA4	Fine-grained carbonate, rhodolith fragments, strongly dolomitized, intergranular porosity, iron-oxide filling the pore space with patchy distribution, ghost grain fabric, and dolomitization-enhanced porosity.	Intergranular porosity plugged by anhydrite	Low	Intertidal to shallow subtidal. SMF 20, FZ 8
G1	Ooidal grainstone	FA4	No micrite, quartz and basement derived fragments act as the nuclei, different cortex thickness (normal and superficial ooids). Cross-bedding and graded bedding less developed compared with facies C2 and C3.	Intergranular, intragranular	High	Shoal complex. Above fair weather wave base. SMF 15-M, FZ 6
D1	Coral boundstone	FA5	In-situ Scleractinian corals deposited in growth position. Detrital limestone filled the space between corals as a matrix. Associated with rudstone and calcareous sandstone.	Vuggy, moldic	Moderate	Rimmed, active wave agitation, above fair weather wave base, SMF 9, FZ 5
D2	Bioclastic wacke to packstone	FA5	Primarily composed of bioclastic fragments (i.e., gastropods) and rhodolith fragments, siliciclastic grains, pervasive dolomitization, grain dissolution filled by cement/micrite.	Intergranular, intragranular, moldic	Moderate	Rimmed, above wave base. SMF 11, SMF 9, FZ 5

[1]SMF = standard microfacies type based on Wilson (1975) and Flügel (2004)
[2]FZ = Facies zone based on Wilson (1975)

3.2 Diagenetic Characteristics

Detailed microscopic studies in thin section revealed several post-depositional alteration features in the Musayr and Wadi Waqb carbonates. These diagenetic processes are summarized below in the relative order of their formation. It includes: microbial micritization, cementation, compaction, neomorphism, dissolution, and dolomitization.

3.2.1 Microbial Micritization

Micritization is typically associated with microbial activity (i.e. borings) on the grain surfaces. Micritization is observed on most of the samples, on both skeletal (i.e., bivalve, gastropods, foraminifera) and non-skeletal grains, as thin micrite envelopes around skeletal grains, micrite patches, and within ooid cortices (Fig. 3.18A).

3.2.2 Cementation

Four different cement fabrics were identified in the carbonate samples: (i) isopachous cement, as the first generation of cement on the skeletal and non-skeletal grain rims, and in some cases growing on micritic envelopes as a nucleation substrate (as shown in Fig. 3.18B). (ii) Blocky cement, usually filling the pore spaces with euhedral and equigranular cements, considered the second cement generation. It forms by the dissolution of unstable to metastable skeletal grains because of newly introduced undersaturated diagenetic fluids (Fig. 3.18C). (iii) Drusy cement, observed in only a few samples as subhedral-anhedral cements with an average size of 0.1-0.5 mm. Subhedral-anhedral cement was always observed between the grains, filling the pore space and beginning as fine crystals near the grain surface, becoming coarser towards the center of the pore space (Fig. 3.18D). (iv) Dog-tooth cement, which was only found on a few samples, arranged perpendicularly from

the grain surfaces (using thin micrite envelopes as a substrate). The crystal size ranged from ten to hundred micrometers, with scalenohedral and rhombohedral shapes (Figs. 3.18E).

3.2.3 Dissolution

Dissolution of the carbonate grains and matrix is normally generated by diffusion and infiltration of $CaCO_3$-undersaturated fluids or intensive chemical compaction. It is observed in most of the carbonate samples where the metastable to unstable skeletal grain shells (i.e., gastropods and corals, Figs. 3.18H and I) and ooids are present. This process plays a significant role in the post-depositional modification of the samples, particularly in the creation of secondary porosities (i.e., moldic and vuggy).

3.2.4 Neomorphism

Based on Tucker and Wright (1990), neomorphism mostly occurs due to the availability of water through dissolution-precipitation processes, and results in changes to mineralogy. The petrography studies identified two different types of neomorphism in the samples. (i) Aggrading neomorphism, defined as the transformation from fine micrite to coarser calcite microspar patches or lenses. This type is mostly observed on mud-dominated lithofacies. (ii) Calcitization including replacement of aragonitic shells and cements by calcite. Evidence of this process is the presence of minute relics of bioclast shells in the form of neomorphic calcite, typically found in grain-dominated lithofacies (Fig. 3.18F to J).

3.2.5 Dolomitization

Dolomitization is the most dominant diagenetic feature recognized in the samples of the Wadi Waqb carbonate from both the surface and subsurface (Hughes and Johson, 2005)

whereas the dolomitization in Musayr Formation is only restricted along the fractures. Two generations of dolomitization are observed in these samples (i) filling the pore spaces (Figs. 3.18L) (ii) superimposed on the skeletal and basement-derived grains (Fig. 3.18L). The fabric of the dolomite cement is observed as equigranular, revealing little intercrystalline porosity, and preserving the original textures. The crystals show euhedral, subhedral, and anhedral shapes between 50 and 200 microns in size, and the typical fabric is a xenotopic mosaic of anhedral crystals.

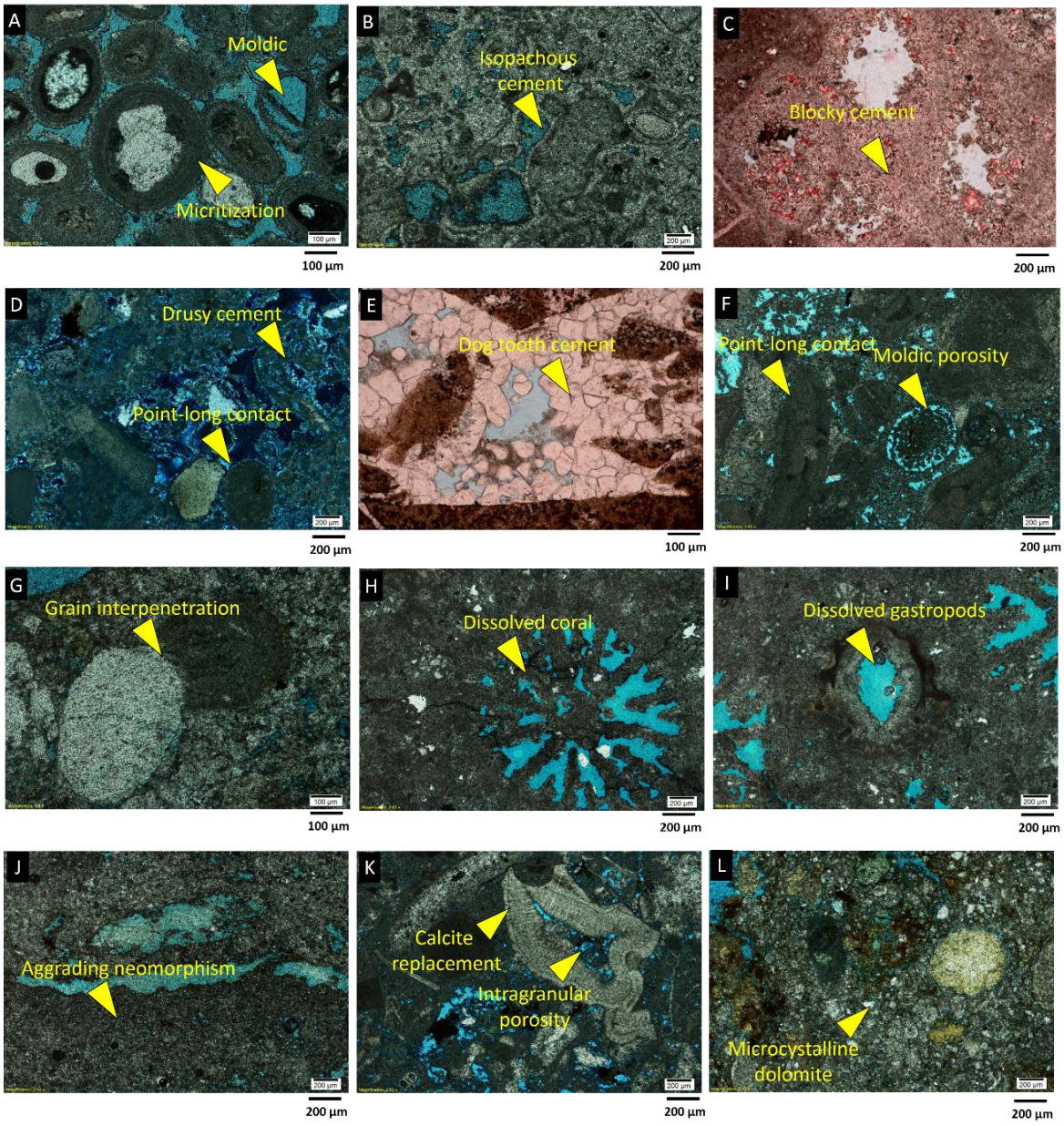

Figure 3.18 Examples of different diagenetic textures captured in thin-section micrographs. **(A)**. Ooid grainstone facies with intensive micritization within the cortices and well developed isophachous cement. Inter-intragranular and moldic porosities are abundant in this facies (XPL). **(B)** and **(G)**. This grain-dominated facies shows intensive grain dissolution and neomorphism (replacement), and has created moldic porosity (XPL). **(C)**. Pervasive blocky cementation with moldic porosity (PPL). **(D)**. Iron oxide cement

surrounding basement-derived fragments. (XPL) **(E)**. Skeletal grains fully replaced grains by dolomite and the presence of microcrystalline dolomite between pore spaces. The rearrangement of grains due to mechanical compaction is also suggested (PPL). **(F)**. Rhodolith fragment surrounded by equigranular isophachous blocky cement (XPL). **(H)**. This image indicates two generations of dolomite, the first one fills the pore space and the later euhedral dolomite crystals are superimposed on the basement-derived fragments (PPL). **(I)**. Intensive micritization and replacement of skeletal grains (PPL). **(J)**. Moldic and channel porosity (PPL). **(K)**. Grain interpenetration with suture contact suggests that chemical compaction occurred in the deeper burial stage of diagenesis (PPL). **(L)**. Grain dissolution, drusy cementation, mechanical compaction and microcrystalline dolomite (PPL).

Table 3.3 Geochemical signatures of Musayr Formation. Representative samples were taken from two different locations, which are Wadi Al-Hamd and Maqna area.

Location	Sample ID	Ca	Mg	Fe	Mn	Na	Sr	$\delta^{13}C$	$\delta^{18}O$	Dolomite	Calcite
		%	%	ppm	ppm	ppm	ppm	‰	‰	%	%
Wadi Alhamd	WH-4	10,98	0,11	732,6	891,3	700,6	42,1	-2,68	-9,41	0	100
	WH-5	31,75	0,13	1033,6	1949,1	365,0	110,6	-2,71	-9,74	0	100
	WH-6	10,09	0,08	302,3	664,3	580,9	31,5	-2,74	-10,08	0	100
	WH-7	27,55	0,28	2008,5	1578,3	753,0	112,9	-2,57	-9,11	0	100
	WH-8	11,55	0,18	1394,3	422,8	1097,2	29,5	-0,45	-7,58	0	100
	WH-9	28,09	0,12	392,3	1167,7	571,4	136,0	-0,74	-9,09	0	100
	WH-10	42,71	0,16	306,2	1215,6	393,4	152,7	-0,47	-9,81	0	100
Maqna	M-3	42,04	0,26	990,4	1939,6	277,1	280,4	-0,56	-6,91	0	100
	M-4	24,43	0,30	1629,9	2489,8	4474,3	134,2	-4,72	-9,93	0	100

	M-5	21,02	0,51	3556,5	1506,8	3397,5	136,3	-4,72	-9,14	0	100
	M-6	15,71	0,56	3560,3	1776,8	2919,5	170,5	-2,89	-9,39	0	100
	M-7	35,56	0,34	1404,5	2429,4	980,0	201,5	-2,59	-9,72	0	100
	M-8	37,35	0,36	1366,4	1962,5	470,5	294,5	-0,98	-8,47	0	100
	M-9	32,80	0,29	1684,5	873,6	367,9	1347,8	1,77	-9,42	0	100
	M-10	44,06	0,23	453,0	796,9	356,5	2032,0	3,09	-8,41	0	100

3.3 Trace Elements

3.3.1 Musayr Formation

The elemental analyses of the Musayr Formation are listed in Table 3.3.

Sr (Strontium). The Sr concentration in the Musayr carbonate ranges from 29.5 to 2032 ppm (mean av. 347 ppm). Maqna location shows relatively higher strontium concentration in comparison with Wadi Al-Hamd area.

Na (Sodium). The Na concentration in the Musayr carbonate ranges from 277 to 4474 ppm (mean av. 1180 ppm). Higher sodium concentration is observed in the lower part of Musayr Formation succession in Maqna area.

Fe (Iron) and Mn (Manganese). The Fe and Mn concentrations in the Musayr carbonates range from 302 to 3560 ppm (mean av. 1388 ppm) and from 422 to 2489 ppm (mean av. 1444 ppm), respectively. Siliciclastic input in the lower part of Musayr Formation may responsible for higher iron concentration.

3.3.2 Wadi Waqb Member

The elemental analyses of the Wadi Waqb member are listed in Table 3.4.

Sr (Strontium). The Sr concentration in the Wadi Waqb carbonate ranges from 71 to 1264 ppm (mean av. 195 ppm). This study shows that Sr values in limestone dolomitic limestone (low magnesium calcite) (av. 335 ppm) are much higher than dolomites (mean av. 443 190 ppm). We also observed higher Sr concentration (av. 332 pm) in platform deposit than slope deposit (av. 153 ppm) from both localities. The difference in Sr partitioning between

dolomites and calcites may be responsible for the lower Sr concentration in dolomite than calcite (Land 1980; Veizer 1983). In a typical carbonate system, Ca generally substitutes for Sr to form a more stable mineral. However, dolomitization typically results in substantially lower Sr.

Na (Sodium). The Na concentration in the Wadi Waqb carbonate ranges from 155 to 6185 ppm (mean av. 1967 ppm). The data shows that there is only small difference between Na concentration in platform and slope deposits.

Fe (Iron) and Mn (Manganese). The Fe and Mn concentrations in the Wadi Waqb carbonates range from 465 to 5234 ppm (mean av. 1769 ppm) and from 206 to 8446 ppm (mean av. 2269 ppm), respectively. The average Fe and Mn concentrations of dolomites (av. 1518 ppm) are higher lower than those of the limestonedolomitic (av. 2281 ppm). In constrast, Mn concentration in the dolomite (av. 2896 ppm) samples are higher than dolomitic limestone (av. 558 ppm). There is no significant difference of Fe and Mn concentrations recognized from platform and slope deposits. However, significantly higher concentration of both elements are found from Wadi Waqb locality (av. 2031 ppm of Fe and av. 3110 ppm of Mn) compare to samples collected from Ad-Dubaybah locality (av. 1270 ppm of Fe and av. 535 ppm of Mn)

Table 3.4 Geochemical signatures of Wadi Waqb Member. Representative samples were taken from two different locations, which are Wadi Waqb and Ad-Dubaybah locations.

Location	Sample ID	Ca	Mg	Fe	Mn	Na	Sr	$\delta^{13}C$	$\delta^{18}O$	Dolomite	Calcite
		%	%	ppm	ppm	ppm	ppm	‰	‰	%	%
Wadi Waqb	P1	23.4	12.63	1136	1031	1595	141	1.95	3.30	100	0
	P2	23.5	13.08	1755	1358	530	103	2.23	3.21	100	0
	P3	26.8	8.94	4308	734	2332	431	0.78	0.88	85	15
	P4	24.0	13.30	3072	2900	487	71	1.51	2.20	100	0
	P5	29.6	5.20	5235	637	2420	521	0.75	1.20	45	55
	P6	42.4	0.00	796	858	1445	270	1.42	-0.71	0	100
	P7	33.0	5.14	2729	350	6815	473	0.55	0.87	50	50
	P8	39.1	2.89	1962	385	1913	522	0.34	-0.91	48	52
	P9	22.6	12.98	2374	2529	1267	1264	1.73	3.08	100	0
	P9a	25.3	13.80	2243	2219	1183	235	1.51	3.68	100	0
	P10	21.9	12.80	1703	2308	1310	114	1.66	3.32	100	0
	WW-US1	22.7	13.47	1147	1741	1383	196	0.96	3.40	100	0
	WW-US2	23.6	13.91	1168	1944	1701	157	0.79	3.93	100	0
	WW-US3	22.7	13.34	1024	2151	1681	137	0.71	3.96	100	0
	WW-US4	39.6	22.18	1029	8447	3969	232	-0.87	3.42	100	0
	WW-US5	24.5	13.66	465	7669	1346	205	-2.03	3.56	100	0

	G2-1	23.8	12.65	2088	4799	365	78	1.24	2.26	96	4
	G2-2	23.9	12.92	957	4078	650	84	0.84	2.31	100	0
	G2-4	22.5	12.21	2461	6388	814	107	0.00	2.33	100	0
	G2-5	22.1	11.96	1936	5425	3972	269	0.42	2.69	100	0
	G2-6	22.0	11.95	1940	5419	4070	273	0.14	2.99	100	0
	G2-7	24.4	12.96	2702	6553	1234	311	0.16	2.19	100	0
	3	22.4	11.33	2472	1610	5072	214	1.97	3.09	100	0
Ad-Dubaybah	DU-US1	22.4	13.32	649	633	821	88	0.70	-4.18	100	0
	DU-US2	25.0	14.21	691	670	441	123	0.71	-3.53	100	0
	DU-US3	22.6	13.52	822	529	572	85	0.10	-5.13	100	0
	DU-US4	22.2	13.00	619	418	9409	95	0.12	-5.60	100	0
	DU-US5	20.7	11.61	1622	594	249	107	-0.09	-3.33	93	7
	DU-US6	25.4	13.47	1070	521	177	96	-0.08	-4.86	96	4
	DU-US7	19.4	11.71	797	463	4817	91	-0.37	-3.47	100	0
	DU-US8	25.5	12.12	925	462	286	102	-0.11	-4.61	86	14
	DU-US9	19.0	11.34	4485	1031	1306	139	-0.27	-7.28	100	0
	DU-US10	23.1	11.54	1326	357	397	197	2.04	-2.57	89	11
	DU-US11	41.7	0.00	965	206	155	164	0.22	-7.25	0	100

3.4 Mineralogy

The XRD analysis was performed on the selected samples with the detection limit focus solely on carbonate minerals (aragonite, calcite, and dolomite). The result show most of the samples on Wadi Waqb locality have more than 85% dolomite mineral, except four samples that are dominated by calcite. Similar mineralogy trend has also observed on the Ad-Dubaybah locality where most of the samples are dolomite. In contrast, samples from Musayr Formation are mostly composed of calcite.

3.5 Stable Isotopes

Carbon and oxygen isotopes have been used to decipher the diagenetic environment conditions and the paleofluids responsible for the diagenetic alteration processes in the Musayr and Wadi Waqb carbonates. Previous studies have demonstrated that $\delta^{13}C$ values from shallow marine carbonates are not readily affected by diagenetic alterations (Magaritz, 1983; Banner & Hanson, 1990). However, $\delta^{18}O$ values for marine carbonate rocks are easily influenced by burial and meteoric diagenesis (Choquette and James, 1988).

3.5.1 Musayr Formation

The stable isotope values of the Musayr carbonate sequences in both localities are presented in Table 3.3. The $\delta^{18}O$ values range between -10.08 and -6.91‰ (av. -9.08‰,), and $\delta^{13}C$ values range between -4.72 and 3.09‰ (av. -1.60‰) (Table 3.3).

3.5.2 Wadi Waqb Member

The stable isotope values of the Wadi Waqb member in both localities are presented in Table 3.4 and Figure 3.19. The $\delta^{18}O$ values range between -7.28 and 3.68‰ (av. 0.13‰,), and $\delta^{13}C$ values range between -0.87 and 4.47‰ (av. 0, 64‰) (Table 3.4).

CHAPTER 4

DISCUSSIONS

4.1 Global vs. Regional Forcing Mechanisms

4.1.1 Carbonate Factory

Pomar (2001a; 2001b) showed the significant role of interplay between depositional geometries and carbonate factories in understanding the evolution of carbonate platforms throughout the geological record. Different types of carbonate factories have been assigned to characterize carbonate platforms. For example, carbonate rimmed and isolated platforms, as observed in this study, are primarily dominated by chlorozoan factories (sensu James, 1997). Conversely, heterozoan factories are frequently observed in the carbonate ramp succession (sensu James, 1997. The Musayr Formation contains photozoan and chlorozoan factories (sensu James 1997), dominated by red algae and large benthic foraminifera, with minor presences of coated grains and low diversity of biota components. Corals were found in this succession as transported clast in the middle ramp environment. The Wadi Waqb member contains a chlorozoan factory (sensu James, 1997) that is comprised of scleractinian corals, coralline red algae, benthic and planktonic foraminifera and coated grains with high biota diversity (i.e brachiopods, echinoids and bivalve).

In the two early Miocene examples examined here, corals occur in both succession, yet it plays a different role. The Musayr Formation corals are interpreted built as discrete mounds in proximal middle ramp zone, lived below the wave action within photic-mesophotic zone. This living position is unlikely for tropical corals and oppose with modern tropical corals that require intensive light and shallow conditions (e.g., Hallock and Schalager, 1986).

However, this condition have been found in adjacent Cenozoic carbonate platforms, such as Mediterannean (Halfar and Mutti, 2005; Benisek et al., 2012; Pomar et al., 2014). The absence of in-situ corals as a wave resistant rimmed in the Musayr Formation might be explained by two different mechanisms: (i) active erosion and long subaerial exposure of the platform margin, or (ii) abundance of coralline red algae because of enhanced nutrient levels and presence as an active bioerosion agent. The second mechanism may suitable to elucidate this phenomenon because of the domination of coralline red algae appears to be the main carbonate factory in the Musayr Formation. The fluorishment of coralline red algae during Miocene time has also been reported from Mediterranean region (Halfar and Mutti, 2005) which may coincide with the condition when the Musayr Formation was deposited.

In contrast, the Wadi Waqb member corals were well flourish and occurred as a three-dimensional wave resistant rimmed up to sea level. The Wadi Waqb carbonate shows that carbonate production and sedimentation maintain pace with the accommodation space created by subsidence. This describes the vertical growth of a wave-resistant rim that is controlled by high carbonate productivity in the platform margin and basement fault activity, which seems to have occurred throughout most of the Miocene. The difference in corals living mode and diversity of biota between the Musayr Formation and the Wadi Waqb member may imply distinct nutrients conditions throughout early Miocene time in the Midyan Basin.

4.1.2 Relative Sea-Level

The strong influence of relative sea-level fluctuations has been recorded in many ancient carbonates (e.g., Pomar, 2001a; Pomar, 2005; Laya et al., 2013). The Midyan basin has

experienced an overall rise in relative sea level during the Miocene driven by tectonic subsidence superimposed on high-frequency glacio-eustatic fluctuations from the formation and melting of ice (Tubbs et al., 2014). The major role of sea level variations in these studied sections controlled the carbonate factory capacity. During the high stand condition, the carbonate factory would have thrived and kept pace with relative sea level rise, and tended to develop an aggradation-progradation system. Relative sea level fall may lead to platform erosion and reef deposition because of subaerial exposure. The erosion processes transport sediments into the slope area, where they are deposited as gravity flow sediment.

Although the large-scale driving controls of platform development in the Midyan Basin have been determined in this study, the mechanisms responsible for transported carbonate material remain unknown. This study hypothesize that either 1) the upper part of the carbonate platform was subaerially exposed, which led to the erosion of carbonate materials towards the slope, or 2) a continued sea level rise that was followed by an increase in carbonate production that exceeded the platform capacity, causing the platform to become unstable and material to be transported into the basin. The first mechanism has been invoked in this study to explain this phenomenon by using several lines of evidence, such as: outsized clast material in the slope, the angle of repose that can reach up to 40^0 and also the diagenesis study have identified pervasive extend of meteoric diagenesis on the studied carbonate platforms that may associated with local subaerial exposure in this region.

4.1.3 Tectonic Activity

The development of these two different carbonate platforms was primarily controlled by the basin topography when the carbonates were established. In addition, the fulcrum / pivot location may also have contributed to the platform geometries. For example, if the fulcrum was located above the sea level when subsidence/uplift occurred, it would have increased the accommodation space and tended to develop progradation with downward thickening. Alternatively, if the fulcrum was located below sea level, it would have exposed the precursor sediments and decreased the accommodation space. The presence of paleohighs may also help the carbonate factory flourish by trapping the clastic sediment fairways around the carbonate platforms. This study propose that tectonic activity was playing a significant role in controlling the establishment and development of carbonate platform geometries for the two carbonate platforms, as opposed to other external controls, such as sea level and orbital forcing.

4.2 Variations of Architecture and Cycles in the Early Miocene Syn-Rift Carbonate

Cross and Bosence (2008) described variations in carbonate platform architecture development based on the maritime rift basin of the Gulf of Suez. This study has found that similar architectures are also recognized in the contiguous Red Sea Rift.

The Musayr Formation outcrops represent a syn-rift hangingwall dipslope carbonate ramp, the deposits of which interfinger with siliciclastics towards the basin (Fig. 3.4). There are

two models proposed by Cross and Bosence (2008) which are largely based on the fulcrum location, and which invoke deposition either (i) downdip of the fault-block fulcrum, which will typically create retrogradational depositional geometries, or aggradational ro progradational geometries if sediment flux is high relative to accommodation generation, or (ii) updip of the fault-block fulcrum, which will lead to regressive but offlapping depositional sequences driven by relative sea level fall. The Musayr Formation is interpreted to relate to the former structural model. However, the presence of an overall aggradational to progradational stacking pattern of shallowing upward cycles within the Musayr carbonates is interpreted as evidence of high (and increasing) carbonate productivity at this time, such that carbonate sediment flux outpaced the temporal increase in accommodation space on the carbonate ramp (Fig. 3.4).

The Wadi Waqb Member located at the Wadi Waqb locality appears to represent a normal fault-controlled isolated carbonate platform (Fig. 3.10). Thick packages of slope deposits found in this location indicate the availability of accommodation space on the downthrown side of the syn-depositionally active fault (Fig. 3.10). High carbonate productivity on the platform margin and interior occurred because the platform-top was isolated from any significant siliciclastic drainage fairways. The morphology of the footwall-derived slope deposits is progradational, controlled by the morphology and topography of the faulted margin. No cyclicity is evident within the upper to mid-slope deposits (Fig. 3.10). The absence of cycles may due to; (i) high carbonate productivity on the platform margin and across the platform-top causing an unstable platform edge and the shedding of excess material onto the slope, obscuring any signal of short-term tectonic or sea level fluctuations, and/or (ii) the location of the carbonate platform possibly being in the middle

of a normal fault segment where highest subsidence rate occur, such that again any short-term relative sea-level changes are obscured by the locally and continuously high subsidence rate.

The Ad-Dubaybah location represents a different type of carbonate platform of the Wadi Waqb Member. The Ad-Dubaybah site is comparable with Abu Shaar platform, Gulf of Suez (Cross and Bosence, 2008). Each represents a relay zone carbonate platform (Fig. 3.17). However, the Ad-Dubaybah location involves the significant local input of siliciclastics compared to the Abu Shaar platform, presumably related to the nearby position of drainage entry points across the rift shoulder. The occurrence of this carbonate platform is associated with the now hard-linked fault set that creates abrupt topographic changes along the rift margin and that allowed the development of an attached carbonate platform with rimmed margin, probably before the rift margin faults became hard-linked (Fig. 3.17). One of the main characteristics of this platform and also the main difference with the Wadi Waqb location is the presence of repetitive shoaling-upward cycles within the outer platform margin to upper slope environments. To explain the occurrence of these parasequences at this study site, two mechanisms may be proposed: (i) The superimposition of high frequency sea level fluctuations over some continuous but relatively low rate of tectonic displacement. It is possible that we can observe the signal of high frequency glacio-eustatic sea level variations because the carbonate platform is located towards the tip of the normal fault where low subsidence rates would have occurred. (ii) Stick-slip movement on one or both of the normal faults, cycles being driven by such processes having been described before by Smalley et al (1985). Each fault event moves the hangingwall down instantaneously, generating a flooding surface, with the shoaling-up,

progradational to aggradational depositional phase representing the period of quiescence before the next seismic event. In the case of the Ad-Dubaybah platform, this would require that seismic displacements on the fault to the east of the platform dominated over any fault displacements on the fault bounding the western side of the platform. To date, this study cannot strictly resolve which forcing mechanism is the more plausible explanation for the presence of cycles in this location. However, the magnitude of accommodation generation implied by each cycle's thickness is too great to be simply related to any one coseismic slip event on a continental normal fault segment.

4.3 Autocyclicity vs. Allocyclicity on Syn-Rift Carbonate Platforms

This study explores whether in maritime rift basin carbonate platforms, seismically driven cycles may be responsible for the development of 5^{th} order depositional cycles, resulting from high-frequency syn-sedimentary fault activity that might generate a recurrent motif in carbonate deposition (Satterley, 1996; Benedictis et al., 2007; Hamon and Merzeraud, 2008; Chow et al., 2013). Alternatively, 4^{th}-5^{th} order depositional cycles (of a magnitude of metres to a few tens of metres) may be accounted for by orbitally-driven glacio-eustatic fluctuations. This scale of cyclicty may be predicted to occur in the carbonates of the Midyan Basin because the Early Miocene was part of the global icehouse episode, in which glacio-eustatic fluctuations were probably a moderately high-amplitude and high-rate phenomenon. Reefs and platforms are particularly sensitive to Milankovitch forcing because they respond to both sea-level cycles and environmental change driven by orbital perturbations (Goldhammer, 1990; Schlager, 2005).

This study proposes that glacio-eusatically induced allocyclic cycles in these carbonate platforms are only apparent (as typically 5-8m thick parasequences) in the middle ramp of the Musayr Formation and in the upper slope and platform margin deposits of specific locations within the Wadi Waqb Member, locations where syn-depositional tectonic displacements may have occurred at low rates. This allocyclicity is represented by repetitive shallowing-upward parasequences separated by flooding surfaces (e.g.., Figs 3.15 and 3.16). The relationship between parasequence expression and the lateral variation in tectonic displacement rates in these carbonate platforms is analogous to that described for syn-rift siliciclastic successions by Gawthorpe et al. (1994) and Collier & Gawthorpe (1995).

4.4 Depositional Evolution of Syn-Rift Carbonates in Midyan Peninsula

Late Aquitanian (N4)

During this time the first major marine incursion was flooded Midyan Peninsula (Tubbs et al., 2014). This marine incursion was characterized by the development of stromatolitic facies deposited in the Maqna area and surrounding. This facies represent a beginning of Musayr Formation. This condition was subsequently followed by an increasing amount of siliciclastic supply due to active weathering of Proterozoic basement. The abundant presence of oyster may suggest brackish environment due to mixing of normal seawater circulation and fresh water input that might coming from hinterland (Tucker and Wright, 1990; Hughes and Johson, 2005). Musayr Formation only developed locally in western

part of Midyan Peninsula, which may suggest the distribution of paleo-highs during that time that allowed Musayr Formation to nucleate (Fig. 4.1)

Early to Middle Burdigalian (N5-N6)

Rapid subsidence represented the climax stage of the normal rift extension during this time. This condition allowed a widespread creation of accommodation space in the Midyan Peninsula. It developed deep marine turbidites deposit (Burqan Fm) due to its narrow shelf and steep slope basin morphology (Fig. 4.1). The carbonate production was shut off because of active siliciclastic input and the inability of carbonate producers to keep up with the increasing of relative sea level rise.

Late Burdigalian (N7)

Before this time, the tectonic activities were slowing down, it was associated with the Mid-Clysmic event that been recognized in Egypt side of Red Sea (Hughes and Johnson, 2005; Tubbs et al., 2014). Following this, several local paleohighs were created due to tectonic readjustment (Fig. 4.1). These paleohighs bounded by fault and allowed Wadi Waqb member of Jabal Kibrit Formation to growth. The development of Wadi Waqb member is characterized by the development of basal lag deposit characterized by inclusion of well polished pebbly to cobbly size clasts in the carbonate sequence at the base of the succession as a product of reworking process of Proterozoic basement due to transgressive processes. The paleohighs also created an isolation of carbonate platform from the silicilastic fairways and allows the carbonate to produce and reach the keep up stage.

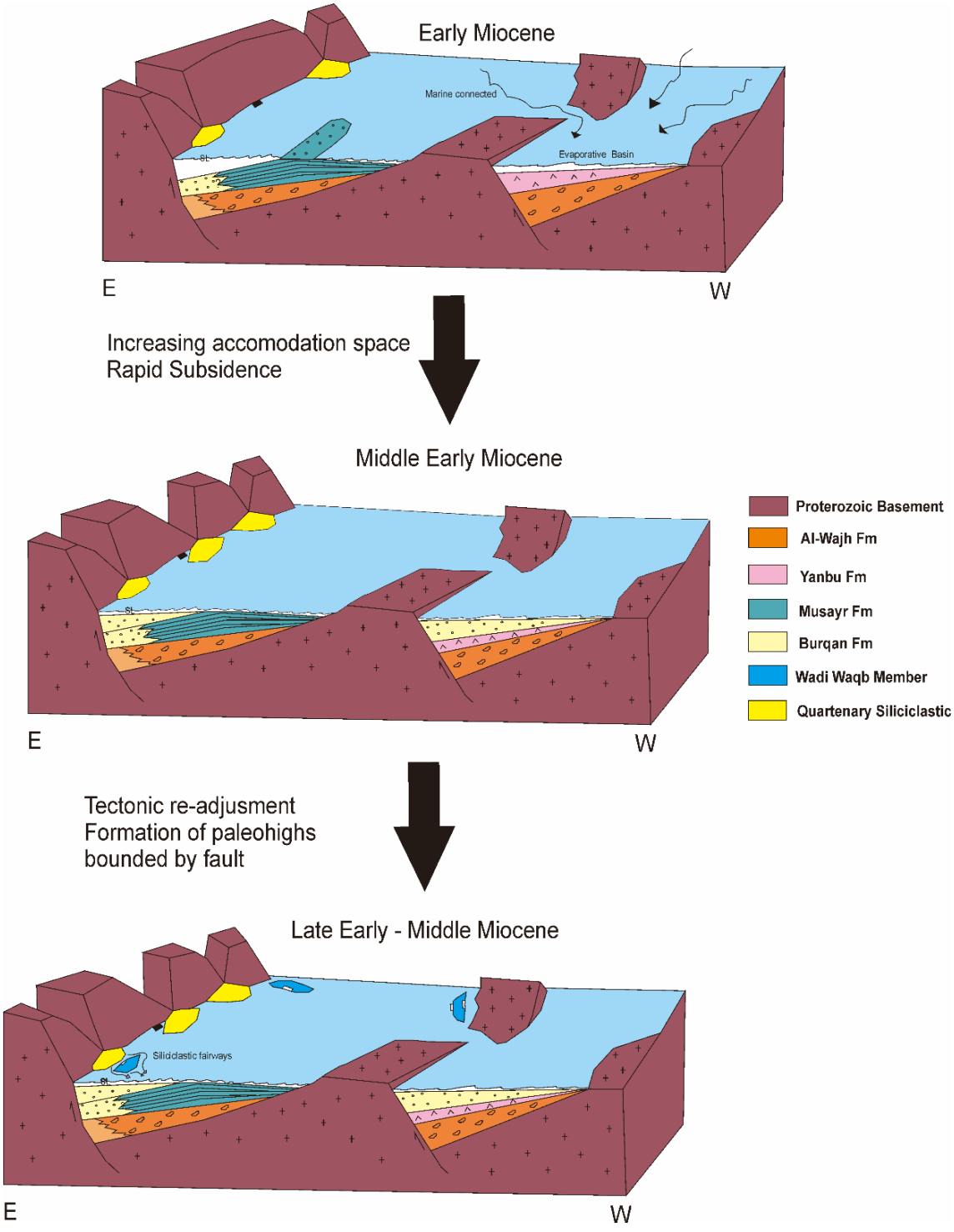

Figure 4.1 3D block diagrams showing the evolution of the Midyan Peninsula from Early Miocene (Late Aquitanian) to the Late Burdigalian.

4.5 Diagenetic Environment and Paragenesis

Sedimentary-petrographic analysis has been utilized to determine different diagenetic environments. Three distinct environments are recognized; shallow marine, burial and near surface meteoric diagenesis (Fig. 4.2). This study indicate that some of the diagenetic features are associated to their original mineralogy and depositional texture (e.g., cementation, selective dissolution) while some (dolomitization) are related to paleofluids conditions infiltrate the platform. The three diagenetic environments and their characteristics are discussed below.

4.5.1 Shallow Marine

The major diagenetic processes that modified porosity under shallow water, normal marine conditions were microbial micritization, marine phreatic cementation (equigranular isopachous cement), mechanical compaction and early stage dolomitization. Considering the Miocene ocean chemistry which belong to aragonite seas (Stanley and Hardy, 1999), the cement was originally precipitated as aragonite fibrous or high magnesium bladed cements (Moore, 2001). Ghost texture of circumgranular cement are observed on the thin section and suggest the later modification of the marine cement by dolomitization and/or recrystallization by meteoric fluids (Fig. 3.18F). The presence of isopachous cement (Fig. 3.18F and M) suggests that the sediment was fully submerged under water with a low sedimentation rate during its formation (Ehrenberg et al., 2002).

Creation of micrite envelopes by microbores organisms surrounding the bioclast and non-bioclast grains may also help the nucleation and provide a substrate of marine cements to

growth. This process has been observed in the modern carbonates in the Red Sea (Koeshidayatullah and Ramadan, 2014). The most common type of porosity in this diagenetic setting is associated with selective dissolution of aragonite bioclasts and ooids.

The early stage dolomitization can be readily observed on the Wadi Waqb locality samples where different stage of dolomitization occurred. The most common dolomitization model associated with early stage dolomite is seepage reflux brines where intensive evaporation took place; hence, the Mg^{2+} concentration on the seawater will increase and provide suitable fluids conditions for dolomitization. The presence of relatively enriched $\delta^{18}O$ may also be used as a line of evidence to support this interpretation.

4.5.2 Burial

Burial diagenesis realm of the Wadi Waqb carbonate sequences is characterized by the presence of intensive compaction, dissolution caused by undersaturated connate water and hydrocarbon filling into the pore space, late stage dolomitization were observed post-date the dissolution. Nested fabrics (Fig. 3.18M) resulted by late stage mechanical compaction were readily recognized under the thin section. Severe reduction of intergranular porosity in grain-dominated facies were also identified. The formation of concavo-convex and sutured grain contacts by chemical compaction (Fig. 3.18K) was prevalent in the mud-supported facies where well-developed circumgranular marine cements are absent (e.g., Moore and Druckman, 1981; Shinn and Robin, 1983). Late stage dolomite cements were common throughout, with most occurring as fabric preserved dolomite bodies with euhedral to subhedral crystal morphologies (Fig. 3.18H).

The timing of hydrocarbon migration may be revealed by looking at the relationship from late stage dolomitization that post-date the dissolution caused by hydrocarbon filling. This relation only observed in the Wadi Waqb locality samples. More samples are needed in order to come up with a reasonable timing of the migration.

4.5.3 Meteoric

This diagenetic realm is the most dominant in the Musayr Formation and Wadi Waqb member in Ad-Dubaybah locality and most likely associated with relative sea level lows that allow the carbonate sequences to subaerially exposed and formed meteoric lenses. The structural context of these platform carbonates is such that they may have been exposed to footwall uplift late in the rift phase prior to late transgression and burial by evaporites of the early post-rift subsidence phase.

Meteoric diagenesis is characterized by clear blocky (Fig. 3.18F) and drusy mosaic cements, followed by selective dissolution by using fractures as the pathways, and dedolomitization. Most of the meteoric cements formed as low magnesium calcite and progressively occluded primary pore spaces in the grain-dominated carbonate facies and filled the fractures.

Considering the climatic setting of study area during Miocene time was arid (the groundwater flow was likely encountered a zone of refluxing hypersaline water near the shoreline), the formation of mixing zone were plausible. This condition may hindered the massive dissolution and instead it favors sulfate mineralization and dolomitization (Lucia, 1999). This study suggest that the dolomitization was actually formed in the early stage by hypersaline brines that later on recrystallized by the presence of meteoric lenses within the

platform. This model has been reported on the adjacent Miocene carbonate succession in Egypt side (Coniglio et al., 1988).

Dedolomitization can be identified in some samples, mostly from the platform interior part on the Wadi Waqb locality. This dedolomitization occurred in two modes: (i) full replacement of the previously dolomite mineral and (ii) partially replaced the dolomite mineral where it formed mostly on the core of the dolomite mineral because the low degree of stability of the mineral as a result of rapid cementation process.

4.6 Stable Isotopes

Relatively high values of $\delta^{18}O$ often indicate extensive evaporation, likely related to the development of the evaporites of the intraformational and younger deposit (i.e. Mansiyah evaporites) (Fig. 4.3). In addition, this enrichment may be due to the relatively high $\delta^{18}O$ identified in dolomites over calcite. Widespread distribution of $\delta^{18}O$ in the Wadi Waqb carbonate samples from both Wadi Waqb and Ad-Dubaybah localities may be related to the presence of different fluid types during diagenesis, indicative of deposition in an open system with high fluid-rock interaction (Meyers 1989). Three possible mechanisms can explain the exceptionally low $\delta^{18}O$ values at Ad Dubaybah: (i) an increase in temperature during burial diagenesis (e.g., Choquette and James 1987; Nelson and Smith 1996) and/or (ii) the infiltration of meteoric fluids; (iii) later recrystallization by meteoric fluids of previously dolomite succession.

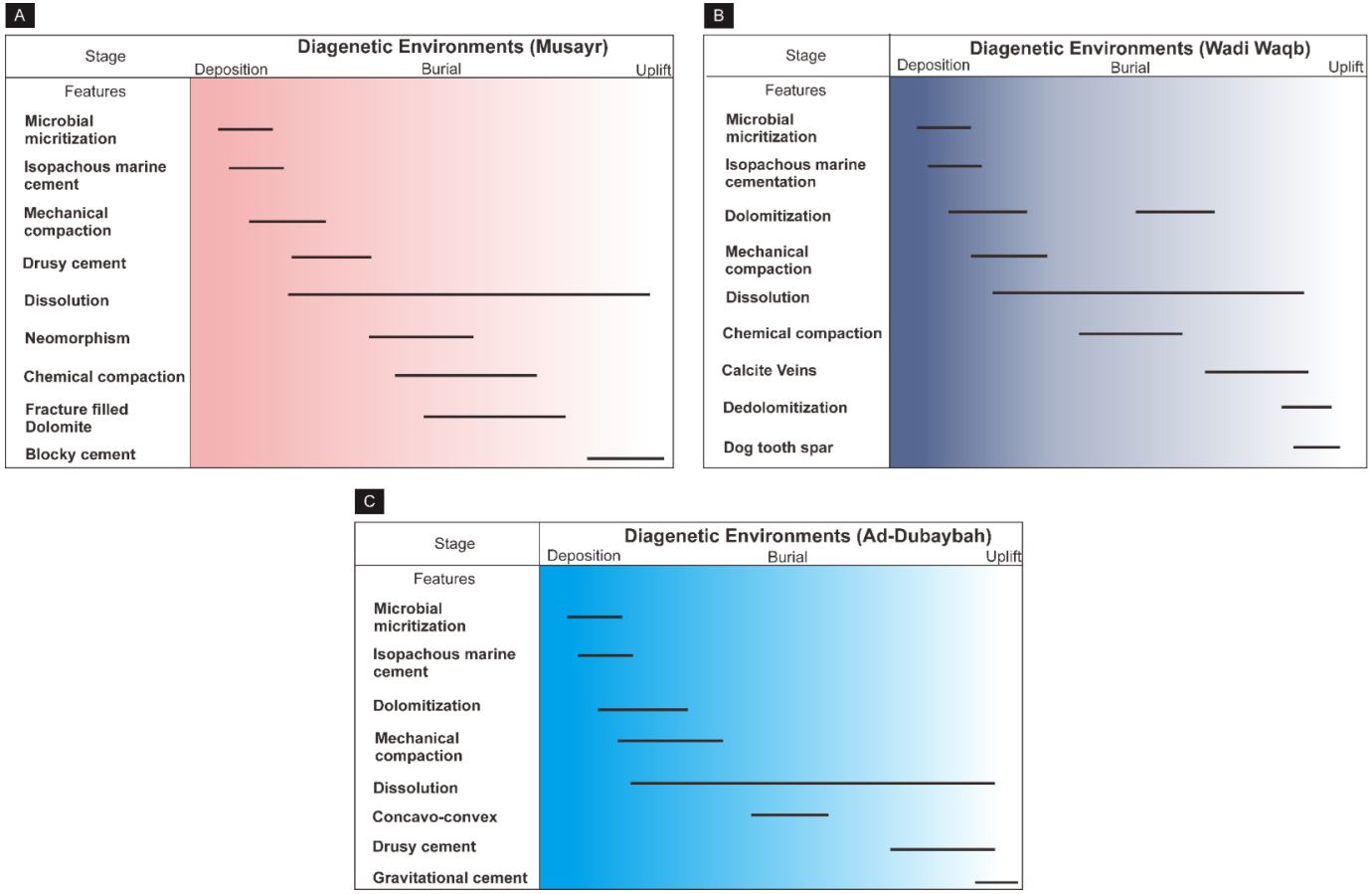

Figure 4.2 Paragenetic sequences of the Early Miocene syn-rift carbonates. (A). Musayr Formation dominated by intensive chemical compaction. (B). Wadi Waqb location characterized by two stages of dolomitization and dedolomitization. (C). Ad-Dubaybah location characterized by pervasive meteoric diagenesis with moderate chemical compaction.

From the samples can be readily observed that low $\delta^{18}O$ values are associated with low trace element concentration (Fig. 4.4). The most possible explanation of this three proposed mechanism is the later crystallization of meteoric water that modify the dolomite of Ad-Dubaybah sequence. Carbon isotopes reflect the original inorganic carbon, and are less susceptible to temperature dependent fractionation than oxygen ^{18}O and ^{16}O, explaining the relatively narrow range of $\delta^{13}C$ values recorded here.

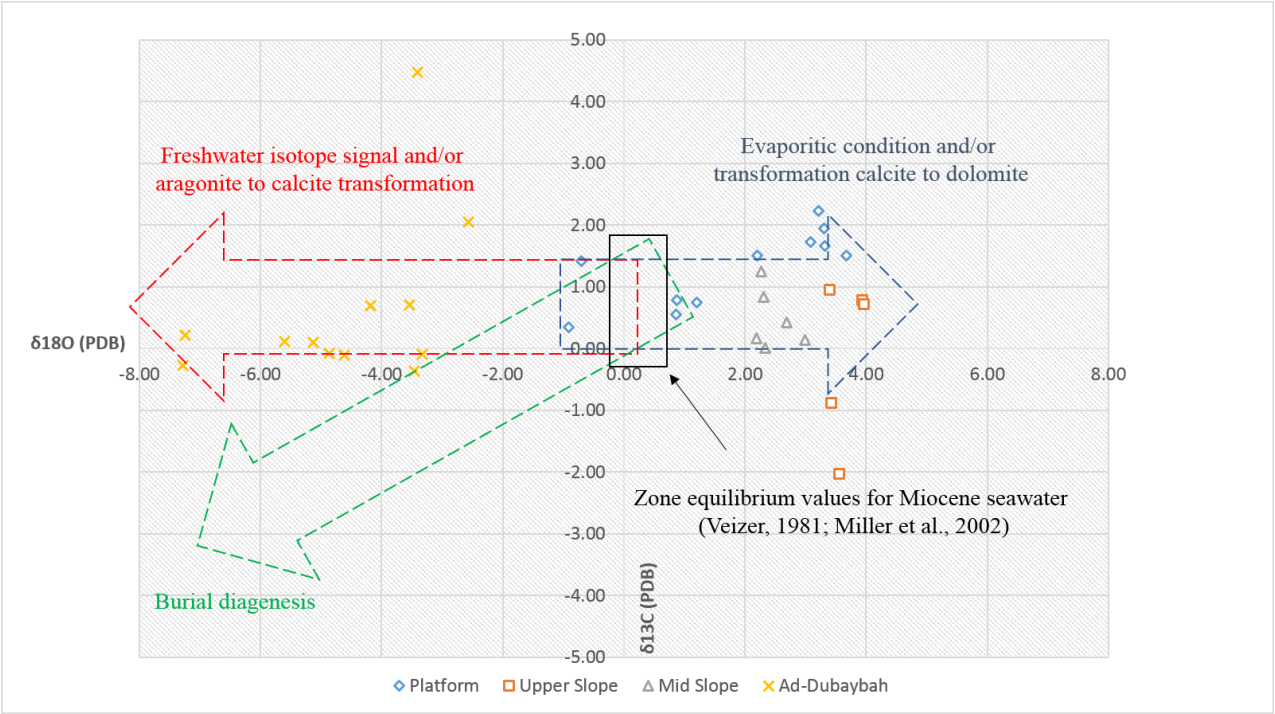

Figure 4.3 Cross plot between $\delta^{18}O$ and $\delta^{13}C$ of the Wadi Waqb carbonates showing two different trends: (1) positive carbon and oxygen isotope values in the Wadi Waqb locality; and (2) negative oxygen isotope values of Wadi Waqb carbonate in the Ad-Dubaybah locality.

4.7 Trace Elements

Incorporation of Fe, Mn, Na, and Sr within carbonate materials has provided a useful proxy for interpreting carbonate diagenesis (Table 3.3 and Table 3.4). Typically, the variations in concentration of these trace elements are used to compare ancient and modern carbonates, which can help determine mineralogical and compositional changes through time. However, there are known issues with this approach, such as the mineralogical variations induced by switching marine conditions from calcite to aragonite seas throughout the Phanerozoic (Sandberg, 1983; Gröcke et al., 1999).

Cross-plots between stable isotopes and trace elements are presented in Figures 4.4 and 4.5. They show that Fe, Mn, and Sr have a negative correlation with both carbon and oxygen isotopes for the Wadi Waqb locality. In contrast, no correlation can be obtained from the Ad-Dubaybah locality due to its low concentrations of trace elements compare to Wadi Waqb locality. The significant difference of trace elements concentrations found in both localities may suggest distinct degree of fluid rock interaction (Brand & Veizer, 1980; Moore 1990). The high concentration of trace elements in Wadi Waqb locality may indicate active fluid rock interaction within open diagenetic system whereas the Ad-Dubaybah carbonate may show inactive fluid rock interaction within the same system (Fig. 4.4). Different tectonic activities between these two localities may responsible in governing the degree of fluid rock interactions.

Negative correlations may indicate the extent of meteoric diagenesis in the Wadi Waqb locality, and/or they may be indicative of the dolomitizing fluid conditions in the dolomitic samples. In suboxic to anoxic diagenetic fluids principally in shallow to deep burial

environments, Fe, Mn and Sr can be present in higher concentrations than in sea-water (Tucker, 1983; 1986). In these samples we observed dolomite minerals with preserved fabric and mimetic textures assembled during the early dolomitization processes, and we may subsequently rule out the hypothesis of diagenesis occurring under deep burial conditions.

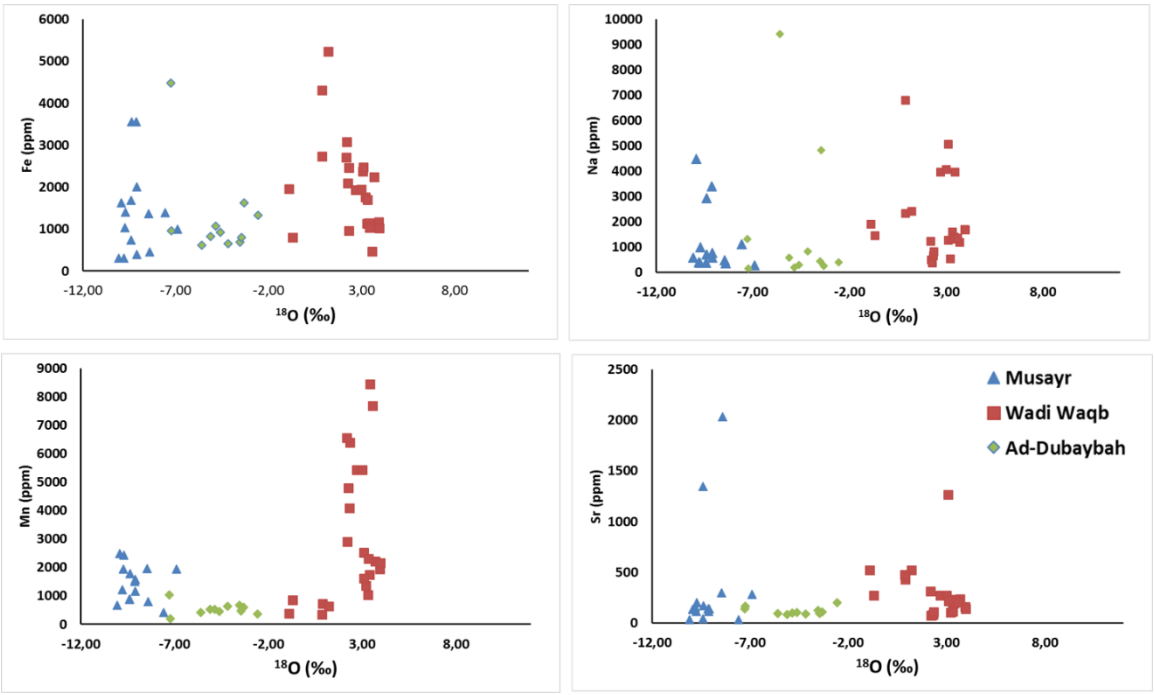

Figure 4.4 Cross plots of carbon isotope and trace element concentrations (Fe, Mn, Sr. and Na) for Musayr and Wadi Waqb carbonates. Negative correlation between Fe and Mn concentrations suggest strong influence of meteoric fluids.

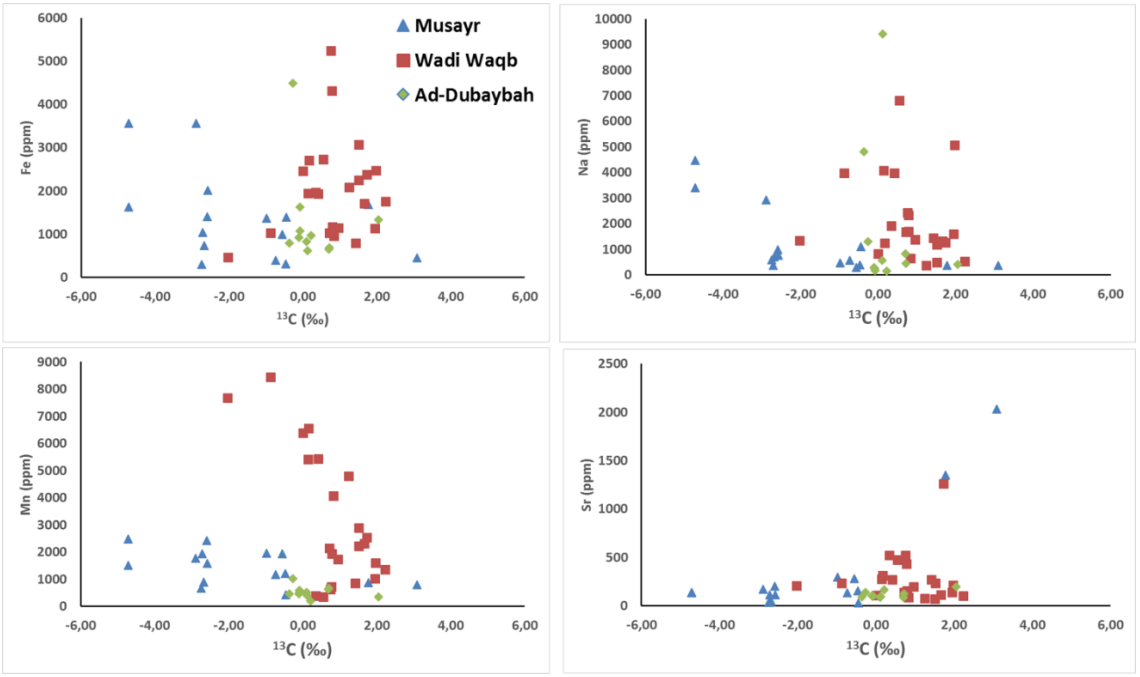

Figure 4.5 Cross plots between oxygen isotopes and various types of trace elements (Fe, Mn, Sr, and Na) for Musayr and Wadi Waqb carbonates. Negative correlation between Fe, Mn, and δ18O may suggest the extent of meteoric diagenesis in the Wadi Waqb carbonate at the Wadi Waqb locality. The Wadi Waqb carbonate at the Ad-Dubaybah location shows significant low trace-element concentrations.

4.8 The Role of Facies and Diagenesis in the Porosity Development

The Wadi Waqb carbonate succession has been interpreted as the main carbonate reservoir in this study area (Hughes and Johnson, 2005; Hughes, 2014). However, no single published article currently discusses the diagenetic history and its control on the reservoir quality due to porosity. The diagenetic features recognized from the studied samples have

indicated two major implications and are summarized in Figure 4.8: (i) porosity creation by burial and meteoric dissolution and neomorphism, and (ii) porosity destruction by dolomitization and cementation from both marine and meteoric fluids.

The variability of diagenesis throughout the platform shows that the slope deposits have much more developed porosity than the platform margin and interior. This is in total contradiction with the equivalent carbonate succession in the Gulf of Suez (Coniglio et al., 1988) where the most porous section is found in the open marine platform. This is due to the dual effect of dolomitization and also the occurrence of remenant porosity from the platform transported into the slope deposits.

This study conclude that, a strong facies control on the distribution of porosity in the Wadi Waqb carbonate is a function of the (1) original sediment composition, (2) synsedimentary cementation and internal sedimentation, (3) differential dolomitization intensity and function throughout the platform, and (4) the extent of meteoric percolation within the platform.

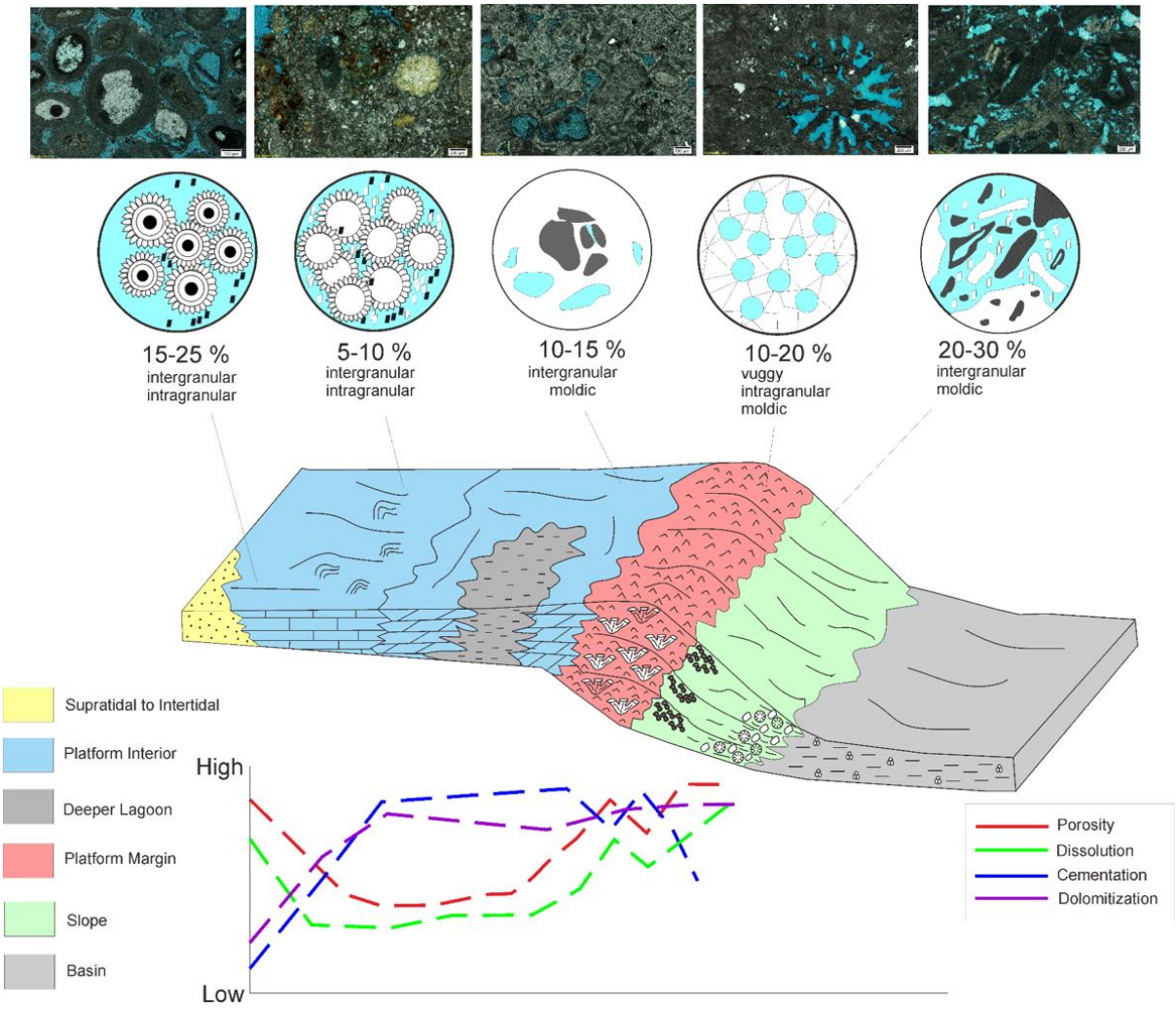

Figure 4.6 The distribution of various diagenetic products within the Wadi Waqb carbonate platform. This model suggests that the most porous section is found in the slope. The porosity distribution is strongly controlled by the intensity of dissolution and cementation.

CHAPTER 5

CONCLUSION AND RECOMMENDATION

5.1 Conclusions

This study presents the reconstruction of new depositional models and an assessment of the internal architecture for Early Miocene carbonate platforms (of the Musayr Formation and of the Wadi Waqb Member) of the Red Sea Rift, NW Saudi Arabia. Carbonates were developed on fault block highs, contemporaneous with siliciclastic deposition within the structurally controlled deeper hangingwall fairways. The Early Miocene carbonate platforms show distinct platform geometries. The Musayr Formation was deposited in a homoclinal carbonate ramp environment, located on the hangingwall dipslope of a syn-depositionally active half graben, where coralline red algae and large benthic foraminifera were the main carbonate producers. The Wadi Waqb Member is here interpreted as having been developed on fault-bounded, carbonate-rimmed platforms, located on fault block highs within the Midyan Red Sea rift segment. Slope deposits are characterized by steep bedding geometries (up to 40^{o} dips) and clinoform progradation. Although the Musayr and Wadi Waqb carbonates formed in similar tectonic and climatic settings overall, the resulting depositional geometries are distinct from one another, due to contrasting local basin structure contexts and differences in their carbonate factories.

Parasequence-scale cyclicities related to periodic rise and fall of relative sea level may result from glacio-eustatic forcing or potentially from cycles of co-seismic displacement in areas close to major active faults. Parasequence sets are observed on a hangingwall dipslope carbonate ramp of the Musayr Formation and in platform edge and upper slope

deposits of the Wadi Waqb Member at the Ad-Dubaybah location. Both locations may have been areas of subdued tectonic displacement rate, the latter perhaps due to the net local displacement rate arising from subsidence on a fault to the east and an uplift component from the fault bounding the western side of the platform. This is consistent with there being a greater likelihood of retaining a glacio-eustatic expression in stratigraphic architectures in localities where syn-rift tectonic displacement rates and sediment flux rates are minimal. Autochthonous carbonates, including Sclerectinian corals and rhodoliths, may have formed preferentially during periods of relative sea level rise over the platform margin and upper slope. High carbonate productivity across the platform-top environments would have allowed progradation and gravitational reworking of material down the slope, across the fault-controlled platform margins. However, allochthonous carbonate resedimentation on the slope may also have been enhanced when the platform-top was subaerially exposed and eroded, whether by tectonic uplift and/or glacio-eustatic sea level fall. At the first order, the architectures of these fault-bounded carbonate platforms are primarily due to syn-rift fault activity, with a superimposed (low magnitude) glacio-eustatic signal only locally evident. The tectonic activity was induced by fault block motion and rotation during extension. This activity governed the position of the platforms, their geometries, and the creation of accommodation space across the basin, and hence provided a fundamental control upon the location and nature of carbonate factories.

The diagenetic history of the Early Miocene Wadi Waqb carbonates includes compaction, cementation, microbial micritization, dissolution, neomorphism, and dolomitization. Three major diagenetic environments were identified: shallow marine, burial and near surface diagenetic environments. The $\delta^{18}O$ and $\delta^{13}C$ values are distinct between the Wadi Waqb

carbonates (3.9 to -7.2‰, and -2.03 to 2.23‰, respectively) and the Ad-Dubaybah locality (-2.57‰ to -7.28‰ and -0.37‰ to 2.04‰, respectively). The wide spread in $\delta^{18}O$ values suggests high intensity of diagenesis on the carbonate sequences.

Trace-element concentrations at the Wadi Waqb locality show negative correlations with carbon and oxygen isotopes, whereas the Ad-Dubaybah locality shows decreasing concentration following the oxygen isotope trends. Based on petrographic evidence, diagenesis had a dual effect on the development of carbonate porosity. The destruction of porosity is mostly due to compaction and cementation, whereas the creation of porosity is typically caused by intensive dissolution and late stage dolomitization. This study indicates that the platform slope is the most porous section and has highest reservoir quality compared to the platform margin and interior. There are four mechanisms controlling the distribution of porosity within the platform: (1) original sediment composition, (2) synsedimentary cementation and internal sedimentation, (3) different dolomitization intensity throughout the platform and (4) the extent of meteoric percolation within the platform. The findings of this study may be used as analogue for syn-rift carbonate platforms elsewhere and ultimate application of this study shows the impact of various paleofluid types on different diagenetic alterations and related reservoir quality.

5.2 Future Recommendations

Some limitations have been encountered in this study and additional necessary works need to be done in the future. Therefore, I would like to recommend few things as mentioned below:

- Detailed sampling strategy might be necessary in order to link the diagenesis into sequence stratigraphic framework.
- Porosity and permeability measurements may be further required to analyze the reservoir quality evolution.
- Link the architectural model established in this study into the subsurface data in order to test the validity of the model.
- Clumped isotope analysis need to be done to unravel the paleotemperature of dolomitizing fluids.

References

Aissaoui, D.M., M. Coniglio, N.P. James., B.H. Purser., (1986). Diagenesis of a Miocene reef-platform: Jebel Abu Shaar, Gulf of Suez, Egypt. In J.H. Schroeder and B.H. Purser (Eds.), Reef Diagenesis. Springer-Verlag, Berlin, p. 112-131.

Banner, J. L., & Hanson, G. N. (1990). Calculation of simultaneous isotopic and trace element variations during water-rock interaction with applications to carbonate diagenesis. Geochimica et Cosmochimica Acta, 54(11), 3123-3137.

Bayer, H.J. Heitzl, H., Jado, A.R., Ruscher, B. and Voggenreitter, W. (1988). Sedimentary and structural evolution of the northwest Arabian Red Sea margin. Tectonophysics, 153, 137-151.

Benedictis, D. D., Bosence, D., & Waltham, D. (2007). Tectonic control on peritidal carbonate parasequence Formation: an investigation using forward tectono-stratigraphic modelling. Sedimentology, **54(3)**, 587-605.

Benisek, M.-F., Marcano, G., Betzler, C. & Mutti, M. (2012). Facies and Stratigraphic Architecture of a Miocene Warm-Temperate to Tropical Fault-Block Carbonate Platform, Sardinia (Central Mediterranean Sea), in Carbonate Systems during the Oligocene-Miocene Climatic Transition (eds M. Mutti, W. Piller and C. Betzler), Wiley-Blackwell, Oxford, UK.

Bolhar, R., & Van Kranendonk, M. J. (2007). A non-marine depositional setting for the northern Fortescue Group, Pilbara Craton, inferred from trace element geochemistry of stromatolitic carbonates. Precambrian Research, 155(3), 229-250.

Bosence, D. (2005). A genetic classification of carbonate platforms based on their basinal and tectonic settings in the Cenozoic. Sedimentary Geology, **175(1)**, 49-72.

Bosworth, W., Sultan, M., Stern, R. J., Arvidson, R. E., Shore, P., & Becker, R. (1993). Nature of the Red Sea crust: A controversy revisited: Comment and Reply. Geology, 21(6), 574-576.

Bosworth, W., Crevello, P., Winn, R.D., Steinmetz, J. (1998). Structure Sedimentation and basin dynamics during rifting of the Gulf of Suez, and north-western Red Sea B.H. Purser, D.W.J. Bosence (Eds.), Sedimentation and tectonics of rift basins: Red SeaGulf of Aden, Chapman and Hall, London pp. 77–96

Bosworth, W. & McClay, K (2001). Structural and stratigraphic evolution of the Gulf of Suez Rift, Egypt: A synthesis. In P.A. Ziegler, W. Cavazza, A.H.F. Robertson and S. Crasquin-Soeau (Eds.), Peri-Tethyan Rift/Wrench Basins and Passive Margins. Memoir Musee Naturale Histoire, Peri-Tethys Memoir, **186 (6)**, 567-606.

Bosworth, W., Huchon, P., & McClay, K. (2005). The Red Sea and Gulf of Aden basins. Journal of African Earth Sciences, **43(1)**, 334-378.

Bover-Arnal, T., Salas, R., Moreno-Bedmar, J. A., & Bitzer, K. (2009). Sequence stratigraphy and architecture of a late Early–Middle Aptian carbonate platform succession from the western Maestrat Basin (Iberian Chain, Spain). Sedimentary Geology, **219(1)**, 280-301.

Brand, U., & Veizer, J. (1980). Chemical diagenesis of a multicomponent carbonate system--1: Trace elements. Journal of Sedimentary Research, 50(4).

Brand, U., & Morrison, J. O. (1987). Diagenesis and pyritization of crinoid ossicles. Canadian Journal of Earth Sciences, 24(12), 2486-2498.

Brand, U. (2004). Carbon, oxygen and strontium isotopes in Paleozoic carbonate components: an evaluation of original seawater-chemistry proxies. Chemical Geology, 204(1), 23-44.

Brandano, M., Frezza, V., Tomassetti, L., Pedley, M., & Matteucci, R. (2009). Facies analysis and palaeoenvironmental interpretation of the late Oligocene Attard Member (lower Coralline Limestone Formation), Malta. Sedimentology, **56(4)**, 1138-1158.

Carr, I. D., Gawthorpe, R. L., Jackson, C. A., Sharp, I. R., & Sadek, A. (2003). Sedimentology and sequence stratigraphy of early syn-rift tidal sediments: the

Nukhul Formation, Suez Rift, Egypt. Journal of Sedimentary Research, **73(3)**, 407-420.

Choquette, P.W., & James, N.P., (1987). Diagenesis in limestones-3. The deep burial environment. Geoscience Canada 14:3–35.

Clark, M. D. (1985). Late Proterozoic crustal evolution of the Midyan region, northwestern Saudi Arabia. Geology, 13(9), 611-615.

Clark, M.D. (1986). Explanatory Notes to the Geologic Map of the Al Bad' Quadrangle, sheet 28A, Kingdom of Saudi Arabia. Saudi Arabian Deputy Ministry for Mineral Resources Geoscience Map Series GM-81A, C, scale 1:250,000, with text, 46 p.

Collier, R.E.Ll. & Gawthorpe, R.L. (1995). Neotectonics, drainage and sedimentation in central Greece: Insights into coastal reservoir geometries in syn-rift sequences. In: Lambiaise, J.J. (Ed.), Hydrocarbon Habitat in Rift Basins, Special Publication of the Geological Society, London, no. **80**, 165-181.

Coniglio, M., N.P. James & D.M. Aissoui (1988). Dolomitization of Miocene carbonates, Gulf of Suez, Egypt. Journal of Sedimentary Petrology, v. 58, p. 100-119.

Coniglio, M., N.P. James & D.M. Assaoui (1996). Abu Shaar complex (Miocene) Gulf of Suez, Egypt: Deposition and diagenesis in an active rift setting. In E.K. Franseen, M. Esteban, W.C. Ward and J.-M. Rouchy (Eds.), Models for carbonate stratigraphy from Miocene reef complexes of Mediterranean regions. Society of Economic Paleontologists and Mineralogists, Concepts in Sedimentology and Paleontology, **5**, 367-384.

Cross, N. E., & Bosence, D. W. J. (2008). Tectono-sedimentary models for rift-basin carbonate systems. Controls on Carbonate Platform and Reef Development, SEPM, Special Publication, **89**, 83-105.

Dickson, J.A.D., (1966). Carbonate identification and genesis as revealed by staining. J Sediment Petrol 36:441–505.

Dorobek, S. L. (2008). Tectonic and depositional controls on syn-rift carbonate platform sedimentation. Controls on Carbonate Platform and Reef Development, SEPM, Special Publication, **89**, 57-81.

Dunham RJ. (1962). Classification of carbonate rocks according to their depositional texture. In: Ham WE, editor. Classification of Carbonate Rocks, AAPG Memoir, **1**, 108– 21.

Ehrenberg, S. N., Pickard, N. A. H., Svånå, T. A., & Oxtoby, N. H. (2002). Cement Geochemistry of Photozoan Carbonate Strata (Upper Carboniferous-Lower Permian), Finnmark Carbonate Platform, Barents Sea. Journal of Sedimentary Research, 72(1), 95-115.

Embry AF, Klovan JE. (1971). A Late Devonian reef tract on northeastern Banks Island. NWT Bulletin of Canadian Petroleum Geology; **19**,730– 81.

Flügel, E. (2004). Microfacies of Carbonate Rocks: Analysis, Interpretation and Application, Springer-Verlag, Berlin, 984 p.

Gardner, W. C., Asif Khan, M., & Al-Hinai, K. G. (1996). Interpretation of Midyan and Sinai Geology from a Landsat TM image. Arabian Journal for Science and Engineering, 21, 571-588.

Gawthorpe, R. L., Fraser, A. J., & Collier, R. E. L. (1994). Sequence stratigraphy in active extensional basins: implications for the interpretation of ancient basin-fills. Marine and Petroleum Geology, **11(6)**, 642-658.

Gawthorpe, R. L., & Leeder, M. R. (2000). Tectono-sedimentary evolution of active extensional basins. Basin Research, **12(3-4)**, 195-218.

Ginsburg, R.N., (1971). Landward movement of carbonate mud: new model for regressive cycles in carbonates. American Association of Petroleum Geology Bulletin. **55**, 340.

Goldhammer, R. K., Dunn, P. A., & Hardie, L. A. (1990). Depositional cycles, composite sea-level changes, cycle stacking patterns, and the hierarchy of

stratigraphic forcing: examples from Alpine Triassic platform carbonates. Geological Society of America Bulletin, **102(5)**, 535-562.

Gröcke, D. R., Hesselbo, S. P., & Jenkyns, H. C. (1999). Carbon-isotope composition of Lower Cretaceous fossil wood: Ocean-atmosphere chemistry and relation to sea-level change. Geology, 27(2), 155-158.

Hallock, P., & Schlager, W. (1986). Nutrient excess and the demise of coral reefs and carbonate platforms. Palaios, 389-398.

Halfar, J., & Mutti, M. (2005). Global dominance of coralline red-algal facies: a response to Miocene oceanographic events. Geology, **33(6)**, 481-484.

Hughes, G.W. & R.S. Johnson (2005). Lithostratigraphy of the Red Sea Region. GeoArabia, **10 (3)**, 49-126.

Hughes, G.W., (2014). Micropalaeontology and palaeoenvironments of the Miocene Wadi Waqb carbonate of the northern Saudi Arabian Red Sea. GeoArabia, **19(4)**, 59-108

Hussein, M. & K. Al-Ramadan. (2009). Microfacies analysis of Wadi Waqb Member (Miocene) in Wadi Aynunah, northwest of Saudi Arabia. Carbonates and Evaporites, **24**, 139-149.

Jackson, M. P. A., Hudec, M. R., & Hegarty, K. A. (2005). The great West African Tertiary coastal uplift: Fact or fiction? A perspective from the Angolan divergent margin. Tectonics, **24(6)**.

James, N. P. (1983). Shelf-slope break in fossil carbonate platforms: an overview.

James, N. P. (1997). The cool-water carbonate depositional realm. Special Publication-SEPM, **56**, 1-22.

Kamal, R.A. & G.W. Hughes 1993. The Ad Dubaybah reef complex, Midyan area, NW Saudi Arabia. Geological Research and Development Division, Miscellaneous Report #1009.

Kendall, C. G. S. C., & Schlager, W. (1981). Carbonates and relative changes in sea level. Marine Geology, **44(1)**, 181-212.

Kerans, C., & Tinker, S. W. (1997). Sequence stratigraphy and characterization of carbonate reservoirs (p. 130). SEPM.

Koeshidayatullah, A., & Al-Ramadan, K. (2014). Unraveling cementation environment and patterns of Holocene beachrocks in the Arabian Gulf and the Gulf of Aqaba: stable isotope approach. Geological Quarterly, 58(2), 207-216.

Kominz, M. A., Browning, J. V., Miller, K. G., Sugarman, P. J., Mizintseva, S., & Scotese, C. R. (2008). Late Cretaceous to Miocene sea-level estimates from the New Jersey and Delaware coastal plain coreholes: An error analysis. Basin Research, 20(2), 211-226.

Land, L. S. (1980). The isotopic and trace element geochemistry of dolomite: the state of the art.

Land, L. S. (1986). Limestone diagenesis—some geochemical considerations. US Geol. Surv. Bull, 1578, 129-137.

Laya, J. C., Tucker, M. E., & Perez-Huerta, A. (2013). Metre-scale cyclicity in Permian ramp carbonates of equatorial Pangea (Venezuelan Andes): Implications for sedimentation under tropical Pangea conditions. Sedimentary Geology, **292**, 15-35.

Leeder, M. R., & Gawthorpe, R. L. (1987). Sedimentary models for extensional tilt-block/half-graben basins. Geological Society, London, Special Publications, **28(1)**, 139-152.

Lees, A., & Buller, A. T. (1972). Modern temperate-water and warm-water shelf carbonate sediments contrasted. Marine Geology, 13(5), p67-p73.

Longman, M. W. (1980). Carbonate diagenetic textures from nearsurface diagenetic environments. AAPG Bulletin, 64(4), 461-487.

Lucia, F. J., Martin, A. J., Solomon, S. T., Hartmann, D. J., (1999). Characterization of petrophysical flow units in carbonate reservoirs: discussion. AAPG bulletin, v. 83(7), 1161-1163.

Lyberis, N. (1988). Tectonic evolution of the Gulf of Suez and the Gulf of Aqaba. Tectonophysics, **153(1)**, 209-220.

Mack, G. H., Leeder, M. R., & Perez-Arlucea, M. (2009). Late Neogene rift-basin evolution and its relation to normal fault history and climate change along the southwestern margin of the Gerania Range, central Greece. Geological Society of America Bulletin, **121(5-6)**, 907-918.

Magaritz, M. (1983). Carbon and oxygen isotope composition of recent and ancient coated grains. In Coated grains (pp. 27-37). Springer Berlin Heidelberg.

Mazzullo, S. J. (2004). Overview of porosity evolution in carbonate reservoirs. Kansas Geological Society Bulletin, 79(1/2), 20-28.

Melim, L.A., Westphal, H., Swart, P.K., Eberli, G.P., Munnecke, A., (2002). Questioning carbonate diagenetic paradigms: evidence from the Neogene of the Bahamas. Marine Geology 185, 27–53.

Meyers, W. J. (1989). Trace element and isotope geochemistry of zoned calcite cements, Lake Valley Formation (Mississippian, New Mexico): insights from water-rock interaction modelling. Sedimentary geology, 65(3), 355-370.

Miller, C. R., James, N. P., & Bone, Y. (2012). Prolonged carbonate diagenesis under an evolving late Cenozoic climate; Nullarbor Plain, southern Australia. Sedimentary Geology, 261, 33-49.

Milliman, J. D. (1974). Marine Carbonates, 375.

Moore, C. H., & Druckman, Y. (1981). Burial diagenesis and porosity evolution, upper Jurassic Smackover, Arkansas and Louisiana. AAPG Bulletin, 65(4), 597-628.

Moore, C. H. (2001). Carbonate Reservoirs: Porosity, Evolution and Diagenesis in A Sequence Stratigraphic Framework: Porosity Evolution and Diagenesis in a Sequence Stratigraphic Framework (**Vol. 55**). Elsevier.

Morse, J. W., & Mackenzie, F. T. (1990). Geochemistry of sedimentary carbonates. Elsevier.

Mougenot, D., & Al-Shakhis, A. A. (1999). Depth imaging sub-salt structures: a case study in the Midyan Peninsula (Red Sea). GeoArabia, 4, 335-463.

Mutti, M., & Hallock, P. (2003). Carbonate systems along nutrient and temperature gradients: some sedimentological and geochemical constraints. International Journal of Earth Sciences, **92(4)**, 465-475.

Nelson, C. S., & Smith, A. M. (1996). Stable oxygen and carbon isotope compositional fields for skeletal and diagenetic components in New Zealand Cenozoic nontropical carbonate sediments and limestones: a synthesis and review. New Zealand Journal of Geology and Geophysics, 39(1), 93-107.

Polis, S. R., Angelich, M. T., Beeman, C. R., Maze, W. B., Reynolds, D. J., Steinhauff, D. M., & Wood, M. V. (2005). Preferential deposition and preservation of structurally-controlled synrift reservoirs: Northeast Red Sea and Gulf of Suez. Geoarabia, 10(1), 97-124.

Pomar, L. (2001). Types of carbonate platforms, a genetic approach. Basin Research, **13**, 313-334.

Pomar, L. (2001) Ecological control of sedimentary accomodation: evolution from a carbonate ramp to rimmed shelf, Upper Miocene, Balearic Islands. Palaeogeography, Palaeoclimatology, Palaeoecology, **175**, 249-272.

Pomar, L., Gili, E., Obrador, A., & Ward, W. C. (2005). Facies architecture and high-resolution sequence stratigraphy of an Upper Cretaceous platform margin succession, southern central Pyrenees, Spain. Sedimentary Geology, **175(1)**, 339-365.

Pomar, L. & Kendall, C. G. S. C. (2007). Architecture of carbonate platforms: a response to hydrodynamics and evolving ecology. Controls on Carbonate Platform and Reef Development. Special Publication, **89**, 187-216.

Pomar, L., Bassant, P., Brandano, M., Ruchonnet, C., & Janson, X. (2012). Impact of carbonate producing biota on platform architecture: Insights from Miocene examples of the Mediterranean region. Earth-Science Reviews, **113(3)**, 186-211.

Pomar, L., Mateu-Vicens, G., Morsilli, M., & Brandano, M. (2014). Carbonate ramp evolution during the Late Oligocene (Chattian), Salento Peninsula, southern Italy. Palaeogeography, Palaeoclimatology, Palaeoecology, **404**, 109-132.

Popp, B. N., Anderson, T. F., & Sandberg, P. A. (1986). Textural, elemental, and isotopic variations among constituents in Middle Devonian limestones, North America. Journal of Sedimentary Research, 56(5).

Posamentier, H.W., Allen, G.P., James, D.P. & Tesson, M. (1992) Forced regression in a sequence stratigraphic framework: concepts, examples and exploration significance. AAPG Memoir, 76, 1687-1709.

Prasada Rao, C., & Adabi, M. H. (1992). Carbonate minerals, major and minor elements and oxygen and carbon isotopes and their variation with water depth in cool, temperate carbonates, western Tasmania, Australia. Marine Geology, 103(1), 249-272.

Prasada Rao, C., (1996). Elemental composition of marine calcite from modern temperate shelf brachiopods, bryozoans and bulk carbonates, eastern Tasmania, Australia. Carbonates and Evaporites, 11(1), 1-18.

Purser, B. H., Philobbos, E. R., & Soliman, M. (1990). Sedimentation and rifting in the NW parts of the Red Sea; a review. Bulletin de la Société géologique de France, 6(3), 371-384.

Ravnas, R., & Steel, R. J. (1998). Architecture of marine rift-basin successions. AAPG bulletin, 82(1), 110-146.

Read, J. F. (1982). Carbonate platforms of passive (extensional) continental margins: types, characteristics and evolution. Tectonophysics, **81(3)**, 195-212.

Read, J.F. (1985) Carbonate Platform Models. AAPG Bulletin, **69**, 1-21.

Roehl, P. O., & Choquette, P. W. (1985). Carbonate petroleum reservoirs.

Rudolph, K. W., & Lehmann, P. J. (1989). Controls on Carbonate Platform and Basin Development.

Sandberg, P. A. (1983). An oscillating trend in Phanerozoic non-skeletal carbonate mineralogy. Nature, 305, 19-22.

Sarg, J. F. (1988). Carbonate sequence stratigraphy.

Saller, A. H., & Vijaya, S. (2002). Depositional and diagenetic history of the Kerendan carbonate platform, Oligocene, central Kalimantan, Indonesia. Journal of Petroleum Geology, 25(2), 123.

Satterley, A. K. (1996). Cyclic carbonate sedimentation in the Upper Triassic Dachstein Limestone, Austria: the role of patterns of sediment supply and tectonics in a platform-reef-basin system. Journal of Sedimentary Research, **66(2)**.

Satterley, A. K. (1996). The interpretation of cyclic successions of the Middle and Upper Triassic of the Northern and Southern Alps. Earth-Science Reviews, **40(3)**, 181-207.

Schlager, W. (1992). Sedimentology and sequence stratigraphy of reefs and carbonate platforms.

Schlager, W. (2005) Carbonate Sedimentology and Sequence Stratigraphy, SEPM Concepts in Sedimentology and Paleontology: **8**, 200 pp.

Schroeder, J. H., & Purser, B. H. (1986). Reef diagenesis: introduction. In Reef Diagenesis (pp. 1-5). Springer Berlin Heidelberg.

Shaaban, M. N., Holail, H. M., & Rashed, M. A. (1997). Dolomitization of middle miocene buildups, Um Gheig area, Red Sea coast, Egypt. Carbonates and Evaporites, 12(2), 264-275.

Shinn, E. A., Robbin, D. M., 1983. Mechanical and chemical compaction in fine-grained shallow-water limestones: Journal of Sedimentary Petrology, v. 53, p. 595-618.

Sibley, D. F., & Gregg, J. M. (1987). Classification of dolomite rock textures. Journal of Sedimentary Research, 57(6).

Strasser, A., Pittet, B., Hillgärtner, H., & Pasquier, J. B. (1999). Depositional sequences in shallow carbonate-dominated sedimentary systems: concepts for a high-resolution analysis. Sedimentary Geology, **128(3)**, 201-221.

Steel, R. J. (1993). Triassic–Jurassic megasequence stratigraphy in the Northern North Sea: rift to post-rift evolution. In Geological Society, London, Petroleum Geology Conference series **4**, 299-315.

Swart, P. K., Thorrold, S., Rosenheim, B., Eisenhauer, A., Harrison, C. G. A., Grammer, M., & Latkoczy, C. (2002). Intra-annual variation in the stable oxygen and carbon and trace element composition of sclerosponges. Paleoceanography, 17(3), 17-1.

Trice, R. (2005). Challenges and insights in optimising oil production from Middle Eastern karst reservoirs. SPE Middle East Oil & Gas Show and Conference, March 12-15, 2005, Bahrain.

Tubbs, R.E., H.G. Aly Fouda, A.M. Afifi, N.S. Raterman, G.W. Hughes & Y.K. Fadolalkarem. (2014). Midyan Peninsula, northern Red Sea, Saudi Arabia: Seismic imaging and regional interpretation. GeoArabia, **19(3)**, 165-184.

Tucker, M. E. (1983). Diagenesis, geochemistry, and origin of a Precambrian dolomite: the Beck Spring Dolomite of eastern California. Journal of Sedimentary Research, 53(4).

Tucker, M. E. (1985). Shallow-marine carbonate facies and facies models. Geological Society, London, Special Publications, **18(1)**, 147-169.

Tucker, M.E., Wright, V.P. (1990). Carbonate Sedimentology. Blackwell Scientific Publications. (482 pp.).

Vahrenkamp, V. C., David, F., Duijndam, P., Newall, M., & Crevello, P. (2004). Growth architecture, faulting, and karstification of a middle Miocene carbonate platform, Luconia Province, offshore Sarawak, Malaysia. AAPG Special Volumes: G. P. Eberli, J. L. Masaferro, and J. F. "Rick" Sarg, 2004, Seismic imaging of carbonate reservoirs and systems: AAPG Memoir 81, p. 329-350.

Veizer, J. (1983). Trace elements and isotopes in sedimentary carbonates. Reviews in Mineralogy and Geochemistry, 11(1), 265-299.

Weissert, H., Lini, A., Föllmi, K. B., & Kuhn, O. (1998). Correlation of Early Cretaceous carbon isotope stratigraphy and platform drowning events: a possible link?. Palaeogeography, Palaeoclimatology, Palaeoecology, **137(3)**, 189-203.

Western, P. G., & Ball, G. J. (1992). 3D Prestack Depth Migration in the Gulf of Suez: A Case History 1. Geophysical prospecting, 40(4), 379-402.

Winefield, P. R., Nelson, C. S., & Hodder, A. P. W. (1996). Discriminating temperate carbonates and their diagenetic environments using bulk elemental geochemistry: a reconnaissance study based on New Zealand Cenozoic limestones. Carbonates and Evaporites, 11(1), 19-31

Wilson, J.L. (1975) Carbonate Facies in Geologic History. Springer, Berlin, 471 pp.

Wilson, M. E., Bosence, D. W., & Limbong, A. (2000). Tertiary syntectonic carbonate platform development in Indonesia. Sedimentology, **47(2)**, 395-419.

Wilson, M. E. (2002). Cenozoic carbonates in Southeast Asia: implications for equatorial carbonate development. Sedimentary Geology, **147(3)**, 295-428.

Vitae

Name	: Ardiansyah Ibnu Koeshidayatullah
Nationality	: Indonesia
Date of Birth	: 03-March-1989
Email	: ardiansyah.ik@gmail.com
Address	: KFUPM, Dhahran
Academic Background	: B. Eng Geology (Bandung Institute of Technology, Indonesia, 2011)

Ardi joined KFUPM as a graduate student at Earth Sciences Department in 2012. Prior to join KFUPM he worked as an exploration geologist in PT. GRG, LAPI ITB where he was involved in different exploration studies from major multinational companies (ExxonMobil, BP, and Repsol SA) in Indonesia, which include subsurface and fieldwork studies. His main research interest is carbonate sedimentology and diagenesis. During his master, he spent two months in Svalbard, Norway to attend a summer school in University of Central Svalbard where he studied Arctic Sedimentology under the supervision of Dr. Maria Jensen. He was also a visiting research student in the Stable Isotope Laboratory in University of Miami, USA where he worked closely with Prof. Peter Swart in analyzing stable isotopes, trace elements and other geochemical analyses of Miocene Red Sea carbonate successions. He attended “Flugel” course in Germany where carbonate sedimentologist around the world were gathered to study carbonate geology. He received

best graduate student of the year in 2014 from Earth Sciences Department and also He was part of the winning Imperial Barrel Award 2015 KFUPM team. He published three journal articles in internationally recognized ISI journals and more than five international conference paper during his master. He is an active member of Dhahran Geosciences Society (DGS), American Association of Petroleum Geologist (AAPG) and European Association of Geoscientist and Engineers (EAGE).

[1] **Koeshidayatullah, A**, and Al-Ramadan, K, (2014). Unraveling Cementation Environ ment and Patterns in Holocene Beachrocks from the Arabian Gulf and the Gulf of Aqaba: A Stable Isotope Approach. Geological Quarterly, v. 58 (2)

[2] Al-Hussaini. A, **Koeshidayatullah, A**, and Al-Ramadan. K., (2015). Formation conditions and diagenetic evolution of Recent Sand Roses along the Arabian Gulf Coastal Region, Eastern Saudi Arabia. Geological Quarterly, v. 59 (1)

[3] **Koeshidayatullah, A,** Al-Ramadan, K, and Hughes, G.W., (2015). Facies Mosaic and Diagenetic Patterns of the Early Devonian (Late Pragian-Early Emsian) Microbialite-Dominated Carbonate Sequences, Qasr Member, Jauf Formation, Saudi Arabia. Geological Journal. In press

[4] **Koeshidayatullah, A**, Al-Ramadan, K, Collier, R.E.L, Hughes, G.W. Variations in Architecture and Cyclicity in Fault-Bounded Carbonate Platforms: Early Miocene Red Sea Rift, NW Saudi Arabia. Sedimentology. Under Review

[5] **Koeshidayatullah, A**, Al-Ramadan, K, and Cantrell, D., 2013. Miocene Carbonate Microfacies Distribution of Tendehantu Formation, Mangkalihat Peninsula: Ap-proach of Reservoir Potential using Outcrop Analogue. AAPG Annual Convention and Exhibition, Pittsburgh, USA.

[6] **Koeshidayatullah, A**, Hughes, G.W, Al-Ramadan, K, and Collier, R., 2014. Facies Distribution and High-Frequency Carbonate Cycles of Midyan Rift Basin: the Early Miocene Musayr Formation, Northwestern Saudi Arabia. 11th Middle East Geo-sciences Conference and Exhibition, GEO 2014, Bahrain.

[7] Collier. R.L., Al-Ramadan. K., Hughes, G.W., Cantrell, D, **Koeshidayatullah, A**, and Al-Hussaini. A. 2014. Syn-rift variations in carbonate facies: Wadi Waqb Member, Midyan, Saudi Arabia. 11th Middle East Geosciences Conference and Exhibition, GEO 2014, Bahrain.

[8] **Koeshidayatullah, A,** and Al-Ramadan, K., 2014. A Multi-Scale Facies Analysis and Diagenetic Evolution of Early Devonian Microbial Carbonate, Qasr Member, Jauf Formation. European Geosciences Union General Assembly, Vienna, Austria.

[9] Trigg, C., Lowe, D., Al-Ramadan, K., and **Koeshidayatullah. A**., 2015. Deep-water Sedimentation in a Proximal Rift Margin Setting: Observation of Syn-Rift Strata, Northern Red Sea. AAPG Annual Convention and Exhibition, Denver.